Strain development of *Gluconobacter oxydans*: Complementation of non-functional metabolic pathways and increase of carbon flux

Ines Kiefler

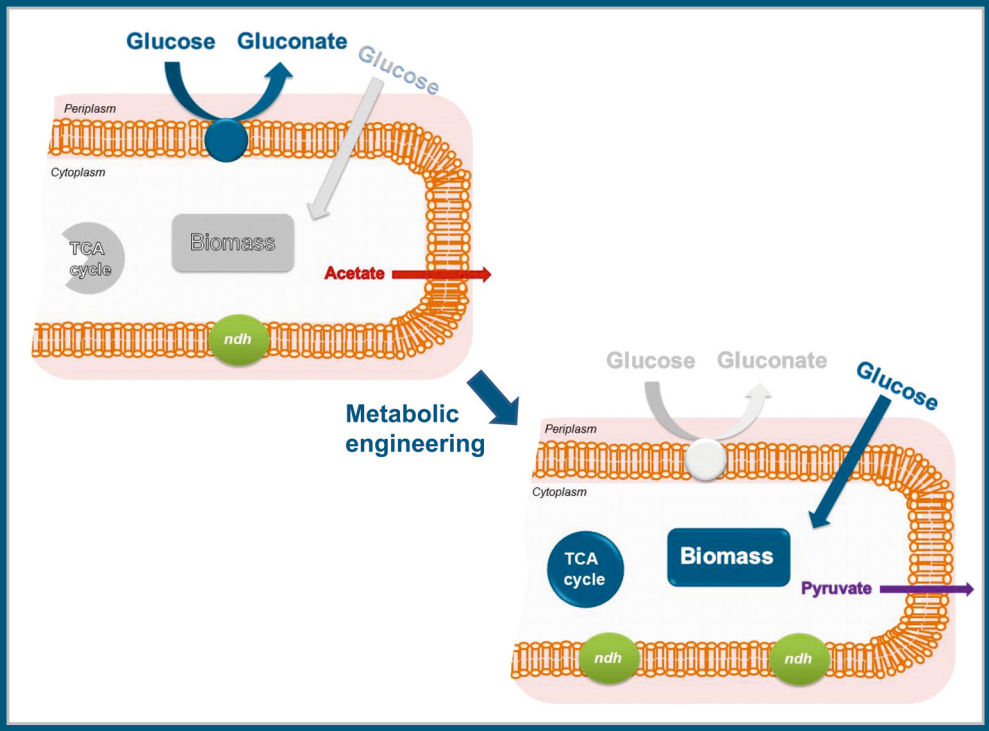

Member of the Helmholtz Association

Gesundheit / Health
Band / Volume 82
ISBN 978-3-95806-158-3

JÜLICH
FORSCHUNGSZENTRUM

Schriften des Forschungszentrums Jülich
Reihe Gesundheit / Health Band / Volume 82

Forschungszentrum Jülich GmbH
Institute of Bio- and Geosciences
Biotechnology (IBG-1)

Strain development of *Gluconobacter oxydans*: Complementation of non-functional metabolic pathways and increase of carbon flux

Ines Kiefler

Schriften des Forschungszentrums Jülich
Reihe Gesundheit / Health

Band / Volume 82

ISSN 1866-1785

ISBN 978-3-95806-158-3

Bibliographic information published by the Deutsche Nationalbibliothek.
The Deutsche Nationalbibliothek lists this publication in the Deutsche Nationalbibliografie; detailed bibliographic data are available in the Internet at http://dnb.d-nb.de.

Publisher and Distributor: Forschungszentrum Jülich GmbH
Zentralbibliothek
52425 Jülich
Tel: +49 2461 61-5368
Fax: +49 2461 61-6103
Email: zb-publikation@fz-juelich.de
www.fz-juelich.de/zb

Cover Design: Grafische Medien, Forschungszentrum Jülich GmbH

Printer: Grafische Medien, Forschungszentrum Jülich GmbH

Schriften des Forschungszentrums Jülich
Reihe Gesundheit / Health, Band / Volume 82

D 61 (Diss. Düsseldorf, Univ., 2016)

ISSN 1866-1785
ISBN 978-3-95806-158-3

The complete volume is freely available on the Internet on the Jülicher Open Access Server (JuSER) unter www.fz-juelich.de/zb/openaccess.

Niemand weiß, was er kann, bis er es probiert hat.

Results described in this this dissertation have been published in the following original publications:

Kiefler I, Bringer S, Bott M (2015) SdhE-dependent formation of a functional *Acetobacter pasteurianus* succinate dehydrogenase in *Gluconobacter oxydans* - a first step toward a complete tricarboxylic acid cycle. Appl Microbiol Biotechnol 99:9147–9160 DOI 10.1007/s00253-015-6972-8.

Kiefler I, Bringer S, Bott M (2016) Metabolic engineering of *Gluconobacter oxydans* 621H for improved growth yield on glucose by prevention of gluconate and acetate formation and completion of the tricarboxylic acid cycle. To be submitted.

Kiefler I, Bringer S, Bott M (2016) Impact of plasmid-based expression of functions for glucose uptake and phosphorylation, glycolysis, and pyruvate oxidation to acetyl-CoA on growth of *Gluconobacter oxydans* IK003.1. To be submitted.

Table of contents

Abbreviations

Δ	Deletion
ATP	Adenosine triphosphate
cdw	Cell dry weight
CoA	Coenzyme A
DCPIP	2,6-dichlorophenolindophenol
DO	Dissolved oxygen
EDP	Entner-Doudoroff Pathway
EMP	Embden-Meyerhof-Parnas pathway
FAD	Flavin adenine dinucleotide
GTP	Guanosine triphosphate
HPLC	High Performance Liquid Chromatography
et al.	et alii
NAD/NADH	Nicotinamide adenine dinucleotide, oxidized/reduced
NADP/NADPH	Nicotinamide adenine dinucleotide phosphate, oxidized/reduced
OD_{600}	Optical density at 600 nm
PPP	Pentose phosphate pathway
PQQ	Pyrroloquinoline quinone
TCA cycle	Tricarboxylic acid cycle
UQ	Ubiquinone

Further abbreviations not included in this section are according to International Standards, as for example listed in the author guidelines of the FEBS Journal.

1. Abstract

The acetic acid bacterium *Gluconobacter oxydans* possesses outstanding metabolic characteristics that are favorable for biotechnological applications in oxidative whole-cell biotransformations. The key feature is the rapid and incomplete regio- and stereoselective oxidation of sugars, sugar alcohols, and other carbon sources in the periplasm by a versatile set of membrane-bound dehydrogenases. Beside the beneficial attributes, the unusual metabolism of *G. oxydans* also poses a problem, which is the low cell yield resulting in high costs for biomass production. This study aimed at an increase of the cell yield of *G. oxydans* on glucose in order to improve its application potential. For this purpose, prevention of incomplete glucose oxidation to gluconate and ketogluconates and complementation of the incomplete tricarboxylic acid (TCA) cycle were selected as promising targets and implemented by construction and characterization of several integration/deletion mutants:

The succinate dehydrogenase from *Acetobacter pasteurianus* was introduced into *G. oxydans*, which naturally lacks this TCA cycle enzyme in addition to succinyl-CoA synthetase. Plasmid-based expression of the structural genes *sdhCDAB* together with the *sdhE* gene encoding a flavinylation factor led to a strain with high succinate dehydrogenase activity, showing functional synthesis of this complex membrane protein containing FAD, three iron-sulfur clusters and heme as prosthetic groups. Genomic integration of the *sdhCDABE* genes with simultaneous deletion of the *gdhS* gene for the cytosolic glucose dehydrogenase led to strain IK001 with considerable succinate dehydrogenase activity.

To improve the NADH oxidation capacity that might be required to handle an increased NADH formation rate resulting from an increased cytoplasmic glucose catabolism, a second NADH dehydrogenase gene *ndh* from *G. oxydans* strain DSM3504 was genomically introduced into strain IK001 with simultaneous deletion of the *pdc* gene encoding pyruvate decarboxylase. The resulting strain IK002.1 also showed an increased cell yield of 12 % compared to the reference strain and secreted pyruvate instead of acetate.

In order to complete the TCA cycle of strain IK002.1 and prevent periplasmic glucose oxidation to gluconate, the succinyl-CoA synthetase genes *sucCD* of *Gluconacetobacter diazotrophicus* were genomically integrated with simultaneous deletion of the *gdhM* gene encoding the membrane-bound glucose dehydrogenase. The resulting strain IK003.1 did not secrete gluconate or 2-ketogluconate anymore, but formed twice as much carbon dioxide as the reference strain, either via the cyclic pentose phosphate cycle or via the TCA cycle. The initial glucose consumption rate was much slower and growth was delayed, but the cell yield was increased by 60 %. Therefore, *G. oxydans* IK003.1 represents a promising strain for industry due to its increased cell yield and a basis for further strain development.

1. Zusammenfassung

Das Essigsäurebakterium *Gluconobacter oxydans* verfügt über herausragende metabolische Besonderheiten, die vorteilhaft für biotechnologische Anwendungen in oxidativen Ganzzellbiotransformationen sind. Die entscheidene Eigenschaft ist die schnelle und unvollständige regio- und stereoselektive Oxidation von Zuckern, Zuckeralkoholen und anderen Kohlenstoffquellen im Periplasma durch ein vielfältiges Angebot an membrangundenen Dehydrogenasen. Neben den nützlichen Attributen wirft der ungewöhnliche Metabolismus von *G. oxydans* auch ein Problem auf, welches in der geringen Zellausbeute besteht und in hohen Kosten für die Biomasseproduktion resultiert. Das Ziel dieser Studie ist die Steigerung der Zellausbeute von *G. oxydans* auf Glucose, um das Anwendungspotenzial zu verbessern. Zu diesem Zweck wurden die Unterbindung der unvollständigen Glucoseoxidation zu Gluconat und Ketogluconaten und die Komplementierung des unvollständigen Tricarbonsäurezyklus als aussichtsreiche Ziele gewählt und durch die Konstruktion und Charakterisierung verschiedener Integrations-/Deletionsmutanten umgesetzt:

Die Succinat-Dehydrogenase von *Acetobacter pasteurianus* wurde in *G. oxydans* eingebracht, da dieses Enzym wie auch die Succinyl-CoA Synthetase des Tricarbonsäurezyklus naturgemäß in *G. oxydans* fehlen. Die plasmid-basierte Expression der strukturellen Gene *sdhCDAB* zusammen mit dem *sdhE*-Gen, welches einen Flavinylierungsfaktor kodiert, führte zu einem Stamm mit einer hohen Succinat-Dehydrogenase Aktivität. Dies zeigte die funktionale Synthese dieses komplexen Membranproteins, das FAD, drei Eisen-Schwefel-Cluster und Häm als prosthetische Gruppen enthält. Die genomische Integration der *sdhCDABE* und gleichzeitige Deletion des *gdhS*-Gens, das die cytosolische Glucose-Dehydrogenase kodiert, ergab Stamm IK001 mit einer beträchtlichen Succinat-Dehydrogenase Aktivität.

Um die Kapazität der NADH-Oxidation zu verbessern, die wahrscheinlich benötigt wird um eine gesteigerte NADH-Bildung zu kompensieren die aus einem erhöhten cytoplasmatischen Glucose-Katabolismus resultiert, wurde ein zweites NADH-Dehydrogenase Gen *ndh* aus *G. oxydans* DSM3504 genomisch in Stamm IK001 integriert und gleichzeitig das *pdc*-Gen, das die Pyruvatdecarboxylase kodiert, deletiert. Der daraus resultierende Stamm IK002.1 zeigte eine verbesserte Zellausbeute von 12 % im Vergleich zum Referenzstamm und sekretierte Pyruvat anstatt Acetat.

Um den Tricarbonsäurezyklus des Stammes IK002.1 zu vervollständigen und die periplasmatische Glucoseoxidation zu Gluconat zu verhindern, wurden die Succinyl-CoA Synthetase Gene *sucCD* von *Gluconacetobacter diazotrophicus* genomisch integriert mit der

simultanen Deletion des *gdhM*-Gens, welches die membrangebundene Glucose-Dehydrogenase kodiert. Der daraus resultierende Stamm IK003.1 sekretierte kein Gluconat oder 2-Ketogluconat mehr, aber bildete zweimal soviel Kohlenstoffdioxid wie der Referenzstamm, entweder über den zyklischen Pentosephosphat-Weg oder den Tricarbonsäurezyklus. Die anfängliche Glucoseverbrauchsrate war wesentlich langsamer und das Wachstum verzögert, aber die finale Zelldichte wurde um 72 % und die Zellausbeute um 60 % gesteigert. Somit repräsentiert *G. oxydans* IK003.1 aufgrund der erhöhten Zellausbeute einen vielversprechenden Stamm für die Industrie und eine Basis für die weitere Stammentwicklung.

2. Introduction

2.1 The organism *Gluconobacter oxydans*

The genus *Gluconobacter* is member of the *Acetobacteraceae* family belonging to the class of α-Proteobacteria (Asai 1935; Kersters et al. 2006). Acetic acid bacteria are Gram-negative, obligately aerobic, ellipsoidal to rod-shaped organisms (De Ley et al. 1984). The family *Acetobacteraceae* includes the genera *Acetobacter*, *Acidomonas*, *Ameyamaea*, *Asaia*, *Gluconacetobacter*, *Gluconobacter*, *Granulibacter*, *Kozakia*, *Komagataeibacter*, *Neoasaia*, *Neokomagataea*, *Saccharibacter*, *Swaminathania* and *Tanticharoenia* (Yamada and Yukphan 2008; Saichana et al. 2015). The different genera are classified into two physiological groups based on the ability to oxidize acetate. Members of *Acetobacter*, *Acidomonas*, *Asaia*, *Gluconacetobacter*, and *Kozakia* possess the genetic requirements for oxidation of acetate and lactate to CO_2. Because of an incomplete tricarboxylic acid (TCA) cycle and the lack of the anaplerotic glyoxylate shunt, *Gluconobacter* is unable to oxidize acetate (Greenfield and Claus 1972; Prust et al. 2005). A distinct differentiation of *Acetobacter* and *Gluconobacter* was first given by 16S rRNA sequence analysis (Sievers et al. 1995). The genus *Gluconobacter* was recommended for biotechnological application already in 1933 due to the ability to rapidly oxidize glucose to gluconic acid without the oxidation of acetate (Asai 1935; Reichstein 1934). The five species *G. oxydans*, *G. frateurii*, *G. cerinus*, *G. albidus* and *G. thailandicus* are counted among the genus *Gluconobacter* (Yamada et al. 1999; Euzeby 2005). Cells of *G. oxydans* are ellipsoidal to rod-shaped and have a growth-depending size of 0.5-0.8 x 0.9-4.2 µm (Fig. 1).

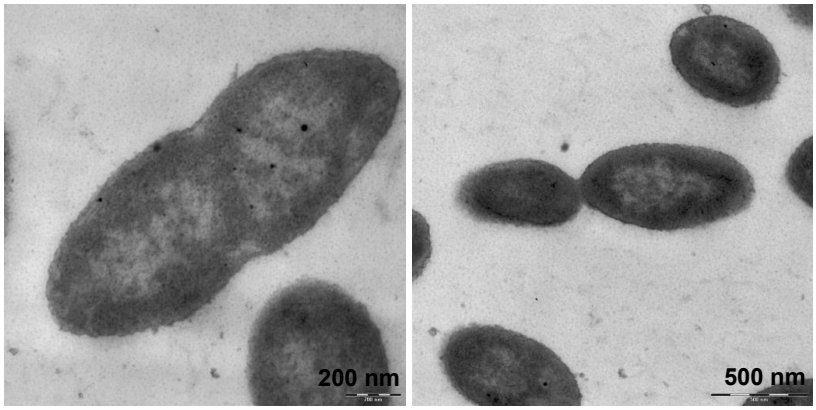

Fig.1: Electron microscopic pictures of *G. oxydans*.
The pictures were kindly provided by M. Hoppert, Department of General Microbiology, Institute of Microbiology and Genetics, University of Göttingen.

Gluconobacter strains are usually thought to be non-pathogenic towards humans or animals, however, there are recent reports on pathogenic *Gluconobacter* strains (Bassetti et al. 2013). Furthermore, the bacteria can cause a bacterial rot of pears and apples (De Ley et al. 1984). The occurrence of this chemoorganotrophic bacterium is mainly in sugary, alcoholic and acidic environments like flowers, fruits, beer and wine. The best substrates for growth of *Gluconobacter* species are the sugars and sugar alcohols D-mannitol, D-sorbitol, glycerol, D-fructose and D-glucose in descending order (De Ley et al. 1984; Kersters et al. 2006; Gupta et al. 2001). Beside the carbon source, *Gluconobacter* requires yeast extract to achieve higher cell densities, due to the fact that growth on defined media is weak (Olijve and Kok 1979a; Raspor and Goranovič 2008). *Gluconobacter* is acidophilic and able to grow at pH 3.6; however, the pH optimum is between 5.5 and 6. The preferred growth temperature is between 25 and 30 °C (De Ley et al. 1984; Olijve and Kok 1979b).

In 2005, the genome sequence of *G. oxydans* 621H was published revealing some special characteristics of this organism (Prust et al. 2005). The total size of the genome amounts to 2.9 Mbp, split into a circular chromosome of 2.7 Mbp and five plasmids (pGOX1-5), ranging from 2.7 kb to 163 kb. The GC content of α-Proteobacteria ranges from 27.5 % (*Ehrlichia ruminantium*) to 65 % (*Rhodopseudomonas palustris*) (Lightfield et al. 2011). With 60.8 %, the GC content of the genomic DNA of *G. oxydans* is in the upper range of this spectrum (Prust et al. 2005; De Ley et al. 1984). Other acetic acid bacteria like *Acetobacter* and *Gluconacetobacter* possess a GC content of 53-63 % and 55-65 %, respectively (Hutkins 2008). In the genome of *G. oxydans*, 2,664 protein-encoding open reading frames (ORFs) were identified. Furthermore, 82 insertion sequences (IS) and 103 transposase genes were found explaining the genetic instability and variability of *G. oxydans* (Kondo and Horinouchi 1997; Prust et al. 2005). Another special characteristic of this organism is the large and diverse number of membrane-bound dehydrogenases and intracellular oxidoreductases (Prust et al. 2005).

2.2 Biotechnological relevance of *G. oxydans*

G. oxydans is distinguished by a multiplicity of membrane-bound and respiratory chain-linked dehydrogenases. Thus, the organism has the favorable ability to rapidly and incompletely oxidize sugars and sugar alcohols regio- and stereoselectively. The catalytic centers of the membrane-integral dehydrogenases are located in the periplasm. Consequently, the uptake of the substrates into the cell is not required and the oxidation products accumulate in large amounts in the media after diffusion through porins in the outer membrane (Matsushita et al. 1994; Kulhanek 1989). Based on these special characteristics, *G. oxydans* is used since the 1930s for industrial applications requiring regio- and

stereoselective oxidations, which would be impossible to perform by classical organic chemistry or result only in poor yields (Gupta et al. 2001; Deppenmeier et al. 2002). The most prominent utilization of the acetic acid bacterium is the oxidation of D-sorbitol to L-sorbose in the Reichstein-Grüssner synthesis of vitamin C. Further major biotechnological applications are: (i) synthesis of the tanning agent dihydroxyacetone via the oxidation of glycerol, (ii) production of 6-amino-L-sorbose from 1-amino-D-sorbitol as a key intermediate in miglitol (anti-diabetic drug) synthesis, and (iii) synthesis of shikimate and 3-dehydroshikimate from quinate (Deppenmeier et al. 2002; Gupta et al. 2001; Macauley et al. 2001; Raspor and Goranovič 2008; Adachi et al. 2003a; Nishikura-Imamura et al. 2014; Mamlouk and Gullo 2013; Pappenberger and Hohmann 2014; Saichana et al. 2015; Schedel 2000). *G. oxydans* whole cells as well as isolated enzymes have found use as biosensors for the analysis of alcohols, sugars or biological oxygen demand (Svitel et al. 2006). The potential of this bacterium for biotechnological applications is not yet exhausted, since genome sequencing revealed a great number of putative dehydrogenases/oxidoreductases of unknown functions (Prust et al. 2005).

2.3 Periplasmic sugar metabolism

Aerobic microorganisms usually oxidize energy sources to CO_2 and water. The generation of energy and precursors for biosynthesis occur during this process. An incomplete oxidation is carried out only under special environmental circumstances (Deppenmeier et al. 2002). Acetic acid bacteria like *G. oxydans* are distinguished by a rapid and incomplete oxidation of sugars and sugar alcohols. The periplasmic oxidation is of high importance for energy generation and carried out by a broad range of membrane-bound dehydrogenases. The resulting oxidation products accumulate near-quantitatively in the medium, often causing acidification of the medium (Olijve and Kok 1979b). Only a small percentage of the carbon source is taken up by the cells for biomass formation resulting in very low growth yields compared to other aerobic bacteria (Olijve and Kok 1979a; Hanke et al. 2013). For example *G. oxydans* strain IFO3293 achieves a value of 0.09 $g_{cdw}/g_{glucose}$, whereas *E. coli* reaches a cell yield of 0.49 $g_{cdw}/g_{glucose}$ and *Bacillus subtilis* of 0.32 $g_{cdw}/g_{glucose}$ (Olijve and Kok 1979a; Hanke et al. 2013; Krajewski et al. 2010; Dauner et al. 2002; Soini et al. 2008).

2.3.1 Mannitol metabolism

The sugar alcohol mannitol is known to be one of the preferred carbon source for biomass production of *G. oxydans* and therefore often used for growth characterization (Gossele et al. 1981). Figure 2 illustrates a scheme of the mannitol catabolism in *G. oxydans*. In growth phase I, mannitol is completely oxidized to fructose by the membrane-bound major polyol dehydrogenase SldAB (GOX0854, *sld*A and GOX0855, *sld*B) in the periplasm. Only a small

amount of the carbon source is taken up into the cytoplasm via a putative mannitol/sorbitol transporter (GOX2182-2185) (Prust et al. 2005). Although the presence of an NADP-dependent mannitol dehydrogenase converting mannitol to fructose was reported (Deppenmeier et al. 2002; Adachi 1999), there is recent evidence that intracellular mannitol is not oxidized. On the one hand mannitol was shown to serve as a compatible solute and on the other hand mannitol did not promote growth of a *sldAB* deletion mutant (Peters et al. 2013b; Zahid et al. 2015). In the second growth phase fructose is converted to 5-ketofructose, accompanied by a reduced growth rate in comparison to phase I. In *G. japonicus,* a membrane-bound fructose dehydrogenase was identified catalyzing this oxidation, however a gene encoding this enzyme is absent in *G. oxydans,* suggesting that an intracellular enzyme is responsible for 5-ketofructose synthesis (Kawai et al. 2013). Part of the fructose enters the cytoplasm via an unknown transporter, followed by the fructose kinase (GOX0284, *frkA*) mediated activation to fructose 6-phosphate. The precursor entering the pentose phosphate pathway (PPP) or the Embden-Meyerhof-Parnas (EDP) pathway is glucose 6-phosphate formed by the conversion of fructose 6-phosphate via glucose 6-phosphate isomerase (GOX1704, *pgi*).

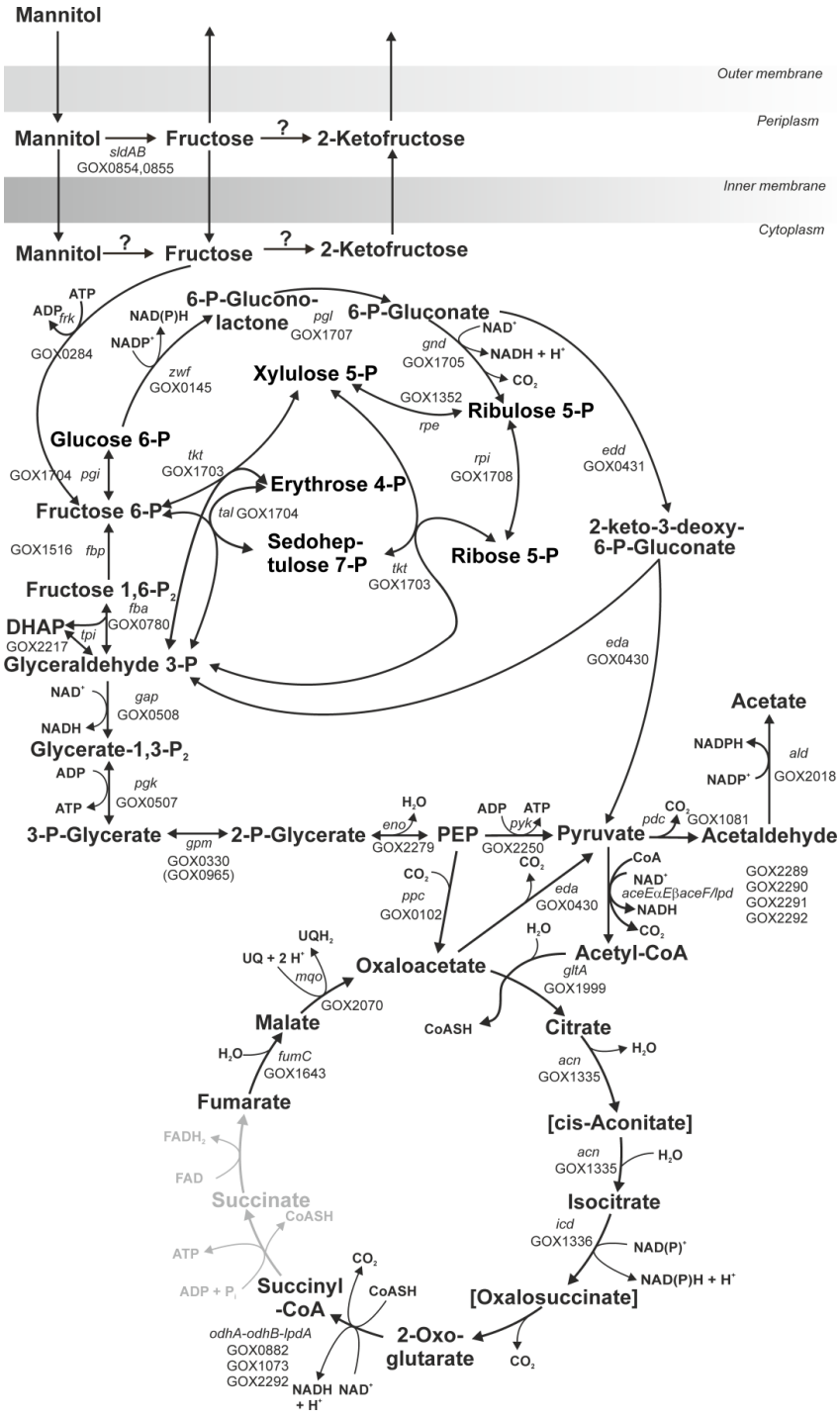

Fig. 2: Scheme of mannitol metabolism by *G. oxydans*.

2.3.2 Glucose metabolism

The glucose metabolism of *G. oxydans* is of great interest since glucose is a favorable carbon source in industry. Thus, in recent years studies were made concerning the growth behavior and physiology of this organism on glucose. An overview of the central carbon metabolism of *G. oxydans* on the substrate glucose is presented in Figure 3. Glucose catabolism in *G. oxydans* proceeds mainly via the PPP, while the EDP only plays a minor role (Richhardt et al. 2013a; Hanke et al. 2013). Growth on glucose is divided into two different metabolic phases, phase I and II. In phase I, the major amount of glucose, almost 90 %, is oxidized in the periplasm to gluconate by the PQQ-dependent membrane-bound glucose dehydrogenase (GOX0265, *gdhM*); consequently gluconate accumulates in the media. The remaining 10 % of glucose is taken up by the cells via an unknown transport system. The presence of an incomplete PEP: carbohydrate phosphotransferase system (PTS) lacking the EIIC and EIIB components suggests a regulatory function rather than a transporter function (Zhang et al. 2014). In the cytoplasm, glucose is mainly oxidized to gluconate by a soluble NADP-linked glucose dehydrogenase (GOX2015, *gdhS*). A small fraction of the intracellular glucose is phosphorylated to glucose-6-phosphate by glucokinase (GOX1182, *glk*A and GOX2419, *glk*B) and predominantly metabolized via the PPP. The first phase is characterized by high growth rates accompanied by high oxygen consumption and low CO_2 production (Levering et al. 1988; Pronk et al. 1989; Hanke et al. 2013; Prust et al. 2005; Olijve and Kok 1979a). At the start of the second growth phase glucose is almost completely oxidized to gluconate. Gluconate is then either taken up into the cells or periplasmatically converted to ketogluconates. During growth on glucose at pH values below 5, gluconate is mainly oxidized in the periplasm to 5-ketogluconate (5-KGA) by the membrane-bound PQQ-dependent sorbitol dehydrogenase (GOX0854-0855, *sldAB*) (Ano et al. 2011). At pH 6 gluconate is converted to 2-ketogluconate (2-KGA) by the membrane-bound flavoprotein gluconate-2-dehydrogenase (GOX1230-1232, *gndSLC*) (Weenk et al. 1984; Hölscher et al. 2009; Prust et al. 2005). Gluconate is taken up into the cytoplasm by a permease (GOX2188, *gntP*) and is either oxidized to 5-ketogluconate by an NADP-dependent gluconate-5 dehydrogenase (GOX2187, *gno*) or phosphorylated by gluconate kinase (GOX1709, *gntK*) to 6-phosphogluconate, which is catabolized via the PPP and the EDP (Pronk et al. 1989; Prust et al. 2005; Klasen et al. 1995; Hanke et al. 2013; Merfort et al. 2006 a). The second growth phase is accompanied by a reduced biomass formation, an increase of CO_2 formation and a reduced requirement for oxygen (Hanke et al. 2013).

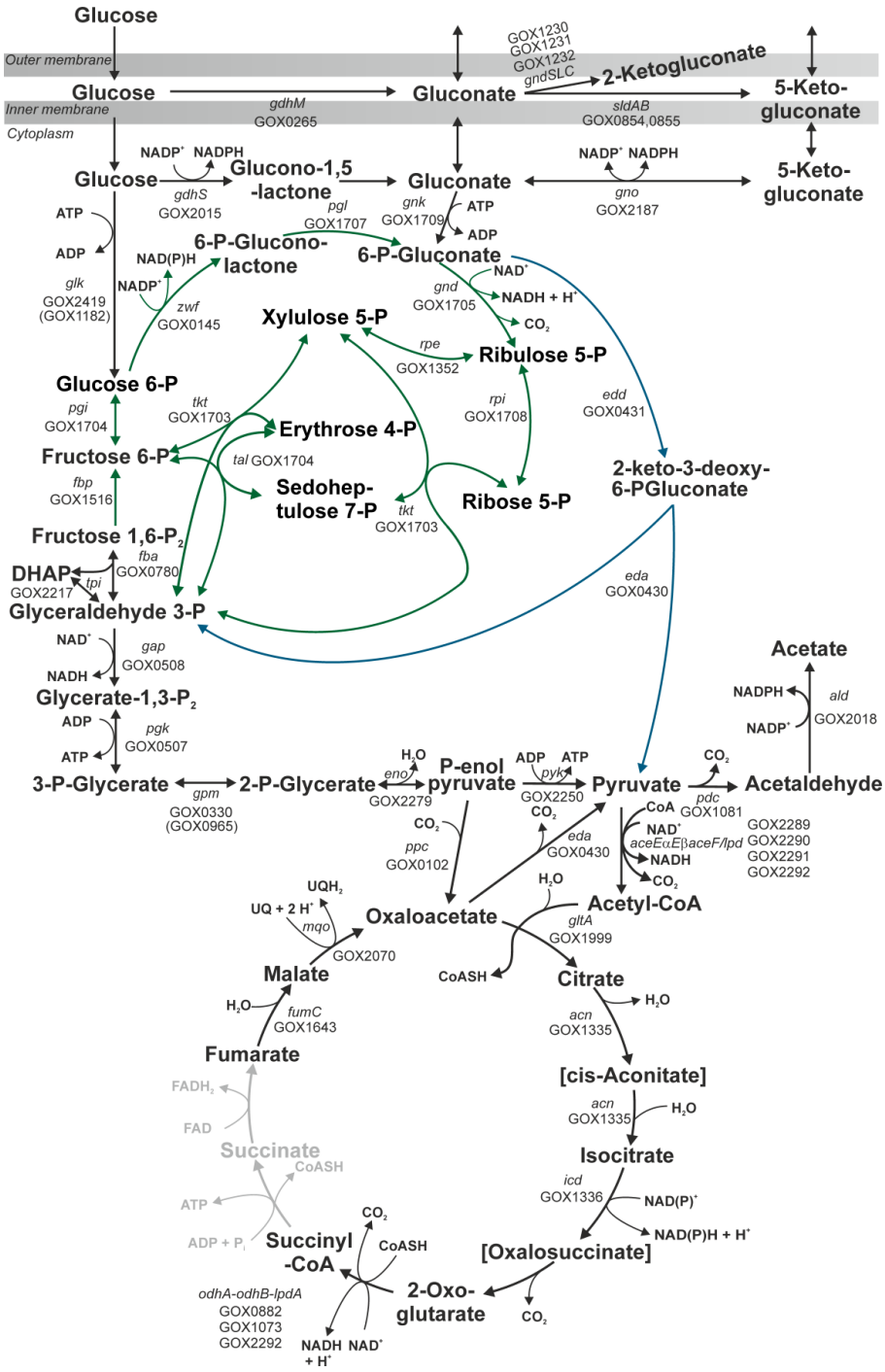

Fig. 3: Scheme of glucose metabolism by *G. oxydans.*

2.4 Cytoplasmic sugar metabolism

2.4.1 Pentose phosphate pathway and Enter-Doudoroff pathway

Genome annotation of *G. oxydans* revealed the presence of all genes for the oxidative pentose phosphate pathway (PPP) and the Entner-Doudoroff pathway (EDP). However, the Embden-Meyerhof-Parnas (EMP) pathway is non-functional due to the absence of a gene for phosphofructokinase and the TCA cycle is incomplete as it lacks the genes for succinyl-CoA synthetase and succinate dehydrogenase (Greenfield and Claus 1972; Prust et al. 2005). Consequently the PPP and EDP are the only pathways for intracellular sugar metabolism in *G. oxydans* sharing 6-phosphogluconate as the common substrate (Prust et al. 2005; Deppenmeier et al. 2002; Kersters and De Ley 1968). Part of the intracellular carbon source is converted to acetate accumulating in the medium. Acetate is produced by the decarboxylation of pyruvate to acetaldehyde via pyruvate decarboxylase (GOX1081, *pdc*) followed by the oxidation to acetate by NADP-dependent acetaldehyde dehydrogenases (GOX1122 and GOX 2018, *aldA* and *aldB*) (Krajewski et al. 2010; Peters et al. 2013a; Prust et al. 2005).

In 1955, the presence of all enzymes of the PPP was already demonstrated and genome annotation confirmed the existence of the corresponding genes (Prust et al. 2005; Hauge et al. 1955). Due to the absence of phosphofructokinase, the PPP proceeds cyclic (Hanke et al. 2013). Fructose 6-phosphate formed by either glucose 6-phosphate isomerase/transaldolase (GOX1704, *pgi*/*tal*) or transketolase (GOX1703, *tkt*) is converted to glucose 6-phosphate, entering the oxidative PPP again (Prust et al. 2005; Hanke et al. 2013; Siedler et al. 2012). Glucose 6-phosphate isomerase (Pgi) and transaldolase (Tal) form a bifunctional enzyme in *G. oxydans* (Sugiyama et al. 2003). The PPP key enzymes glucose 6-phosphate dehydrogenase (GOX0145, *zwf*) and 6-phosphogluconate dehydrogenase (GOX1705, *gnd*) were shown to have dual coenzyme specificities *in vitro* (Tonouchi et al. 2003). *In vivo*, these enzymes depend on $NADP^+$ and NAD^+, respectively (Rauch et al. 2010). The oxidative PPP represents the most important way for the phosphorylative degradation of sugars and polyols to CO_2 (Richhardt et al. 2012, 2013a; Hanke et al. 2013).

In 1968, it was shown that the EDP is active in *G. oxydans* (Kersters and De Ley 1968). In accordance, genome sequencing revealed the existence of the genes encoding the key enzymes 6-phosphogluconate dehydratase (GOX0431, *edd*) and 2-dehydro-3-deoxy-6-phosphogluconate (KDPG) aldolase (GOX0430, *eda*) (Prust et al. 2005). However, various experiments demonstrated that the EDP is less important than the PPP and even dispensable in *G. oxydans* (Hanke et al. 2013; Richhardt et al. 2012, 2013a). The PPP and EDP pathways differ with respect to energetic efficiency and formation of reduction equivalents. The cyclic PPP (1) yields 7 mol NAD(P)H and the EDP (2) only 2 mol NAD(P)H

when catabolizing 1 mol glucose 6-phosphate (Kruger and von Schaewen 2003).

1) 1 glucose 6-phosphate + 2 ADP + 7 NAD(P) + Pi → 1 pyruvate + 3 CO_2 + 7 NAD(P)H + 2 ATP
2) 1 glucose 6-phosphate + 2 ADP + 2 NAD(P) + Pi → 2 pyruvate + 2 NAD(P)H + 2 ATP

2.4.2 Incomplete pathways and consequences: Embden-Meyerhof-Parnas pathway and tricarboxylic acid cycle

2.4.2.1 Embden-Meyerhof Parnas pathway

The EMP pathway (glycolysis) is a central metabolic pathway of glucose degradation to pyruvate taking place in the cytosol. The complete pathway was elucidated in 1940 and consists of 10 reaction steps. As mentioned above, the EMP pathway in *G. oxydans* is non-functional due to the absence of a *pfk* gene (Prust et al. 2005) resulting only in the supply of precursor metabolites for biosynthesis. Pfk catalyzes the irreversible ATP-dependent phosphorylation of fructose 6-phosphate to fructose 1,6-bisphosphate. In *E. coli* it was shown that Pfk activity is allosterically stimulated by AMP and ADP and allosterically inhibited by phosphoenolpyruvate (PEP) and ATP (Lau and Fersht 1987; Blangy et al. 1968). Although Pfk is a key enzyme in the EMP pathway, it is lacking in many obligately aerobic organisms (Baart et al. 2010). Nevertheless, *G. oxydans* possesses the other 9 essential genes of the EMP pathway which are listed in Table 1.

2.4.2.2 The tricarboxylic acid cycle

The tricarboxylic acid (TCA) cycle is an ubiquitous metabolic pathway in aerobic organisms by which acetyl-CoA is completely decarboxylated to CO_2. The TCA cycle has two functions: first the generation of energy via the oxidation of acetyl-CoA to CO_2 under formation of NADH, NADPH and $FADH_2$ and second the supply of 2-oxoglutarate and oxaloacetate as precursors for biosynthesis of amino acids belonging to the glutamate and aspartate family. The TCA cycle is composed of eight enzymes, of which *G. oxydans* possesses only six (Table 1), resulting in an incomplete pathway only providing precursor metabolites for biosynthesis. Genome sequencing revealed a gene for a type II citrate synthase (GOX1999, *gltA*). *Acetobacter aceti* contains a citrate synthase (G-15977, *aarA*) which is insensitive to NADH (Duckworth et al. 2013). Based on a 73 % amino acid sequence identity of the citrate synthases from *A. aceti* and *G. oxydans*, an insensitivity to NADH of *G. oxydans* citrate synthase appears likely. Furthermore, genes coding for an

aconitase (GOX1335, *acn*) of family II, isocitrate dehydrogenase (GOX1336, *icd*), 2-oxoglutarate dehydrogenase (GOX0882, *odhA*; GOX1073, *odhB*; GOX2292, *lpdA*), a class II fumarase (GOX1643, *fumC*), and malate: quinone oxidoreductase (GOX2070, *mqo*) were identified. Genes coding for succinyl-CoA synthetase (*sucCD*) and succinate dehydrogenase (*sdh*) are absent in the genome of *G. oxydans* (Prust et al. 2005; Greenfield and Claus 1972). Based on the importance of the TCA cycle complementation via heterologous expression of *sucCD* and *sdh* genes in *G. oxydans* in the present work, the next two sections deal with a brief overview of succinyl-CoA synthetase (Scs) and succinate dehydrogenase (Sdh).

Table 1: Enzymes and genes of the EMP pathway and the TCA cycle present in *G. oxydans*

	Enzyme	GOX number
EMP pathway	Glucokinase	(GOX1182, *glkA*)*, GOX2419 (*glkB*)
	Glucose-6-phosphate isomerase	GOX1704 (*pgi*)
	Fructose-bisphosphate aldolase	GOX0780 (*fba*)
	Triosephosphate isomerase	GOX2217, (GOX2284)* (*tpi*)
	Glyceraldehyde 3-phosphate dehydrogenase	GOX0508 (*gap*)
	Phosphoglycerate kinase	GOX0507 (*pgk*)
	Phosphoglycerate mutase	GOX0330, (GOX0965)* (*gpm*)
	Enolase	GOX2279 (*eno*)
	Pyruvate kinase	GOX2250 (*pyk*)
TCA cycle	Citrate synthase	GOX1999 (*gltA*)
	Aconitase	GOX1335 (*acn*)
	Isocitrate dehydrogenase	GOX1336 (*icd*)
	2-Oxoglutarate dehydrogenase	GOX0882 (*odhA*) GOX1073 (*odhB*) GOX2292 (*lpdA*)
	Fumarase	GOX1643 (*fumC*)
	Malate: quinone oxidoreductase	GOX2070 (*mqo*)

* Brackets symbolize genes probably encoding the corresponding enzyme.

2.4.2.2.1 Succinyl-CoA synthetase

Succinyl-CoA synthetase (Scs) occurs in prokaryotes as well as in eukaryotes. The enzyme catalyzes the only substrate-level phosphorylation in the TCA cycle (Bridger 1974; Nishimura 1986). Thereby, succinyl-CoA conversion to succinate leads to nucleoside

triphosphate formation during aerobic metabolism. The reaction of succinyl-CoA synthetase is reversible and particularly during anaerobic growth, succinyl-CoA is provided for ketone catabolism and heme biosynthesis (Park et al. 1997). Scs consists of α (SucD) and β (SucC) subunits. Gram-positive bacteria and higher organisms possess αβ-heterodimers, whereas $(\alpha\beta)_2$-tetramers usually occur in Gram-negative bacteria (Bridger 1971; Wolodko et al. 1986). The nucleotide specificity of Scs differs; Gram-negative bacteria like *E. coli* tend to use ATP and GTP as coenzymes, with a preference for ATP. In eukaryotes, such as *Saccharomyces cerevisiae,* the enzyme is only specific for ATP (Bridger 1974; Przybyla-Zawislak et al. 1998). The CoA binds to the α-subunit of the enzyme, comprising the active reaction site with a conserved histidine residue which is transiently phosphorylated during enzymatic catalysis. Substitution of the histidine residue by another amino acid yields an inactive enzyme (Bridger 1974; Wolodko et al. 1986; Majumdar et al. 1991). The β-subunit represents the nucleotide binding site and determines the nucleotide specificity (Johnson et al. 1998; Joyce et al. 1999).

2.4.2.2.1 Succinate dehydrogenase

Succinate dehydrogenase (Sdh) is found in aerobic organisms and is part of the TCA cycle. Additionally the enzyme represents complex II of the respiratory chain and is therefore also called succinate:quinone oxidoreductase (Sqr). Sdh catalyzes the oxidation of succinate to fumarate in the TCA cycle and the reduction of ubiquinone in the membrane. The enzyme is decisive for intermediary metabolism as well as energy production in bacteria and eukaryotes under aerobic conditions (Hägerhäll 1997; Hederstedt 2003). Many bacterial and eukaryotic Sdhs consist of two hydrophilic subunits, a flavoprotein (SdhA) and iron-sulfur protein (SdhB) and two hydrophobic membrane-anchored subunits SdhC and SdhD, containing a heme *b* and the binding site for ubiquinone (Fig. 4). However, most Gram-positive bacteria possess only three subunits due to an apparent fusion of subunit C and D to a single membrane-anchored polypeptide (Hederstedt 2003; Hägerhäll and Hederstedt 1996; Hederstedt 1999; Lancaster et al. 1999).

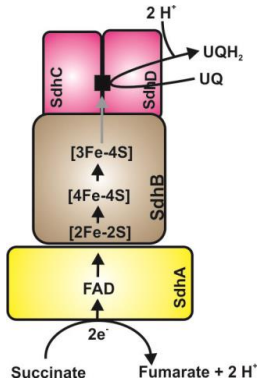

Fig. 4: Scheme of the succinate dehydrogenase (Sdh) of *E. coli*. Flavoprotein subunit SdhA, iron-sulfur subunit SdhB, cytochrome b subunit SdhC and membrane anchor subunit SdhD.

According to Hägerhäll, Sqrs can be divided into three functional classes due to the quinone substrate and *in vivo* function of the enzyme. Class I Sqrs catalyze the oxidation of succinate and the reduction of a high potential quinone like ubiquinone. Enzymes of class I are common and are found in mammalian mitochondria and many pro- and eukaryotes. All quinol:fumarate reductases (Qfr) so far investigated belong to class II, as they oxidize a low potential quinol such as menaquinol and reduce fumarate. Class III Sqrs are found in Gram-positive bacteria and archaebacteria. This class of enzyme catalyzes the oxidation of succinate and the reduction of a low potential quinone like menaquinone (Hägerhäll 1997).

2.5 Respiratory chain of *G. oxydans*

A characteristic feature of *G. oxydans* is the large and diverse number of membrane-bound dehydrogenases transferring electrons directly to ubiquinone of the respiratory chain (Prust et al. 2005). PQQ, FAD as well as heme *c* serve as cofactors of the dehydrogenases (Shinagawa et al. 1990; Matsushita et al. 2003; Matsushita et al. 1994). Figure 5 shows a scheme of the core components of the respiratory chain of *G. oxydans*. The organism *G. oxydans* possesses a type II monomeric non-proton-pumping NADH dehydrogenase (*ndh*) transferring electrons from NADH to the ubiquinone pool, whereas a proton-translocating NADH:ubiquinone oxidoreductase (complex I) is absent (Prust et al. 2005). From the ubiquinone pool onwards, the respiratory chain of *G. oxydans* is branched due to two terminal ubiquinol oxidases, cytochrome bo_3 oxidase and cytochrome *bd* oxidase. Based on the cyanide insensitivity of *G. oxydans* cytochrome *bd*, Matsushita and coworkers designated this enzyme as cyanide-insensitive oxidase CIO and the corresponding genes *cioA* and *cioB* instead of *cydA* and *cydB* (Mogi et al. 2009; Miura et al. 2013). The two terminal oxidases catalyze the transfer of the electrons from ubiquinol to molecular oxygen

(Matsushita et al. 1987; Matsushita et al. 1989; Prust et al. 2005; Ameyama et al. 1987; Miura et al. 2013). The bo_3 oxidase is encoded by the *cyoBACD* genes (GOX1911-1914) and belongs to the superfamily of heme-copper oxygen reductases, with heme *b*, heme *o* and a copper ion as cofactors (Matsushita et al. 1987; Prust et al. 2005). The reaction catalyzed by bo_3 oxidase participates in the generation of proton motive force in two ways. On the one hand via the oxidation of ubiquinol at the periplasmic site of the membrane, with the release of protons from the cytoplasm in the periplasm and the transfer of electrons to the o_3-Cu center. On the other hand proton motive force is established by using free energy associated with electron transfer from ubiquinol to dioxygen for proton-pumping across the membrane (Puustinen et al. 1989; Verkhovskaya et al. 1997). It is assumed that cytochrome bo_3 oxidase is the main component for proton extrusion via the respiratory chain (Richhardt et al. 2013b). The cyanide-insensitive oxidase CIO possesses heme b_{558}, b_{595} and heme *d* as prosthetic groups (Prust et al. 2005; Mogi et al. 2009; Miura et al. 2013). In contrast to bo_3 oxidase, the CIO is non-proton pumping and generates proton motive force only by ubiquinol oxidation at the periplasmic site (Miller and Gennis 1985). The level of CIO increases by a pH change from 6 to 4, suggesting an impact at low pH values (Matsushita et al. 1989; Hanke et al. 2012). In *E. coli* it was demonstrated that the bo_3 oxidase is synthetized maximally under high oxygen conditions, whereas *bd* oxidase is predominantly abundant under microaerobic conditions (D'mello et al. 1996; Georgiou et al. 1988). In *G. oxydans* bo_3 oxidase possesses a high oxygen affinity contrary to CIO exhibiting a low oxygen affinity. However, the K_M value for oxygen of *G. oxydans* CIO is 10-fold higher than the one for *bd* oxidase of *E. coli* (Richhardt et al. 2013b; Miura et al. 2013). Interestingly, *G. oxydans* also possesses genes encoding a cytochrome bc_1 complex (GOX0565-0567), containing a heme *c*, two heme *b* and one [Fe-S]-cluster as prosthetic groups. Furthermore, genome sequencing revealed a gene for a soluble cytochrome c_{552} (GOX0258). However, genes for subunits I, II and III of cytochrome *c* oxidase are absent in the genome of *G. oxydans,* raising the question of the function of the cytochrome bc_1 complex, because reduced cytochrome c_{552} cannot be reoxidized by complex IV (Prust et al. 2005; Matsutani et al. 2014; Hanke et al. 2012). The electron transport chain builds up an electrochemical proton gradient which is used to generate ATP via two F_1F_0-type ATP synthases. The corresponding genes are organized in three clusters located at different positions on the chromosome. The hydrophobic membrane-bound subunits of the first ATP-synthase are encoded by cluster I (GOX1110-1113), whereas cluster II (GOX1310-1314) encodes the hydrophilic enzyme part. The H^+-dependent ATP synthase represents an ortholog of the ATP synthases of *Acetobacter pasteurianus* IFO 3283-01, *Gluconacetobacter diazotrophicus* PAl 5 and other α-proteobacteria. Custer III (GOX2167-2175) encodes the second ATP synthase, which might use sodium as coupling ion (Prust et al. 2005; Hanke et al. 2012; Dibrova et al. 2010).

Since *G. oxydans* produces NADPH via the PPP by glucose 6-phosphate dehydrogenase (GOX0145, *zwf*) as well as via the incomplete cytoplasmic oxidations by the soluble NADP-linked glucose dehydrogenase (GOX2015, *gdhS*) and gluconate-5 dehydrogenase (GOX2187, *gno*), it is assumed that the organism generates NADPH efficiently; NADP regeneration however is likely to be problematic. Genome annotation of *G. oxydans* revealed genes for a proton-translocating nicotinamide adenine dinucleotide transhydrogenase (GOX0310-0312, *pntA1A2B*) (Prust et al. 2005). In bacteria and many animal mitochondria, the reversible hydride transfer between NADPH + H^+ and NAD^+ is coupled by such transhydrogenases to translocate protons across the membrane (Cotton et al. 2001; Bizouarn et al. 2002). Thus, transhydrogenase is probably involved in (i) regeneration of NADP and (ii) the translocation of protons from the cytoplasm in the periplasm, thereby participating in the formation of the electrochemical proton gradient (Deppenmeier and Ehrenreich 2009; Prust et al. 2005).

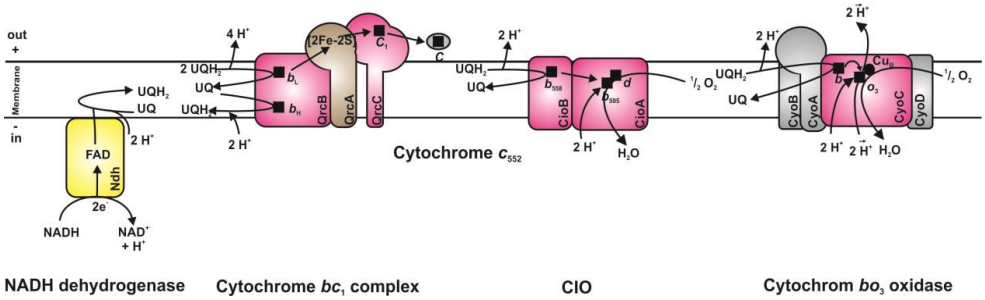

Fig. 5: Scheme of the core components of the respiratory chain of *G oxydans*.

2.6 Aims of this thesis

The biotechnological interest in *G. oxydans* is mainly based on the rapid and incomplete oxidation of sugars and sugar alcohols in the periplasm by various membrane-integral dehydrogenases. Caused by the periplasmic oxidation of the major part of the carbon source and the incompleteness of the TCA cycle, biomass formation and cell yields of *G. oxydans* are very low, leading to increased costs of biotechnological processes with this species. In this work, the main focus is the optimization of biomass production leading to increased cell yields of *G. oxydans* on the favorable substrate glucose, thereby decreasing the costs for biomass synthesis and improving/enabling industrial applications. To this end, prevention of glucose oxidation to gluconate by deletion of genes encoding the membrane-bound dehydrogenase (GOX0265, *gdhM*) and the cytosolic glucose dehydrogenase (GOX2015, *gdhS*) is necessary. Glucose uptake should be improved by the heterologous expression of

the glucose facilitator gene (*glf*). Through the heterologous expression of a phosphofructokinase gene (*pfkA*), intracellular glucose degradation via the EMP pathway should be enabled, thereby avoiding carbon loss through usage of the PPP or the EDP. Furthermore, the pyruvate decarboxylase gene (GOX1081, *pdc*) should be deleted to prevent acetaldehyde formation and consequently acetate production. Additionally, the overexpression of the homologous pyruvate dehydrogenase complex genes (GOX2289, *aceE*α; GOX2290, *aceE*β; GOX2291, *aceF*; GOX2292, *lpd*) should allow increased rates of oxidative decarboxylation of pyruvate to acetyl-CoA. Through the genomic integration of heterologous genes encoding succinyl-CoA synthetase (*sucCD*) and succinate dehydrogenase (*sdhCDABE*) a complete oxidation of acetyl-CoA via the TCA cycle should be enabled. As complete glucose oxidation via glycolysis and the TCA cycle leads to an increased NADH formation rate and the necessity for increased NADH reoxidation rates, a second *ndh* gene coding for NADH dehydrogenase should be integrated into the genome of *G. oxydans*. The metabolically engineered strains should be characterized with respect to their growth behavior, substrate consumption, product formation, and the activities of the enzymes encoded by the genomically integrated or plasmid-based homologous and heterologous genes. Furthermore, the activities of the TCA cycle enzymes already present in the parent strain should be measured to determine possible carbon flux limitations in the TCA cycle that need to be removed.

3. Results

Gluconobacter oxydans is an acetic acid bacterium that is used industrially in oxidative biotransformations due to its exceptional capability for regio- and stereoseletive oxidations of a variety of carbohydrates in the periplasm. The incomplete periplasmic oxidations and a restricted cytoplasmic catabolism caused by the absence of a functional glycolysis and tricarboxylic acid cycle lead to a very low cell yield that increases the costs for biomass production. This thesis aimed at an increased cell yield from glucose by metabolic engineering of *G. oxydans* 621H.

The publication “SdhE-dependent formation of a functional *Acetobacter pasteurianus* succinate dehydrogenase in *Gluconobacter oxydans* - a first step toward a complete tricarboxylic acid cycle“ (Applied Microbiology and Biotechnology, vol. 99, pp. 9147–9160) describes the successful plasmid-based synthesis of a heterologous succinate dehydrogenase in *G. oxydans*. The work revealed the necessity and sufficiency of the accessory protein SdhE for synthesis of an active *A. pasteurianus* Sdh in *G. oxydans*. Furthermore, it was demonstrated that the γ-proteobacterial *Serratia* SdhE protein is able to activate an α-proteobacterial *A. pasteurianus* Sdh in *G. oxydans*.

In the second manuscript “Metabolic engineering of *Gluconobacter oxydans* 621H for improved growth yield on glucose by prevention of gluconate and acetate formation and completion of the tricarboxylic acid cycle” a series of *G. oxydans* strains were constructed by chromosomal integration of genes for succinate dehydrogenase, succinyl-CoA synthetase, and a second NADH dehydrogenase with simultaneous deletion of the genes for periplasmic and cytoplasmic glucose dehydrogenase and pyruvate decarboxylase. The strains were characterized with respect to growth, substrate consumption, product formation, and enzyme activities. The final strain IK003.1 showed a 60 % improved cell yield.

The third manuscript entitled “Impact of plasmid-based expression of functions for glucose uptake and phosphorylation, glycolysis, and pyruvate oxidation to acetyl-CoA on growth of *Gluconobacter oxydans* IK003.1” describes studies aimed at a further improvement of the growth properties and the cell yield of strain IK003.1 by plasmid-based expression of genes for a glucose facilitator and glucokinase, phosphofructokinase, and the pyruvate dehydrogenase complex. Despite the functional synthesis of pyruvate dehydrogenase complex and phosphofructokinase, neither growth nor the cell yield of the recombinant *G. oxydans* strains could be enhanced.

3.1 Insertion of a functional succinate dehydrogenase in *G. oxydans*

Own contribution to this publication: about 70 %. I performed all experimental work described in the publication and wrote a draft of the manuscript. I am first author of the publication.

Published in Applied Microbiology and Biotechnology; DOI 10.1007/s00253-015-6972-8

Impact factor: 3.337

SdhE-dependent formation of a functional *Acetobacter pasteurianus* succinate dehydrogenase in *Gluconobacter oxydans*—a first step toward a complete tricarboxylic acid cycle

Ines Kiefler[1,2] · **Stephanie Bringer**[1,2] · **Michael Bott**[1,2]

Received: 21 July 2015 / Revised: 17 August 2015 / Accepted: 27 August 2015 / Published online: 23 September 2015

Abstract The obligatory aerobic α-proteobacterium *Gluconobacter oxydans* 621H possesses an unusual metabolism in which the majority of the carbohydrate substrates are incompletely oxidized in the periplasm and only a small fraction is metabolized in the cytoplasm. The cytoplasmic oxidation capabilities are limited due to an incomplete tricarboxylic acid (TCA) cycle caused by the lack of succinate dehydrogenase (Sdh) and succinyl-CoA synthetase. As a first step to test the consequences of a functional TCA cycle for growth, metabolism, and bioenergetics of *G. oxydans*, we attempted to establish a heterologous Sdh in this species. Expression of *Acetobacter pasteurianus sdhCDAB* in *G. oxydans* did not yield an active succinate dehydrogenase. Co-expression of a putative *sdhE* gene from *A. pasteurianus*, which was assumed to encode an assembly factor for covalent attachment of flavin adenine dinucleotide (FAD) to SdhA, stimulated Sdh activity up to 400-fold to 4.0 ± 0.4 U (mg membrane protein)$^{-1}$. The succinate/oxygen reductase activity of membranes was 0.68 ± 0.04 U (mg membrane protein)$^{-1}$, indicating the formation of functional Sdh complex capable of transferring electrons from succinate to ubiquinone. *A. pasteurianus* SdhE could be functionally replaced by SdhE from the γ-proteobacterium *Serratia* sp. According to these results, the accessory protein SdhE was necessary and sufficient for heterologous synthesis of an active *A. pasteurianus* Sdh in *G. oxydans*. Studies with the Sdh-positive *G. oxydans* strain provided evidence for a limited functionality of the TCA cycle despite the absence of succinyl-CoA synthetase.

Keywords *Gluconobacter oxydans* · Citrate cycle · Succinate dehydrogenase

✉ Stephanie Bringer
st.bringer-meyer@fz-juelich.de

✉ Michael Bott
m.bott@fz-juelich.de

[1] Institute of Bio- and Geosciences, IBG-1: Biotechnology, Forschungszentrum Jülich, 52425 Jülich, Germany

[2] The Bioeconomy Science Center (BioSC), c/o Forschungszentrum Jülich, 52425 Jülich, Germany

Introduction

Gluconobacter oxydans is an α-proteobacterial species that is exceptionally suited for oxidative biotransformations due to its many membrane-bound dehydrogenases, which oxidize a large variety of substrates in the periplasm regio- and stereoselectively. It is used industrially for several purposes, the most prominent being vitamin C production (Deppenmeier et al. 2002; Adachi et al. 2003; Pappenberger and Hohmann 2014; Gupta et al. 2001; Macauley et al. 2001; Raspor and Goranovič 2008). A handicap for a broader use of *G. oxydans* is its low biomass yield, which is caused by a number of metabolic peculiarities. The carbohydrates serving as energy and carbon sources are incompletely oxidized in the periplasm, leading to partially oxidized products that remain unmetabolized in the medium. For example, glucose is oxidized to about 90 % in the periplasm to the end products gluconate and ketogluconate and less than 10 % is metabolized in the cytoplasm (Hanke et al. 2013). Similarly, mannitol is periplasmatically oxidized to fructose and 5-ketofructose (Richhardt et al. 2012). The cytoplasmic oxidation capabilities are restricted because several enzymes of central metabolic pathways are absent. *G. oxydans* 621H is deficient in glycolysis due to the absence of a gene for phosphofructokinase and a functional tricarboxylic acid (TCA) cycle due to the absence of genes for Sdh and succinyl-CoA synthetase (Prust et al.

2005). Sugars and sugar alcohols are metabolized primarily via the pentose phosphate pathway (PPP), which runs partially cyclic, and to some extent by the Entner–Doudoroff pathway (Hanke et al. 2013). Due to the incomplete TCA cycle, pyruvate cannot be oxidized completely via this pathway. Instead, a significant fraction of pyruvate is converted to acetate by the action of pyruvate decarboxylase and acetaldehyde dehydrogenase (Krajewski et al. 2010).

In order to elucidate the impact on bioenergetics and in particular on the biomass yield, we initiated studies to redirect glucose oxidation from the periplasm to the cytoplasm and allow a complete cytoplasmic oxidation of pyruvate by restoring glycolysis and the TCA cycle. As a first step in this direction, we attempted to introduce a heterologous Sdh complex (EC 1.3.5.1), also known as complex II or succinate/quinone oxidoreductase. The rationale for choosing this starting point was that the risk of failure was considered as particularly high, as Sdh is a membrane protein complex composed of at least three subunits containing a covalently linked flavin adenine dinucleotide (FAD) prosthetic group in the flavoprotein subunit SdhA, three iron–sulfur clusters in the iron–sulfur protein subunit SdhB, and a cytochrome *b* in subunit(s) C or C and D. Thus, formation of an active heterologous Sdh enzyme presumably requires additional proteins besides the Sdh structural proteins. Using genes from *Acetobacter pasteurianus*, we were able to functionally synthesize a heterologous Sdh complex in *G. oxydans*.

Materials and methods

Materials

Chemicals were obtained from Sigma-Aldrich (Taufkirchen, Germany), Qiagen (Hilden, Germany), Merck (Darmstadt, Germany), and Roche Diagnostics (Mannheim, Germany).

Bacterial strains, plasmids, media, and growth conditions

Genomic DNA of *Serratia* sp. ATCC39006 was purchased from LGC Standards, Wesel, Germany. The bacterial strains and plasmids used in this study are listed in Table 1. The *Escherichia coli* strains were cultivated in lysogeny broth (LB) medium or on LB agar plates at 37 °C (Bertani 1951, 2004). When required, kanamycin was added to a final concentration of 50 μg mL^{-1}. *Corynebacterium glutamicum* ATCC13032 was precultured in brain heart infusion medium (BHI, Difco, Detroit, USA) overnight at 30 °C and 120 rpm. Main cultures were grown in CGXII minimal medium containing 30 μg protocatechuic acid L^{-1} (Keilhauer et al. 1993) with 4 % (*w*/*v*) glucose. *A. pasteurianus* (DSM3509 = NBRC3191) was precultured in 20 mL tomato juice medium (Chen et al. 2011) in 100 mL baffled shaking flasks at 30 °C and 140 rpm. Main cultures were grown in basic medium (Chen et al. 2011) containing 10 g L^{-1} yeast extract, 10 g L^{-1} peptone, 2 g L^{-1} K_2HPO_4, and 10 g L^{-1} glucose supplemented with 4 % ethanol at 30 °C and 140 rpm. Genomic data were taken from the genome sequence of *A. pasteurianus* IFO 3283_01 (Azuma et al. 2009). *G. oxydans* ATCC 621H Δ*upp* (ATCC 621H is identical to DSM2343), which lacks the *upp* gene for uracil phosphoribosyltransferase (Peters et al. 2013), was obtained from Dr. Armin Ehrenreich (Technical University of Munich, Germany). This strain was used as reference strain and will be referred to as *G. oxydans* in the following text. The strain was cultivated on mannitol medium containing 220 mM (4 % *w*/*v*) mannitol, 5 g L^{-1} yeast extract, 2.5 g L^{-1} $MgSO_4 \times 7\ H_2O$, 1 g L^{-1} $(NH_4)_2SO_4$, 1 g L^{-1} KH_2PO_4, and 10 μM thymidine. The initial pH value of the medium was 6.0. *G. oxydans* possesses a natural resistance toward cefoxitin; as a precaution to prevent bacterial contaminations, cefoxitin was added to the media at a concentration of 50 μg mL^{-1}. When required for plasmid maintenance, 50 μg mL^{-1} kanamycin was added. Precultures were grown in baffled shaking flasks at 30 °C and 140 rpm. Main cultures were grown in 500 mL baffled shaking flasks containing 100 mL mannitol medium. Incubation was at 140 rpm and 30 °C in an Infors shaker (Basel, Switzerland).

Cultivations under controlled conditions of pH and oxygen were performed in 250 mL mannitol medium using a bioreactor system (DASGIP, Jülich, Germany) composed of four 400-mL vessels, each equipped with electrodes for measuring the dissolved oxygen concentration (DO) and the pH. The system allows to constantly control these two parameters. The carbon dioxide concentration in the exhaust gas was measured continuously by an infrared spectrometer and the oxygen concentration by a zirconium dioxide sensor. The pH was kept at pH 6.0 by automatic titration of 2 M NaOH and 2 M HCl. The oxygen availability was kept constant at 15 % DO by mixing air, O_2, and N_2. Calibration was performed by gassing with air (100 % DO) and N_2 (0 % DO). The agitation speed was kept constant at 900 rpm. Control and recording of all data was carried out by the software "Fedbatch Pro" (DASGIP, Jülich, Germany).

Cloning and DNA techniques

DNA manipulation was performed by standard methods as described by Sambrook and Russel (Sambrook and Russell 2001). Competent cells of *E. coli* were prepared with $CaCl_2$ and transformed as described by Hanahan (Hanahan et al. 1991). DNA sequencing was performed by Eurofins MWG Operon (Ebersberg, Germany). Oligonucleotides were synthesized by Biolegio (Nijmegen, Netherlands) and are listed in Table 1.

Table 1 Bacterial strains, plasmids, and oligonucleotides used in this work

Strain or plasmid or oligonucleotide	Description or primer sequence (5′ → 3′)	Source, reference, or restriction site
Strain		
E. coli TOP10	F *mcr*A Δ(*mrr*-*hsd*RMS-*mcr*BC) Φ80*lac*ZΔM15 Δ*lac*X74 *rec*A1 *ara*D139 Δ(*ara leu*) 7697 *gal*U *gal*K *rps*L (StrR) *end*A1 *nup*G	Invitrogen, Darmstadt, Germany
E. coli S17-1	Δ*rec*A, *end*A1, *hsd*R17, *sup*E44, *thi*-1, *tra*$^{+}$	Simon et al. 1983
G. oxydans Δ*upp*	*G. oxydans* 621H derivative with a deletion of GOX0327 coding for uracil phosphoribosyl-transferase	Peters et al. 2013
C. glutamicum ATCC1302	ATCC1302, wild-type strain	American Type Culture Collection
A. pasteurianus DSM3509	DSM3509, wild-type strain	DSMZ - Deutsche Sammlung von Mikroorganismen und Zellkulturen GmbH, Germany
Plasmid		
pBBR1p384	Kan^{R}; pBBR1MCS-2 derivative containing the 5′-UTR of GOX0384	U. Deppenmeier (Bonn University); (Kovach et al. 1995)
pBBR1p384-sdh	Kan^{R}; pBBR1p384-derivative expressing *sdhCDAB* (APA01_00310–00,340) from *A. pasteurianus*	This work
pBBR1p384-sdh-sdhE$_{Ace}$	Kan^{R}; pBBR1p384-derivative expressing *sdhCDAB* (APA01_00310–00,340) and *sdhE* (APA01_11050) from *A. pasteurianus*	This work
pBBR1p384-sdh-p$_{nat}$-sdhE$_{Ace}$	Kan^{R}; pBBR1p384-derivative expressing *sdhCDAB* (APA01_00310–00,340) and 5′-UTR *sdhE* (APA01_11050) from *A. pasteurianus*	This work
pBBR1p384-sdh-p$_{nat}$-sdhE$_{Ser}$	Kan^{R}; pBBR1p384-derivative expressing *sdhCDAB* (APA01_00310–00,340) and 5′-UTR *sdhE* (Ser39006_1161) from *Serratia* sp. ATCC39006	This work
Oligonucleotide		
sdh_forw_*Hin*dIII	GTATATAAGCTTGACGGGGTACGA GGCAGACA	*Hin*dIII
sdh_rev_*Cla*I	GCGCGCATCGATTCTTCGCTTGGG TTACAAAA	*Cla*I
p384_seq_forw	AAGACGCAGCGGAATGAGAG	
p384_seq_rev	CTTCCGGCTCGTATGTTGTG	
pnat11050_forw_*Sal*I	CGAATTGTCGACCAGCCTGCGGT CTGTAATGC	*Sal*I
11050_rev_*Xho*I	GCGTAACTCGAGCTGTGCTGTCA TCCCGGTAT	*Xho*I
11050_forw_*Xho*I	CTATATCTCGAGCGGTATAGGATA CCAGCGCC	*Xho*I
11050_rev_*Apa*I	CTATATGGGCCCCTGTGCTGTCAT CCCGGTAT	*Apa*I
pnat1161-forw-*Xho*I	CAATTTCTCGAGGCTTTAAGCGA ATGACTTCA	*Xho*I
1161-rev-*Kpn*I	CTATATGGTACCAATGTCACCAGC CCCAGCCA	*Kpn*I

Plasmid-based expression of *sdhCDAB* and *sdhE*

For expression of the *sdh* genes of *A. pasteurianus* in *G. oxydans*, the broad-host-range plasmid pBBR1p384 (Kallnik et al. 2010) was used. The genes *sdhCDAB* (APA01_00310-00340) were amplified from genomic DNA of *A. pasteurianus* using the oligonucleotides sdh_forw_*Hin*dIII and sdh_rev_*Cla*I and Phusion DNA polymerase (Finnzymes, Thermo Scientific, Vantaa, Finland). The 3763 bp PCR product was phosphorylated with T4 polynucleotide kinase and cloned into dephosphorylated *Sma*I-restricted pUC18. From one of the recombinant clones giving a 3.76-kbp product after colony PCR with sdh_forw_*Hin*dIII/sdh_rev_*Cla*I, pUC18-sdh was isolated. The *sdhCDAB* insert was excised with *Cla*I and *Hin*dIII and subsequently cloned with a 20-bp 5′ UTR containing the 5′-ACGAGG-3′ ribosome binding site into the *Cla*I/*Hin*dIII-linearized vector pBBR1p384. After verification of positive clones by colony PCR with oligonucleotides p384_seq_forw and p384_seq_rev, the *sdh* genes of the resulting plasmid pBBR1p384-sdh were sequenced in order to exclude unwanted mutations. Subsequently, pBBR1p384-sdh was transferred by conjugation into *G. oxydans* using *E. coli* S17-1 as donor (Richhardt et al. 2012). Positive clones were selected by their kanamycin resistance.

For construction of the expression plasmids pBBR1p384-sdh-sdhE$_{Ace}$ and pBBR1p384-sdh-p$_{nat}$-sdhE$_{Ace}$, the putative *sdhE* gene (APA01_11050) of *A. pasteurianus* was amplified by PCR with Phusion DNA polymerase from genomic DNA either without its putative promoter using oligonucleotides 11050_forw_*Xho*I and 11050_rev_*Apa*I or with its assumed native promoter using oligonucleotides pnat11050_forw_*Sal*I and 11050_rev_*Xho*I. The 464-bp PCR product without promoter was digested with *Apa*I/*Xho*I and cloned into pBBR1p384-sdh restricted with *Apa*I and *Xho*I. The 714-bp PCR product including the putative native promoter was cut with *Sal*I/*Xho*I and cloned into pBBR1p384-sdh cut with *Sal*I and *Xho*I. Construction of plasmid pBBR1p384-sdh-p$_{nat}$-sdhE$_{Ser}$ carrying the *sdhE* gene (Ser39006_1161) of *Serratia* sp. ATCC39006 with its assumed native promoter was performed analogously using oligonucleotides pnat1161-forw-*Xho*I/1161-rev-*Kpn*I. The 664-bp PCR product was cut with *Kpn*I/*Xho*I and cloned into pBBR1p384-sdh cut with *Kpn*I/*Xho*I. The resulting plasmids pBBR1p384-sdh-sdhE$_{Ace}$, pBBR1p384-sdh-p$_{nat}$-sdhE$_{Ace}$, and pBBR1p384-sdh-p$_{nat}$-sdhE$_{Ser}$ were transferred by conjugation into *G. oxydans* as described previously (Richhardt et al. 2012). Positive clones were selected by their kanamycin resistance.

Membrane isolation for Sdh assay

For membrane preparation, *G. oxydans* cells were cultivated in 500 mL mannitol medium and *C. glutamicum* cells in 500 mL CGXII minimal medium with 4 % (*w*/*v*) glucose at 30 °C and 100 rpm (Infors shaker, Basel, Switzerland). *A. pasteurianus* was cultivated in 500 mL basic medium (Chen et al. 2011) supplemented with 4 % (*v*/*v*) ethanol at 30 °C and 100 rpm. After 16 h *G. oxydans* (OD_{600} 1.5–3.2) and *A. pasteurianus* (OD_{600} 1.2–1.5) cells were harvested by centrifugation (20 min, ~6500×*g*, 4 °C). *C. glutamicum* cells were harvested in the exponential growth phase at an OD_{600} of 5. Subsequently, the cells were washed with 25 mL 100 mM potassium phosphate buffer pH 7.5 and centrifuged for 5 min at ~10,500×*g*, 4 °C. The cells were resuspended in 10 mL of the same buffer supplemented with Complete Protease Inhibitor Cocktail (Invitrogen, Darmstadt, Germany). *C. glutamicum* cell suspensions were additionally incubated for 30 min at 37 °C with lysozyme (10 mg mL^{-1}). After cell disruption by five passages at 1500 psi through a French pressure cell (SLM Aminco), cell debris was removed by centrifugation (30 min, 16,000×*g*, 4 °C) and the supernatant (cell-free extract) was subjected to ultracentrifugation for 60 min at 230,000×*g* and 4 °C. The membrane pellet was washed in 1 mL 100 mM potassium phosphate buffer pH 7.5 and again subjected to ultracentrifugation (60 min, 230,000×*g*, 4 °C). Then, washed membrane pellet was resuspended in 1 mL of the same buffer and stored at −70 °C until use. Protein concentrations were determined with the bicinchoninic acid (BCA) protein assay (Smith et al. 1985) (Interchim, Montluçon, France) using bovine serum albumin (BSA) as standard. Dilutions of membrane protein suspensions contained 1 mg mL^{-1} BSA to stabilize the membrane protein (Finn et al. 2012).

Enzyme assays

Succinate/DCPIP reductase activity was determined using a method described by Spencer and Guest (Spencer and Guest 1973). The reaction mixture contained 60 mM potassium phosphate buffer, pH 7.5 (buffer A), 2,6-dichlorophenol indophenol (DCPIP, 0.23 mM), *N*-methylphenazine methosulfate (PMS, 2.18 mM), and membrane protein. The reaction was started by addition of disodium succinate (10 mM) to a final volume of 1 mL. Reduction of DCPIP (extinction coefficient at 600 nm is 21 mM^{-1} cm^{-1}) was monitored at 600 nm and 30 °C. One molecule DCPIP is reduced by one molecule of succinate. One unit (U) is defined as 1 μmol DCPIP reduced per min. Succinate/oxygen reductase activity of membrane fractions was determined with a Clark-type oxygen electrode in an oxygen electrode chamber (Oxygraph, Hansatech Instruments, Germany). Oxygen consumption rates of the isolated membranes were measured using a thermostatically controlled, magnetically stirred 2 mL chamber at 30 °C and the Oxygraph Plus software. The electrode was calibrated with air-saturated buffer A (100 % oxygen saturation), and dithionite was added for setting the 0 % oxygen saturation

value. The membrane preparations were diluted with air-saturated buffer A, and the chamber was filled with 500 µL air-saturated membrane dilution. Oxygen consumption was followed after adding 5 µL of a 1 M disodium succinate stock solution in buffer A. One molecule O_2 is reduced by two molecules succinate. One unit (U) is defined as 0.5 µmol O_2 reduced to H_2O per min.

Determination of substrates and products by HPLC analysis

One milliliter culture was centrifuged for 2 min at 16,000 × *g*, and the supernatant was filtered through a 0.2 µm filter (Millipore, MA, USA) prior to HPLC analysis. Mannitol, fructose, and 5-ketofructose were quantified with a Rezex RCM-Monosaccharide 300 × 7.8 mm column (Phenomenex, Aschaffenburg, Germany) at 60 °C using H_2O as the eluent at a flow rate of 0.6 mL min^{-1}. Substances were detected by a refractive index detector. Retention times for 5-ketofructose, fructose, and mannitol were 13.57, 15.31, and 19.98 min, respectively. Calibration curves were made using a series of standards ranging from 5.5 to 28 mM mannitol, fructose or 5-ketofructose. Acetate and fumarate concentrations were measured with an Organic Acid Resin 300 × 8 mm column (CS Chromatographie Service, Langerwehe, Germany) at 25 °C using 8 mM H_2SO_4 as the eluent at a flow rate of 0.6 mL min^{-1}. Acetate and fumarate were detected with an UV detector at 215 nm, and the retention times were 18.15 and 20.42 min, respectively. Calibration curves were made using a series of standards ranging from 1 to 10 mM acetate or fumarate.

Protein identification by mass spectrometry and detection of FAD fluorescence

Ten microgram protein of membrane fractions per lane were separated by SDS-PAGE (4–12 % polyacrylamide gels using a buffer composed of 50 mM MOPS (3-(*N*-morpholino)propanesulfonic acid), 50 mM Tris base, 0.1 % SDS, 1 mM EDTA, pH 7.7). Identification of proteins from gels stained with PageBlue Protein Staining Solution (Thermo Scientific, Schwerte, Germany) was performed by peptide mass fingerprinting of tryptic digests as described (Schaffer et al. 2001), except that peptides were extracted by the addition of 0.2 % (*v*/*v*) trifluoroacetic acid in 30 % (*v*/*v*) acetonitrile. MALDI-TOF-MS was performed with an Ultraflex III TOF/TOF mass spectrometer (Bruker Daltonics, Bremen, Germany). MASCOT software (Perkins et al. 1999) was used to compare the peptide mass patterns obtained with those of all proteins from the theoretical *A. pasteurianus* proteome. The molecular weight search (MOWSE) scoring scheme (Pappin et al. 1993) with a cutoff value of 50 was used for unequivocal identification of proteins.

For detection of fluorescent protein bands in SDS-polyacrylamide gels, proteins were fixed after electrophoresis in 10 % (vol/vol) acetic acid for 1 h. Gels were inspected and photographed on an UV-transilluminator system at 312 nm (PEQLAB Biotechnologie GmbH, Erlangen, Germany). Upon illumination with UV light, subunit A of Sdh was visible because of the fluorescence of the covalently bound flavin (Bafunno et al. 2004).

Results

Expression of the *sdhCDAB* genes from *A. pasteurianus* in *G. oxydans*

For the synthesis of a heterologous Sdh in *G. oxydans*, the *sdhCDAB* genes from *A. pasteurianus* were chosen (Azuma et al. 2009). Like *G. oxydans*, this species is a member of the family *Acetobacteraceae* within the α-proteobacteria and a close phylogenetic relationship might be favorable for functional expression. According to the classification scheme of Hägerhäll, the *sdhCDAB* genes of *A. pasteurianus* encode a succinate/quinone oxidoreductase belonging to class 1, as they reduce the high potential quinone ubiquinone and with respect to the membrane anchor to type C, which is composed of two polypeptides, with three transmembrane helices each, and contain one protoheme IX molecule (Hägerhäll 1997).

In order to express the *A. pasteurianus sdhCDAB* genes in *G. oxydans*, they were amplified from chromosomal DNA and cloned into the expression vector pBBR1p384, in which genes are expressed under control of the promoter of the ribosomal protein gene *rpsL* (GOX0384) (Fig. 1). The resulting plasmid pBBR1p384-sdh was transferred into *G. oxydans* by conjugation, and the membrane fraction of the recombinant strain was tested for succinate/DCPIP reductase activity. Membrane preparations of *G. oxydans* and of *G. oxydans*/pBBR1p384 were used as negative controls, and membrane preparations of *A. pasteurianus* and *C. glutamicum* as positive controls (Bussmann et al. 2009; Azuma et al. 2009). The results of these enzymatic assays are shown in Table 2. As expected, no activity was measured for the two *G. oxydans* negative controls and activities of 0.12 and 3.85 U (mg membrane protein)$^{-1}$ were determined for the *A. pasteurianus* and *C. glutamicum* positive controls. The recombinant *G. oxydans* strain carrying the *A. pasteurianus sdhCDAB* genes showed an extremely low succinate/DCPIP reductase activity of 0.01 U (mg membrane protein)$^{-1}$, which was close to the detection limit of the assay, suggesting that expression of the structural genes was weak or that additional genes are required to form an active Sdh complex. SDS-PAGE of the membrane

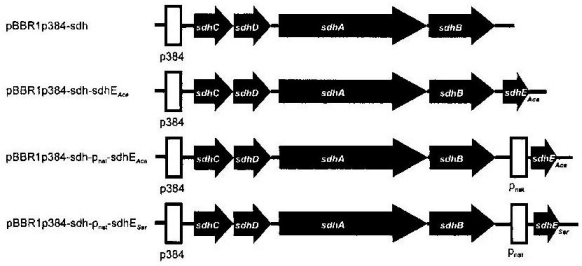

Fig. 1 Scheme of the inserts of the four expression plasmids used for heterologous synthesis of succinate dehydrogenase from *A. pasteurianus* in *G. oxydans*. The promoters used are indicated as p384 or p_{nat}. *Ace*, *A. pasteurianus*; *Ser*, *Serratia*

fraction of *G. oxydans* with plasmid pBBR1p384-sdh revealed a faint band at 67 kDa that was presumed to represent the flavoprotein subunit SdhA (Fig. 2).

Identification of an SdhE homolog in *A. pasteurianus*

Hederstedt et al. reported the lack of covalently bound flavin in the *Bacillus subtilis* Sdh when heterologously produced in *E. coli* and discussed the necessity of host-specific factors that allow FAD attachment (Hederstedt et al. 1987). Recently, McNeil and coworkers identified a novel accessory protein of Sdh in γ-proteobacteria. The SdhE protein promotes covalent FAD attachment to complex II-type enzymes (i.e., Sdh and fumarate reductase) (McNeil et al. 2012; McNeil and Fineran 2013b; McNeil et al. 2014). In order to identify putative SdhE homologs in *A. pasteurianus*, a BlastP search (Altschul et al. 1990) was performed using the SdhE protein of *Serratia* sp. ATCC39006 as query sequence. The 12.2 kDa protein (109 amino acid residues) encoded by the gene with the locus tag APA01_11050 was identified as putative SdhE homolog of *A. pasteurianus*. It showed 27 % sequence identity in a 74 amino acid overlap and differed from *Serratia* sp. SdhE by an N-terminal extension of 20 amino acid residues including eight serine residues. The RGxxE motif containing residues essential for the flavinylation activity of SdhE from *Serratia* was conserved in the APA01_11050 protein. The chromosomal localization of APA01_11050 upstream of the transcription repair factor gene *mfd* and divergent to *recG* was reported to be the typical position of *sdhE* genes in α-proteobacteria (McNeil et al. 2012; McNeil and Fineran 2013a).

In order to test its influence on the formation of an active *A. pasteurianus* Sdh complex in *G. oxydans*, we amplified the APA01_11050 gene and cloned it into pBBR1p384-sdh in two different ways. In pBBR1p384-sdh-sdhE$_{Ace}$, the APA01_11050 gene including its native ribosome binding

Table 2 Specific succinate/DCPIP reductase and succinate/oxygen reductase activities of selected strains

Strain[a]	Succinate/DCPIP reductase activity[b] [U (mg membrane protein^{-1})]	Succinate/oxygen reductase activity[b] [U (mg membrane protein^{-1})]
C. glutamicum ATCC1302	3.85 ± 0.42	0.084 ± 0.005
A. pasteurianus DSM3509	0.12 ± 0.09	0.012 ± 0.005
G. oxydans	<0.01 ± 0.00	n.d.
G. oxydans/pBBR1p384	<0.01 ± 0.00	<0.002 ± 0.000
G. oxydans/pBBR1p384-sdh	0.01 ± 0.00	0.002 ± 0.000[c]
G. oxydans/pBBR1p384-sdh-sdhE$_{Ace}$	0.43 ± 0.07	0.060 ± 0.010
G. oxydans/pBBR1p384-sdh-p$_{nat}$-sdhE$_{Ace}$	3.99 ± 0.40	0.680 ± 0.040
G. oxydans/pBBR1p384-sdh-p$_{nat}$-sdhE$_{Ser}$	0.92 ± 0.15	n.d.

n.d. not determined

[a] *C. glutamicum* and *A. pasteurianus* served as positive controls, and *G. oxydans* and *G. oxydans*/pBBR1p384 served as negative controls

[b] Mean values and standard deviation from three biological replicates are given

[c] Incubation of the membrane fraction of strain *G. oxydans*/pBBR1p384-sdh with 0.1 mM FAD at 30 °C for 30 min prior to the Sdh activity test resulted in a weak stimulation of succinate/oxygen reductase activity to 0.006 ± 0.000 U (mg membrane protein)$^{-1}$

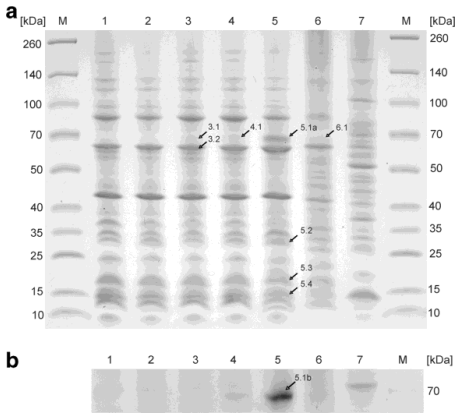

Fig. 2 **a**, Coomassie-stained SDS-PAGE gel loaded with 10 µg membrane protein per lane of the indicated strains. *M*, molecular weight marker; *lane 1*, *G. oxydans*; *lane 2*, *G. oxydans*/pBBR1p384; *lane 3*, *G. oxydans*/pBBR1p384-sdh; *lane 4*, *G. oxydans*/pBBR1p384-sdh-sdhE$_{Ace}$; *lane 5*, *G. oxydans*/pBBR1p384-sdh-p$_{nat}$-sdhE$_{Ace}$; *lane 6*, *A. pasteurianus*; *lane 7*, *C. glutamicum*. **b** FAD-UV analysis of the SDS-PAGE gel loaded with 10 µg membrane protein per lane of the strains indicated in **a**

site, but not its native promoter, was cloned behind *sdhCDAB*, resulting in the artificial operon *sdhCDABE* controlled by the p384 promoter. In the pBBR1p384-sdh-p$_{nat}$-sdhE$_{Ace}$ plasmid, the APA01_11050 gene including its native ribosome binding site and its presumed native promoter was cloned downstream of *sdhCDAB* (Fig. 1). The plasmids were transferred to *G. oxydans* by conjugation, and membrane fractions of the recombinant strains were tested for succinate/DCPIP reductase activity. The strain carrying pBBR1p384-sdh-sdhE$_{Ace}$ showed an activity of 0.43 U (mg membrane protein)$^{-1}$ and the one carrying pBBR1p384-sdh-p$_{nat}$-sdhE$_{Ace}$ one of 4.0 U (mg membrane protein)$^{-1}$ (Table 2). Consequently, the co-expression of *sdhE$_{Ace}$* with *sdhCDAB* was sufficient to allow formation of an Sdh enzyme with succinate/DCPIP reductase activity. The tenfold difference in Sdh activity between the two strains is most likely caused by strongly differing expression levels of *sdhE$_{Ace}$* (see subsequent paragraphs).

Use of *Serratia* SdhE for synthesis of a functional *A. pasteurianus* Sdh in *G. oxydans*

In view of the differences in the amino acid sequences of *Serratia* SdhE and the *A. pasteurianus* SdhE homolog (APA01_11050), we wanted to determine whether SdhE$_{Ser}$ was also able to serve as assembly factor for *A. pasteurianus* Sdh. To this end, we cloned the *sdhE$_{Ser}$* gene (locus tag Ser39006_1161) including its native ribosome binding site and its presumed native promoter behind the *sdhCDAB* genes in plasmid pBBR1p384-sdh (Fig. 1). Transfer of the resulting plasmid pBBR1p384-sdh-p$_{nat}$-sdhE$_{Ser}$ into *G. oxydans* resulted in a recombinant strain with a succinate/DCPIP reductase activity of 0.92 U (mg membrane protein)$^{-1}$ (Table 2). Thus, also SdhE$_{Ser}$ is able to promote covalent FAD attachment to *A. pasteurianus* Sdh and thus functionality of the enzyme.

Analysis of the membrane fraction of the recombinant strains

The membrane proteins of the recombinant *G. oxydans* strains were analyzed by SDS-PAGE (Fig. 2) and subsequent MS analysis (Table 3) in order to test for the presence of the heterologous Sdh subunits and for covalent FAD linkage to SdhA. As shown in Fig. 2a (lane 5, marked with arrow 5.1a), a prominent band with an apparent mass of about 67 kDa became visible in *G. oxydans* carrying pBBR1p384-sdh-p$_{nat}$-sdhE$_{Ace}$, which was identified as SdhA (predicted mass of apo-SdhA 65.9 kDa) by peptide mass fingerprinting (Table 3). SdhA was also identified in the *G. oxydans* strains carrying pBBR1p384-sdh and pBBR1p384-sdh-sdhE$_{Ace}$ and also in the membrane fraction of wild type *A. pasteurianus* (Fig. 2a, lanes 3, 4, and 6, protein bands marked as 3.1, 4.1, and 6.1), but was present in much lower quantities. Besides SdhA, also SdhB (calculated mass 29.3 kDa) could be unequivocally identified in *G. oxydans*/pBBR1p384-sdh-p$_{nat}$-sdhE$_{Ace}$. In the case of SdhC (calculated mass 16.8 kDa) and SdhD (calculated mass 14.7 kDa), one and two peptides could be identified by MALDI-TOF-MS, respectively. Along with the high enzyme activity, these data suggest that all *A. pasteurianus* Sdh subunits were formed in *G. oxydans*.

In order to test the assumed function of SdhE$_{Ace}$ as a protein required for the covalent attachment of FAD to SdhA, the membrane fractions separated by SDS-PAGE were analyzed for FAD-dependent fluorescence by transillumination at 312 nm. As shown in Fig. 2b, a clear band at about 67 kDa was detected in *G. oxydans*/pBBR1p384-sdh-p$_{nat}$-sdhE$_{Ace}$. MS analysis of tryptic digests of this band confirmed that it represents SdhA (Table 3). The peptide SHTVAAQGGIGASLGNMAEDNWR with the flavinylation site H56 was not detectable in the MS spectra, either in the unflavinylated (*m*/*z* 2342) or in the flavinylated state (*m*/*z* = 3128). Weak SdhA fluorescence was also observed for strain *G. oxydans*/pBBR1p384-sdh-sdhE$_{Ace}$, but not for *G. oxydans*/pBBR1p384-sdh. These results are in agreement with a requirement of SdhE for flavinylation of SdhA, as described for *Serratia* SdhE (see "Discussion").

Succinate/oxygen reductase activities

As the succinate/DCPIP reductase assay does not detect the entire reaction catalyzed by Sdh, i.e., the reduction of

No. score	Protein	Predicted mass (kDa)	No. of peptides	Sequence coverage (%)	MOWSE
3.1	APA01_00330 (SdhA)	67	13	32	86
3.2	GOX1902 (GroEL)	58	30	53	132
4.1	APA01_00330 (SdhA)	67	15	29	84
5.1a	APA01_00330 (SdhA)	67	22	33	97
5.1b	APA01_00330 (SdhA)	67	17	31	101
5.2	APA01_00340 (SdhB)	29	7	24	50
5.3	APA01_00310 (SdhC)	17	1	5	8
5.4	APA01_00320 (SdhD)	15	2	34	13
6.1	APA01_00330 (SdhA)	67	4	11	15

5.1a shows the results for the Coomassie-stained gel and 5.1b those for the gel analyzed by FAD-UV

ubiquinone by succinate, we also determined the succinate/oxygen reductase activity of membrane preparations with a Clark-type oxygen electrode. In this assay, ubiquinol is reoxidized by one of the terminal quinol oxidases of *G. oxydans*, cytochrome bo_3 oxidase (Richhardt et al. 2013) or the cyanide-insensitive cytochrome *bd* oxidase CIO (Miura et al. 2013). Significant oxygen consumption rates were measured in strains also possessing succinate/DCPIP reductase activity, whereas no activity was detectable in the *G. oxydans* negative controls (Table 2). Although the succinate/oxygen reductase activities were only 14–17 % of the succinate/DCPIP reductase activities, they confirm that in the presence of SdhE, the *A. pasteurianus* Sdh complex was functionally integrated into the cytoplasmic membrane of *G. oxydans* and transferred the electrons from succinate to ubiquinone. Consequently, it has to be assumed that at least a part of the Sdh population was correctly assembled and fully functional.

Impact of an active Sdh on the metabolism of *G. oxydans*

In order to test the influence of an active Sdh complex on metabolism, the *G. oxydans* strains carrying pBBR1p384, pBBR1p384-sdh-sdhE$_{Ace}$, or pBBR1p384-sdh-p$_{nat}$-sdhE$_{Ace}$ were cultivated in mannitol medium at pH 6 and 15 % DO in a multibioreactor system. *G. oxydans*/pBBR1p384-sdh-sdhE$_{Ace}$ showed similar profiles of growth, mannitol consumption, and product formation as the reference strain/pBBR1p384 (Fig. 3a, b). However, acetate formed during growth was partially reconsumed by the Sdh-positive strain, but not by the reference strain (Fig. 3c). Acetate reconsumption suggests that despite the absence of succinyl-CoA synthetase, the other enzymes of TCA cycle including the heterologous Sdh allow oxidation of acetate to CO_2. Moreover, the Sdh-positive strain, but not the reference strain, transiently excreted low concentrations of fumarate (about 30 μM). In the case of *G. oxydans* with pBBR1p384-sdh-p$_{nat}$-sdhE$_{Ace}$, which exhibits a tenfold higher Sdh activity than pBBR1p384-sdh-sdhE$_{Ace}$, growth ceased after mannitol had been completely oxidized to fructose (Fig. 3d, e). The reduced growth correlated with a reduced fructose oxidation to ketofructose in the second growth phase (Fig. 3e). As observed for *G. oxydans*/pBBR1p384-sdh-sdhE$_{Ace}$, acetate formation was lower than for the reference strain and about 70 μM fumarate was excreted after 28 h (Fig. 3f). The excretion of fumarate points to a limited fumarase activity in the Sdh-positive strain. As discussed below, we assume that succinate, the substrate for Sdh and the precursor of fumarate, is formed by spontaneous hydrolysis of instable succinyl-CoA.

Discussion

G. oxydans lacks the genes for 1-phosphofructokinase, succinyl-CoA synthetase, and succinate dehydrogenase, and therefore, both glycolysis and the TCA cycle are interrupted. In a study on the phylogenetic distribution of 1-phosphofructokinase, it was found that the corresponding gene is missing in most of the analyzed α-proteobacteria (Baart et al. 2010) and its absence in *G. oxydans* is thus not surprising. In contrast, metabolic pathway reconstructions made through comparative genomics by Koonin and Galperin predicted that either Sdh or fumarate reductase is present in the vast majority of organisms, with the exception of pyrococci, spirochetes, and mycoplasmas (Koonin and Galperin 2003). The absence of Sdh and fumarate reductase in *G. oxydans* and the other *Gluconobacter* species with known genome sequence (*G. oxydans* DSM3504, *Gluconobacter thailandicus*, *Gluconobacter frateurii*) thus may be regarded as a rare example of a genus having lost this function. Genes for succinyl-CoA synthetase are also missing in the genome of *G. oxydans* (Prust et al. 2005). Although alternative pathways for succinate formation have been described, e.g., via succinate semialdehyde dehydrogenase or succinyl-coenzyme A (CoA)/

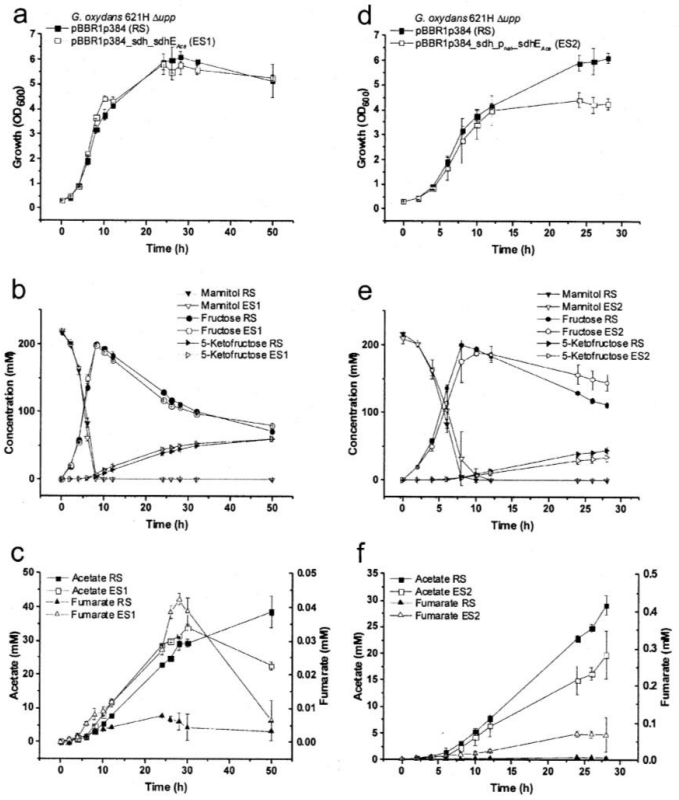

Fig. 3 Growth (**a**, **d**), substrate consumption and product formation (**b**, **c**, **e**, **f**) of *G. oxydans*/pBBR1p384 (reference strain, RS), *G. oxydans*/pBBR1p384-sdh-sdhE$_{Ace}$ (expression strain 1, ES1), and *G. oxydans*/pBBR1p384-sdh-p$_{nat}$-sdhE$_{Ace}$ (expression strain 2, ES2). Mean values and standard deviation from three biological replicates are shown

acetate CoA-transferase (Schweiger et al. 2007; Green et al. 2000; Huynen et al. 1999; Mullins et al. 2008; Yuan et al. 2013), the corresponding genes are not annotated in the *G. oxydans* 621H genome (Prust et al. 2005). The genes for the residual six enzymes of the TCA cycle, i.e., citrate synthase (GOX1999), aconitase (GOX1335), isocitrate dehydrogenase (GOX1336), 2-oxoglutarate dehydrogenase (GOX0882, GOX1072, GOX2292), fumarase (GOX1643), and malate quinone oxidoreductase (GOX2070), are present in *G. oxydans*. However, except for malate/quinone oxidoreductase, the specific activities of these enzymes in cell extracts have not yet been determined. Malate/DCPIP reductase activity in membrane preparations was found to be 0.020 ± 0.008 U (mg membrane protein)$^{-1}$ (data not shown).

As a first step to study the consequences of a functional TCA cycle on biomass yield and growth physiology of *G. oxydans*, we introduced a heterologous Sdh complex, which requires a covalently bound FAD, three iron–sulfur clusters, and a heme group for activity. The covalent binding of FAD is essential for Sdh activity, as it increases its redox potential by about 100 mV and thereby allows electron transfer from succinate to FAD (Cheng et al. 2015). In eukaryotes, where Sdh is located in the inner mitochondrial membrane, four Sdh-specific assembly factors have been identified and characterized (for a recent review see Van Vranken et al. (2015)). Sdh5 of *Saccharomyces cerevisiae* specifically binds to apo-Sdh1 (flavoprotein) and is required for covalent flavinylation by a yet unknown mechanism. Sdh8 binds to flavinylated Sdh1 and is assumed to protect the FAD cofactor from undesired oxidation reactions. Sdh6 and Sdh7 are involved in Sdh2 (iron–sulfur protein) maturation. In addition, biogenesis of the three iron–sulfur clusters of Sdh2 requires

Fig. 4 Multiple sequence alignment of Sdh5/SdhE proteins from *Saccharomyces cerevisiae* (YOL071W), *Serratia* sp. ATCC 39006 (Ser39006_1161), *Azospirillum lipoferum* (AZOLI_1466), *Acetobacter pasteurianus* IFO3283-01 (APA01_11050), *Granulibacter bethesdensis* (GbCGDNIH1_0835), *Gluconacetobacter diazotrophicus* PA1 5 (GDI1885), *Komagataeibacter medellinensis* NBRC 3288 (GLX_05520), and *Komagataeibacter xylinus* E25 (H845_1665). A cluster of eight serine residues in SdhE of *A. pasteurianus* is highlighted in *light grey* and a cluster of four consecutive arginine or lysine residues in the α-proteobacterial SdhE proteins in *dark grey*. The conserved RGXXE motif characteristic of SdhE proteins is highlighted in *black*. *Asterisks* indicate identical amino acids, and *points* indicate conservative substitutions

the ISU and ISA complexes (Van Vranken et al. 2015). In bacteria, much less is known on the maturation of Sdh. Only recently, McNeil and coworkers demonstrated that the YgfY protein of *Serratia* strain ATCC 39006 (a DUF339/COG2938 protein) is required for the covalent attachment of FAD to the flavoprotein subunit SdhA and renamed the protein SdhE (McNeil et al. 2012). They showed that SdhA purified from *Serratia* wild type contained a detectable FAD cofactor, whereas SdhA purified from a Δ*sdhE* mutant lacked FAD. Furthermore, purified Serratia SdhE was able to convert apo-SdhA in cell extracts of the Δ*sdhE* mutant to holo-SdhA when supplemented with FAD (McNeil et al. 2012).

Table 4 Iron–sulfur cluster biosynthesis genes in *G. oxydans* 621H and *A. pasteurianus* IFO3283-01

Gene	Function[a]	*G.oxydans* locus tag	*A. pasteurianus* locus tag	% Amino acid sequence identity (identical aa/total aa)
sufB	FeS assembly SufBCD complex, SU B, scaffold protein	GOX0098	APA01_16620	86 (428/496)
sufC	FeS assembly SufBCD complex, SU C, ABC-type ATPase	GOX0097	APA01_16610	81 (208/256)
sufD	FeS assembly SufBCD complex, SU D	GOX0096	APA01_16600	50 (189/380)
sufS	SufSE complex; cysteine desulfurase; provides sulfur from L-cysteine and relays sulfur from SufS to scaffold	GOX0095	APA01_16590	69 (278/402)
sufE	SufSE complex; cysteine desulfurase; provides sulfur from L-cysteine and relays sulfur from SufS to scaffold	GOX0268	APA01_10250	75 (107/143)
hesB	HesB; iron–sulfur FeS cluster assembly protein	GOX1751	APA01_21200	64 (78/122)
nifR3	NifR3; tRNA-dihydrouridine synthase	GOX0469	APA01_17530	73 (244/333)
nifU	NifU; nitrogen fixing thioredoxin-like protein	GOX0777	APA01_00150	68 (127/186)
nifS	NifS; cysteine desulfurase I	GOX1368	APA01_26020	56 (204/364)
nifS	NifS; cysteine desulfurase II	GOX1369	APA01_26010	61 (169/279)

[a] Functions were in part assigned according to Roche et al. (2013); SU, subunit

SdhE homologs are present in the α-, β-, and γ-proteobacteria and in eukaryotes including humans (McNeil et al. 2012; McNeil and Fineran 2013b; Van Vranken et al. 2015; McNeil and Fineran 2013a). SdhE of *Serratia* is a small soluble protein of 88 amino acids including the highly conserved RGxxE motif (Fig. 4). The mutations G16R and E19A within this motif impaired the activation of Sdh (McNeil and Fineran 2013a). There are a number of interesting differences between SdhE of *Serratia* and Sdh5 of *S. cerevisiae*. Whereas there is evidence for FAD-binding by SdhE (reviewed in McNeil and Fineran 2013b), NMR studies with Sdh5 argue against FAD binding (Eletsky et al. 2012). Moreover, Sdh5 (Hao et al. 2009), but not SdhE (McNeil et al. 2012), was required for Sdh stability and assembly. Furthermore, *Serratia* Sdh retained about 10 % residual activity in the absence of SdhE (McNeil and Fineran 2013a), whereas Sdh5 was strictly required in yeast for maintaining Sdh activity (Van Vranken et al. 2015). These and additional data led to different models of Sdh assembly in *Serratia* and yeast (Van Vranken et al. 2015; McNeil et al. 2012). Our results show that SdhE is required for activation of Sdh not only in γ-proteobacteria but also in α-proteobacteria. We identified the SdhE homolog of *A. pasteurianus* and showed that it is essential for functional synthesis of the *A. pasteurianus* Sdh in the heterologous host *G. oxydans*. Flavinylation of *A. pasteurianus* SdhA was only detected in the presence of SdhE when analyzed by UV-induced fluorescence (Fig. 2b). In contrast to *Serratia*, the residual activity of *A. pasteurianus* Sdh in the absence of SdhE was negligible, resembling the essentiality of Sdh5 for Sdh activity in yeast.

A. pasteurianus SdhE shows only 27 % sequence identity to SdhE of *Serratia* and contains an N-terminal extension of 23 amino acids, which includes the striking sequence motif SSPSSSSSAS (Fig. 4). The function of the N-terminal region is not known yet, but the fact that the SdhE protein of *Serratia* was also able to activate the *A. pasteurianus* Sdh in *G. oxydans* shows that it is not essential for interaction with SdhA and flavinylation. Moreover, this experiment showed for the first time that a γ-proteobacterial SdhE is able to activate an α-proteobacterial Sdh. The functionality of this chimeric combination of Sdh core proteins and flavinylation chaperone is presumably due to the conserved surface region of SdhE/Sdh5 (Lim et al. 2005), which includes the functionally important residues G16 and E19 ($SdhE_{Ser}$ numbering) (McNeil and Fineran 2013b) and therefore is key for interaction with SdhA. Compared to SdhE proteins, SdhA proteins are highly conserved, with the flavinylated histidine residue (H56 in the case of *A. pasteurianus* SdhA) and the conserved FAD-binding motif GXGXXG being located in the N-terminal region (Dym and Eisenberg 2001). In a recent study with *E. coli* Sdh, it was shown that SdhA-R286 plays an essential role in the mechanism of covalent flavinylation and that SdhA-H242 plays a role in its efficiency and completeness (Cheng et al. 2015). Exchange of either R286 or H242 reduced covalent FAD binding by >95 % and about 70 %, respectively (Cheng et al. 2015). Both residues are conserved in *A. pasteurianus* SdhA (H253, R297). Flavinylation of the yeast Sdh1 subunit was reported to be dependent on two spatially close C-terminal arginine residues that are distant from the FAD-binding site, Arg582 and Arg638 (Kim et al. 2012). Also, these residues are conserved in *A. pasteurianus* SdhA (R547, R601), indicating that many steps of flavin attachment are conserved in eukaryotes and proteobacteria.

The result that co-expression of *sdhE* was sufficient to obtain an active *A. pasteurianus* Sdh complex with succinate/oxygen reductase activity of the *G. oxydans* membrane fraction indicates that a holo-complex was formed that is able to transfer the electrons from succinate via FAD in SdhA and the three iron–sulfur clusters in SdhB to the ubiquinone binding site at the membrane-bound SdhCD subunits. Thus, the systems for iron–sulfur cluster formation in *G. oxydans* are apparently able to recognize apo-SdhB and to correctly insert the [2Fe-2S], [3Fe-4S], and [4Fe-4S] clusters into a protein which is naturally absent in the cell. Although the presence of the clusters still needs to be confirmed by a more direct approach, the process of holo-SdhB formation presumably does not require any additional specific assembly proteins. *G. oxydans* and *A. pasteurianus* both possess the Suf and the Nif systems for iron–sulfur cluster biogenesis (Roche et al. 2013; Prust et al. 2005; Deppenmeier and Ehrenreich 2009), and the homologous proteins show 50–92 % amino acid sequence identity (Table 4).

G. oxydans possesses at least eight FAD-dependent membrane-bound dehydrogenases. In other *Gluconobacter* species, four homologous enzymes were purified and shown to contain covalently bound FAD/gluconate dehydrogenase from *Gluconobacter dioxyacetonicus* IFO 3271 (Shinagawa et al. 1984; Toyama et al. 2007), 2-keto-gluconate dehydrogenase from *Gluconobacter melanogenus* IFO 3293 (Shinagawa et al. 1981; McIntire et al. 1985), sorbitol dehydrogenase from *G. frateurii* (Toyama et al. 2005), and fructose dehydrogenase from *Gluconobacter japonicus* (Kawai et al. 2013). The mechanism by which FAD is covalently attached to the large subunits of these heterotrimeric membrane proteins is as yet unknown. If it does not occur autocatalytically, other flavinylation proteins without sequence similarity to SdhE await their discovery.

The presence of an active Sdh complex in *G. oxydans* did not lead to improved growth on mannitol. On the contrary, the strain with the highest Sdh activity of 4 U (mg membrane protein)$^{-1}$ even showed growth inhibition in the second phase of cultivation on mannitol, where fructose is slowly oxidized to 5-ketofructose (Richhardt et al. 2012). The low energy availability under these conditions in combination with the metabolic burden of strong Sdh overexpression might be

responsible for the growth impairment. Nevertheless, the presence of an active Sdh in *G. oxydans* caused a significantly decreased acetate formation and the excretion of small amounts of fumarate. While the decreased acetate production implies an elevated flux of pyruvate into the TCA cycle, the appearance of fumarate in the culture supernatant reflects the presence of a functional Sdh complex and an apparently limiting activity of fumarate hydratase, which is a class II fumarase C. As *G. oxydans* does not contain genes for succinyl-CoA synthetase, the Sdh substrate succinate might be slowly formed by spontaneous hydrolysis of succinyl-CoA (Lambeth and Muhonen 1993; Reeves et al. 1971).

Obviously, the regression of central metabolic functions displayed by *G. oxydans* is no disadvantage in its natural habitat. Rather, the organism evolved a vigorous periplasmic oxidation activity involving one of the most active bacterial respiratory chains (Sootsuwan et al. 2008). Future work will reveal if the low growth yield of *G. oxydans* can be improved by complete supplementation of the TCA cycle by introduction of a heterologous succinyl-CoA synthetase into the Sdh-positive strain.

Acknowledgments The scientific activities of the Bioeconomy Science Center were financially supported by the Ministry of Innovation, Science and Research within the framework of the NRW Strategieprojekt BioSC (no. 313/323-400-002 13). We are most grateful to Uwe Deppenmeier (Universität Bonn) for providing plasmid pBBR1p384.

Conflict of interest The authors declare that they have no conflict of interest.

Ethical statement This article has been prepared following principles of ethical and professional conduct.

References

Adachi O, Moonmangmee D, Toyama H, Yamada M, Shinagawa E, Matsushita K (2003) New developments in oxidative fermentation. Appl Microbiol Biotechnol 60(6):643–653. doi:10.1007/s00253-002-1155-9

Altschul SF, Gish W, Miller W, Myers EW, Lipman DJ (1990) Basic local alignment search tool. J Mol Biol 215(3):403–410

Azuma Y, Hosoyama A, Matsutani M, Furuya N, Horikawa H, Harada T, Hirakawa H, Kuhara S, Matsushita K, Fujita N, Shirai M (2009) Whole-genome analyses reveal genetic instability of *Acetobacter pasteurianus*. Nucleic Acids Res 37(17):5768–5783. doi:10.1093/nar/gkp612

Baart GJ, Langenhof M, van de Waterbeemd B, Hamstra HJ, Zomer B, van der Pol LA, Beuvery EC, Tramper J, Martens DE (2010) Expression of phosphofructokinase in *Neisseria meningitidis*. Microbiology 156(Pt 2):530–542. doi:10.1099/mic.0.031641-0

Bafunno V, Giancaspero TA, Brizio C, Bufano D, Passarella S, Boles E, Barile M (2004) Riboflavin uptake and FAD synthesis in *Saccharomyces cerevisiae* mitochondria: involvement of the Flx1p carrier in FAD export. J Biol Chem 279(1):95–102. doi:10.1074/jbc.M308230200

Bertani G (1951) Studies on lysogenesis. I. The mode of phage liberation by lysogenic *Escherichia coli*. J Bacteriol 62(3):293–300

Bertani G (2004) Lysogeny at mid-twentieth century: P1, P2, and other experimental systems. J Bacteriol 186(3):595–600. doi:10.1128/Jb.186.3.595-600.2004

Bussmann M, Emer D, Hasenbein S, Degraf S, Eikmanns BJ, Bott M (2009) Transcriptional control of the succinate dehydrogenase operon *sdhCAB* of *Corynebacterium glutamicum* by the cAMP-dependent regulator GlxR and the LuxR-type regulator RamA. J Biotechnol 143(3):173–182

Chen XH, Lou WY, Zong MH, Smith TJ (2011) Optimization of culture conditions to produce high yields of active *Acetobacter* sp. CCTCC M209061 cells for anti-prelog reduction of prochiral ketones. BMC Biotechnol 11:110. doi:10.1186/1472-6750-11-110

Cheng VW, Piragasam RS, Rothery RA, Maklashina E, Cecchini G, Weiner JH (2015) Redox state of flavin adenine dinucleotide drives substrate binding and product release in *Escherichia coli* succinate dehydrogenase. Biochemistry 54(4):1043–1052. doi:10.1021/bi501350j

Deppenmeier U, Ehrenreich A (2009) Physiology of acetic acid bacteria in light of the genome sequence of *Gluconobacter oxydans*. J Mol Microbiol Biotechnol 16(1–2):69–80. doi:10.1159/000142895

Deppenmeier U, Hoffmeister M, Prust C (2002) Biochemistry and biotechnological applications of *Gluconobacter* strains. Appl Microbiol Biotechnol 60(3):233–242. doi:10.1007/s00253-002-1114-5

Dym O, Eisenberg D (2001) Sequence-structure analysis of FAD-containing proteins. Protein Sci 10(9):1712–1728. doi:10.1110/ps.12801

Eletsky A, Jeong MY, Kim H, Lee HW, Xiao R, Pagliarini DJ, Prestegard JH, Winge DR, Montelione GT, Szyperski T (2012) Solution NMR structure of yeast succinate dehydrogenase flavinylation factor Sdh5 reveals a putative Sdh1 binding site. Biochemistry 51(43):8475–8477. doi:10.1021/bi301171u

Finn TE, Nunez AC, Sunde M, Easterbrook-Smith SB (2012) Serum albumin prevents protein aggregation and amyloid formation and retains chaperone-like activity in the presence of physiological ligands. J Biol Chem 287(25):21530–21540. doi:10.1074/jbc.M112.372961

Green LS, Li Y, Emerich DW, Bergersen FJ, Day DA (2000) Catabolism of alpha-ketoglutarate by a *sucA* mutant of *Bradyrhizobium japonicum*: evidence for an alternative tricarboxylic acid cycle. J Bacteriol 182(10):2838–2844

Gupta A, Singh VK, Qazi GN, Kumar A (2001) *Gluconobacter oxydans*: its biotechnological applications. J Mol Microbiol Biotechnol 3(3):445–456

Hägerhäll C (1997) Succinate: quinone oxidoreductases. Variations on a conserved theme. Biochim Biophys Acta 1320(2):107–141

Hanahan D, Jessee J, Bloom FR (1991) Plasmid transformation of *Escherichia coli* and other bacteria. Meth Enzymol 204:63–113. doi:10.1016/0076-6879(91)04006-A

Hanke T, Nöh K, Noack S, Polen T, Bringer S, Sahm H, Wiechert W, Bott M (2013) Combined fluxomics and transcriptomics analysis of glucose catabolism via a partially cyclic pentose phosphate pathway in *Gluconobacter oxydans* 621H. Appl Environ Microbiol 79(7):2336–2348. doi:10.1128/AEM.03414-12

Hao HX, Khalimonchuk O, Schraders M, Dephoure N, Bayley JP, Kunst H, Devilee P, Cremers CW, Schiffman JD, Bentz BG, Gygi SP, Winge DR, Kremer H, Rutter J (2009) SDH5, a gene required for flavination of succinate dehydrogenase, is mutated in paraganglioma. Science 325(5944):1139–1142. doi:10.1126/science.1175689

Hederstedt L, Bergman T, Jornvall H (1987) Processing of *Bacillus subtilis* succinate dehydrogenase and cytochrome b-558 polypeptides. Lack of covalently bound flavin in the *Bacillus* enzyme expressed in *Escherichia coli*. FEBS Lett 213(2):385–390

Huynen MA, Dandekar T, Bork P (1999) Variation and evolution of the citric-acid cycle: a genomic perspective. Trends Microbiol 7(7): 281–291

Kallnik V, Meyer M, Deppenmeier U, Schweiger P (2010) Construction of expression vectors for protein production in *Gluconobacter oxydans*. J Biotechnol 150(4):460–465. doi:10.1016/j.jbiotec.2010.10.069

Kawai S, Goda-Tsutsumi M, Yakushi T, Kano K, Matsushita K (2013) Heterologous overexpression and characterization of a flavoprotein-cytochrome *c* complex fructose dehydrogenase of *Gluconobacter japonicus* NBRC3260. Appl Environ Microbiol 79(5):1654–1660. doi:10.1128/AEM.03152-12

Keilhauer C, Eggeling L, Sahm H (1993) Isoleucine synthesis in *Corynebacterium glutamicum*: molecular analysis of the *ilvB-ilvN-ilvC* operon. J Bacteriol 175(17):5595–5603

Kim HJ, Jeong MY, Na U, Winge DR (2012) Flavinylation and assembly of succinate dehydrogenase are dependent on the C-terminal tail of the flavoprotein subunit. J Biol Chem 287(48):40670–40679. doi:10.1074/jbc.M112.405704

Koonin EV, Galperin MY (2003) Evolution of central metabolic pathways: the playground of non-orthologous gene displacement. In: Sequence - evolution - function: computational approaches in comparative genomics, Chapter 7. Kluwer Academic, Boston

Kovach ME, Elzer PH, Hill DS, Robertson GT, Farris MA, Roop 2nd RM, Peterson KM (1995) Four new derivatives of the broad-host-range cloning vector pBBR1MCS, carrying different antibiotic-resistance cassettes. Gene 166(1):175–176. doi:10.1016/0378-1119(95)00584-1

Krajewski V, Simić P, Mouncey NJ, Bringer S, Sahm H, Bott M (2010) Metabolic engineering of *Gluconobacter oxydans* for improved growth rate and growth yield on glucose by elimination of gluconate formation. Appl Environ Microbiol 76(13):4369–4376. doi:10.1128/aem.03022-09

Lambeth DO, Muhonen WW (1993) The direct assay of kinases and acyl-CoA synthetases by HPLC: application to nucleoside diphosphate kinase and succinyl-CoA synthetase. Anal Biochem 209(1):192–198. doi:10.1006/abio.1993.1102

Lim K, Doseeva V, Demirkan ES, Pullalarevu S, Krajewski W, Galkin A, Howard A, Herzberg O (2005) Crystal structure of the YgfY from *Escherichia coli*, a protein that may be involved in transcriptional regulation. Proteins 58(3):759–763. doi:10.1002/prot.20337

Macauley S, McNeil B, Harvey LM (2001) The genus *Gluconobacter* and its applications in biotechnology. Crit Rev Biotechnol 21(1):1–25. doi:10.1080/20013891081665

McIntire W, Singer TP, Ameyama M, Adachi O, Matsushita K, Shinagawa E (1985) Identification of the covalently bound flavins of D-gluconate dehydrogenases from *Pseudomonas aeruginosa* and *Pseudomonas fluorescens* and of 2-keto-D-gluconate dehydrogenase from *Gluconobacter melanogenus*. Biochem J 231(3):651–654

McNeil MB, Clulow JS, Wilf NM, Salmond GP, Fineran PC (2012) SdhE is a conserved protein required for flavinylation of succinate dehydrogenase in bacteria. J Biol Chem 287(22):18418–18428. doi:10.1074/jbc.M111.293803

McNeil MB, Fineran PC (2013a) The conserved RGxxE motif of the bacterial FAD assembly factor SdhE is required for succinate dehydrogenase flavinylation and activity. Biochemistry 52(43):7628–7640. doi:10.1021/bi401006a

McNeil MB, Fineran PC (2013b) Prokaryotic assembly factors for the attachment of flavin to complex II. Biochim Biophys Acta 1827(5): 637–647. doi:10.1016/j.bbabio.2012.09.003

McNeil MB, Hampton HG, Hards KJ, Watson BN, Cook GM, Fineran PC (2014) The succinate dehydrogenase assembly factor, SdhE, is required for the flavinylation and activation of fumarate reductase in bacteria. FEBS Lett 588(3):414–421. doi:10.1016/j.febslet.2013.12.019

Miura H, Mogi T, Ano Y, Migita CT, Matsutani M, Yakushi T, Kita K, Matsushita K (2013) Cyanide-insensitive quinol oxidase (CIO) from *Gluconobacter oxydans* is a unique terminal oxidase subfamily of cytochrome *bd*. J Biochem 153(6):535–545. doi:10.1093/jb/mvt019

Mullins EA, Francois JA, Kappock TJ (2008) A specialized citric acid cycle requiring succinyl-coenzyme A (CoA):acetate CoA-transferase (AarC) confers acetic acid resistance on the acidophile *Acetobacter aceti*. J Bacteriol 190(14):4933–4940. doi:10.1128/JB.00405-08

Pappenberger G, Hohmann HP (2014) Industrial production of L-ascorbic acid (vitamin C) and D-isoascorbic acid. Adv Biochem Eng Biotechnol 143:143–188. doi:10.1007/10_2013_243

Pappin DJ, Hojrup P, Bleasby AJ (1993) Rapid identification of proteins by peptide-mass fingerprinting. Curr Biol 3(6):327–332

Perkins DN, Pappin DJ, Creasy DM, Cottrell JS (1999) Probability-based protein identification by searching sequence databases using mass spectrometry data. Electrophoresis 20(18):3551–3567. doi:10.1002/(SICI)1522-2683(19991201)20:18<3551::AID-ELPS3551>3.0.CO;2-2

Peters B, Junker A, Brauer K, Mühlthaler B, Kostner D, Mientus M, Liebl W, Ehrenreich A (2013) Deletion of pyruvate decarboxylase by a new method for efficient markerless gene deletions in *Gluconobacter oxydans*. Appl Microbiol Biotechnol 97(6):2521–2530. doi:10.1007/s00253-012-4354-z

Prust C, Hoffmeister M, Liesegang H, Wiezer A, Fricke WF, Ehrenreich A, Gottschalk G, Deppenmeier U (2005) Complete genome sequence of the acetic acid bacterium *Gluconobacter oxydans*. Nat Biotechnol 23(2):195–200. doi:10.1038/nbt1062

Raspor P, Goranovič D (2008) Biotechnological applications of acetic acid bacteria. Crit Rev Biotechnol 28(2):101–124. doi:10.1080/07388550802046749

Reeves HC, Rabi R, Wegener WS, Ajl SJ (1971) Assays of enzymes of the tricarboxylic acid and glyoxylate cycles. In: Norris JR, Ribbons DW (eds) Meth microbiol, vol 6A, Chapter X. Academic Press, London, pp. 448–449

Richhardt J, Bringer S, Bott M (2012) Mutational analysis of the pentose phosphate and Entner-Doudoroff pathways in *Gluconobacter oxydans* reveals improved growth of a Δ*edd* Δ*eda* mutant on mannitol. Appl Environ Microbiol 78(19):6975–6986. doi:10.1128/AEM.01166-12

Richhardt J, Luchterhand B, Bringer S, Büchs J, Bott M (2013) Evidence for a key role of cytochrome bo_3 oxidase in respiratory energy metabolism of *Gluconobacter oxydans*. J Bacteriol 195(18):4210–4220. doi:10.1128/JB.00470-13

Roche B, Aussel L, Ezraty B, Mandin P, Py B, Barras F (2013) Iron/sulfur proteins biogenesis in prokaryotes: formation, regulation and diversity. Biochim Biophys Acta 1827(3):455–469. doi:10.1016/j.bbabio.2012.12.010

Sambrook J, Russell DW (2001) Molecular cloning: a laboratory manual, 3rd edn. Cold Spring Harbor Laboratory Press, Cold Spring Harbor, N.Y.

Schaffer S, Weil B, Nguyen VD, Dongmann G, Günther K, Nickolaus M, Hermann T, Bott M (2001) A high-resolution reference map for cytoplasmic and membrane-associated proteins of *Corynebacterium glutamicum*. Electrophoresis 22(20):4404–4422

Schweiger P, Volland S, Deppenmeier U (2007) Overproduction and characterization of two distinct aldehyde-oxidizing enzymes from *Gluconobacter oxydans* 621H. J Mol Microbiol Biotechnol 13(1–3):147–155. doi:10.1159/000103606

Shinagawa E, Matsushita K, Adachi O (1984) Gluconate dehydrogenase, 2-keto-gluconate yielding, from *Gluconobacter dioxyacetonicus*: purification and characterization. Agric Biol Chem 48:1517–1522

Shinagawa E, Matsushita K, Adachi O, Ameyama M (1981) Purification and charcterization of 2-keto-D-gluconate dehydrogenase from *Gluconobacter melanogenus*. Agric Biol Chem 45:1079–1085

Simon R, Priefer U, Pühler A (1983) A broad host range mobilization system for *in vivo* genetic-engineering-transposon mutagenesis in Gram-negative bacteria. Bio-Technol 1(9):784–791. doi:10.1038/nbt1183-784

Smith PK, Krohn RI, Hermanson GT, Mallia AK, Gartner FH, Provenzano MD, Fujimoto EK, Goeke NM, Olson BJ, Klenk DC (1985) Measurement of protein using bicinchoninic acid. Anal Biochem 150(1):76–85

Sootsuwan K, Lertwattanasakul N, Thanonkeo P, Matsushita K, Yamada M (2008) Analysis of the respiratory chain in ethanologenic *Zymomonas mobilis* with a cyanide-resistant *bd*-type ubiquinol oxidase as the only terminal oxidase and its possible physiological roles. J Mol Microbiol Biotechnol 14(4):163–175. doi:10.1159/000112598

Spencer ME, Guest JR (1973) Isolation and properties of fumarate reductase mutants of *Escherichia coli*. J Bacteriol 114(2):563–570

Toyama H, Furuya N, Saichana I, Ano Y, Adachi O, Matsushita K (2007) Membrane-bound, 2-keto-D-gluconate-yielding D-gluconate dehydrogenase from "*Gluconobacter dioxyacetonicus*" IFO 3271: molecular properties and gene disruption. Appl Environ Microbiol 73(20):6551–6556. doi:10.1128/AEM.00493-07

Toyama H, Soemphol W, Moonmangmee D, Adachi O, Matsushita K (2005) Molecular properties of membrane-bound FAD-containing D-sorbitol dehydrogenase from thermotolerant *Gluconobacter frateurii* isolated from Thailand. Biosci Biotechnol Biochem 69(6):1120–1129. doi:10.1271/bbb.69.1120

Van Vranken JG, Na U, Winge DR, Rutter J (2015) Protein-mediated assembly of succinate dehydrogenase and its cofactors. Crit Rev Biochem Mol Biol 50(2):168–180. doi:10.3109/10409238.2014.990556

Yuan Z, Yin B, Wei D, Yuan YR (2013) Structural basis for cofactor and substrate selection by cyanobacterium succinic semialdehyde dehydrogenase. J Struct Biol 182(2):125–135. doi:10.1016/j.jsb.2013.03.001

3.2 Increased cell yield of *G. oxydans* on glucose

Own contribution to this publication: about 70 %. I performed all experimental work described in the publication and wrote a draft of the manuscript. I am first author of the publication.

To be submitted

Metabolic engineering of *Gluconobacter oxydans* 621H for improved growth yield on glucose by prevention of gluconate and acetate formation and completion of the tricarboxylic acid cycle

Abstract

The obligatory aerobic acetic acid bacterium *Gluconobacter oxydans* rapidly oxidizes diverse carbon sources regio- and stereoselectively in the periplasm. The products mainly remain in the medium without being further oxidized. These features are favorable for oxidative biotransformations, e. g. in vitamin C production, but they are unfavorable for biomass formation, as only a small fraction of the carbon sources enter the cytoplasm. Cytoplasmic carbon metabolism is characterized by an interrupted glycolysis and an incomplete tricarboxylic acid (TCA) cycle due to the lack of phosphofructokinase, succinyl-CoA synthetase, and succinate dehydrogenase. Excess pyruvate is converted to acetate via pyruvate decarboxylase and NADP-dependent acetaldehyde dehydrogenase. In order to increase the cell yield on glucose, we sequentially replaced (i) *gdhS* encoding the cytoplasmic NADP-dependent glucose dehydrogenase by the *Acetobacter pasteurianus sdhCDABE* genes for succinate dehydrogenase and the flavinylation factor SdhE (strain IK001), (ii) *pdc* encoding pyruvate decarboxylase by a second *ndh* gene encoding a type II NADH dehydrogenase (strain IK002.1), and (iii) *gdhM* encoding the membrane-bound PQQ-dependent glucose dehydrogenase by *sucCD* from *Gluconacetobacter diazotrophicus* encoding succinyl-CoA synthetase (strain IK003.1). Analysis under controlled cultivation conditions in bioreactors revealed that formation of gluconate, 2-ketogluconate, and acetate was eliminated for IK003.1. The strain excreted some 5-ketogluconate and pyruvate instead of acetate. CO_2 formation was more than doubled compared to the reference strain. Growth of IK003.1 was retarded, but the cell yield was improved by 60 %, allowing a significant reduction of the glucose costs for biomass formation. Furthermore, IK003.1 serves as suitable host for further metabolic engineering addressing bottlenecks in pyruvate and acetyl-CoA oxidation that were identified by enzyme activity measurements.

Introduction

Gluconobacter oxydans is a Gram-negative, strictly aerobic acetic acid bacterium belonging to the α-proteobacteria. Since the 1930s it is in industrial use for vitamin C production and later also for several other oxidative biotransformations. The organism possesses a variety of membrane-bound dehydrogenases facing with their catalytic centers the periplasm and oxidizing monosaccharides and alcohols regio- and stereoselectively (Deppenmeier et al. 2002; Adachi et al. 2003b; Mamlouk and Gullo 2013; Nishikura-Imamura et al. 2014; Macauley et al. 2001; Raspor and Goranovič 2008).

When cultivated on glucose, more than 90 % of the substrate is converted to gluconate, mainly by the membrane-bound PQQ-dependent glucose dehydrogenase and to a lesser extent by the cytoplasmic NADP-dependent glucose dehydrogenase (Hanke et al. 2013). Up to now, the transporter(s) responsible for glucose uptake are not known for *G. oxydans*. The presence of an incomplete PEP: carbohydrate phosphotransferase system (PTS) lacking the EIIC and EIIB components suggests a regulatory rather than a transporter function (Prust et al. 2005). Beside these PTS components, the genome of *G. oxydans* lacks several genes for central metabolic enzymes, such as phosphofructokinase, phosphotransacetylase, acetate kinase, succinyl-CoA synthetase, succinate dehydrogenase, isocitrate lyase, and malate synthase. This results in non-functionality or absence of glycolysis, the tricarboxylic acid (TCA) cycle, and the glyoxylate shunt (Prust et al. 2005) and the inability to utilize acetate as carbon source. Excess pyruvate formed either via the pentose phosphate pathway or the Entner-Doudoroff pathway (Richhardt et al. 2012, 2013a) is converted to acetate via pyruvate decarboxylase and acetaldehyde dehydrogenase with acetaldehyde as intermediate (Krajewski et al. 2010). The aerobic respiratory chain involves two terminal ubiquinol oxidases, cytochrome bo_3 oxidase and a cyanide-insensitive cytochrome *bd*-type oxidase termed CIO (Richhardt et al. 2013b; Miura et al. 2013; Matsushita et al. 1987). The bo_3 oxidase was shown to be of prime importance for energy generation (Richhardt et al. 2013b).

The incomplete periplasmic oxidation of glucose to gluconate and ketogluconates and the restricted intracellular catabolism cause a very low cell yield in the range of 0.1 g cell dry weight (cdw) per g glucose. This makes industrial biomass production for oxidative biotransformations costly. As a first step to establish a functional TCA cycle in *G. oxydans*, we recently described the plasmid-based synthesis of succinate dehydrogenase from *Acetobacter pasteurianus* in *G. oxydans* (Kiefler et al. 2015). This membrane-bound enzyme is composed of four subunits and contains covalently bound FAD, three iron-sulfur clusters, and one heme *b* moiety. Functional expression of the *A. pasteurianus sdhCDAB* genes was dependent on the co-expression of the *sdhE* gene encoding an assembly factor involved in flavinylation of SdhA. Despite high succinate dehydrogenase activity of up to 4 μmol min^{-1}

(mg protein)$^{-1}$, the recombinant *G. oxydans* strain did not reach a higher cell yield than the reference strain (Kiefler et al. 2015).

The aim of the current study was to increase the cell yield of *G. oxydans* 621H from glucose by preventing periplasmic and cytoplasmic glucose oxidation to gluconate as well acetaldehyde and acetate formation from pyruvate and by completion of the TCA cycle. In this way, glucose should be completely metabolized in the cytoplasm allowing for an increased precursor supply for biomass synthesis and the possibility of a complete oxidation of glucose to CO_2 via the TCA cycle.

Materials and methods

2.1. Materials

Chemicals were obtained from Sigma-Aldrich (Taufkirchen, Germany), Qiagen (Hilden, Germany), Merck (Darmstadt, Germany) and Roche Diagnostics (Mannheim, Germany).

2.2. Bacterial strains, plasmids, media and growth conditions

The bacterial strains and plasmids used in this study are listed in Table 1. The *E. coli* strains were cultivated in lysogeny broth (LB) medium or on LB agar plates at 37 °C (Bertani 1951, 2004). When required, kanamycin was added to a final concentration of 50 µg mL^{-1}. *A. pasteurianus* (DSM3509 = NBRC3191) was precultured as described previously (Kiefler et al. 2015). Genomic data were taken from the genome sequence of *A. pasteurianus* IFO 3283_01 (Azuma et al. 2009). *Gluconacetobacter diazotrophicus* DSM5601 was cultivated on 220 mM (4 % w/v) mannitol, 5 g L^{-1} yeast extract, 2.5 g L^{-1} $MgSO_4$ x 7 H_2O, 1 g L^{-1} $(NH_4)_2SO_4$, 1 g L^{-1} KH_2PO_4, pH 6 at 28 °C and 140 rpm. *G. oxydans* ATCC 621H Δ*upp* (ATCC 621H is identical to DSM2343), which lacks the *upp* gene for uracil phosphoribosyltransferase, was kindly obtained from Dr. Armin Ehrenreich (Technical University of Munich, Germany). This strain and *G. oxydans* DSM3504 were cultivated on medium containing 220 mM (4 % w/v) mannitol or 110 mM (2 % w/v) glucose, 5 g L^{-1} yeast extract, 2.5 g L^{-1} $MgSO_4$ x 7 H_20, 1 g L^{1} $(NH_4)_2SO_4$, 1 g L^{-1} KH_2PO_4 and 10 µM thymidine. The initial pH value of the medium was 6.0. *G. oxydans* possesses a natural resistance towards cefoxitin; as a precaution to prevent bacterial contaminations, cefoxitin was added to the media at a concentration of 50 µg mL^{-1}. When required, kanamycin (50 µg mL^{-1}) was added. Precultures were grown in baffled shaking flasks at 30 °C and 140 rpm. Main cultures were grown in 500 mL baffled shake flasks containing 100 mL medium with the carbon source indicated in the text. Incubation was at 140 rpm and 30 °C in an Infors shaker (Basel,

Switzerland) (Kiefler et al. 2015). For the determination of growth parameters with glucose as carbon source, the strains were cultivated in 250 mL of the same medium in a bioreactor system (DASGIP, Jülich, Germany) as described previously (Kiefler et al. 2015).

2.3. Cloning and DNA techniques

DNA manipulation was performed by standard methods as described by Green and Sambrook (Green and Sambrook 2012). For PCR reactions, genomic DNA served as template for the amplification. Competent cells of *E. coli* were prepared with $CaCl_2$ and transformed as described previously (Hanahan et al. 1991). DNA sequencing was performed by Eurofins MWG Operon (Ebersberg, Germany). Oligonucleotides were synthesized by Biolegio (Nijmegen, Netherlands) and are listed in Table 1. Conjugation of *G. oxydans* was performed by using *E. coli* S17-1 as donor strain. *G. oxydans* and *E. coli* main cultures were inoculated to an OD_{600} of 0.15-0.2 and harvested at an OD_{600} of 0.5-0.8. The cultures (50 mL) were centrifuged (10,414 x *g*, 3 min, 4 °C), resuspended in 25 mL 0.9 % NaCl and the procedure was repeated twice. The pellets were resuspended in 0.9 % NaCl and mixed. Cell suspension was dropped on a mannitol plate without antibiotics and incubated over night at 30 °C. Subsequently the cells were scraped from the agar plate and resuspended in 1 mL of mannitol medium. This cell suspension was plated in different dilutions on mannitol plates containing cefoxitin and kanamycin, thereby selecting for *G. oxydans* exconjugants.

2.4. Construction of expression plasmids for succinate dehydrogenase and succinyl-CoA synthetase

For the construction of expression plasmid pBBR1p264-sdh-Pnat-sdhE amplification of insert sdhCDAB-Pnat-sdhE was obtained as described previously (Kiefler et al. 2015). The HindIII/XhoI restricted insert was ligated into the HindIII/XhoI linearized vector pBBR1p264 resulting in the *sdhCDABE* expression plasmid. Expression plasmid pBBR1p264-sucCD was constructed via amplification of the *sucCD* genes from genomic DNA of *G. diazotrophicus* with oligonucleotide pair sucCD_forw_EcoRI/ sucCD_rev_HindIII_2. The insert was restricted with EcoRI/HindIII and cloned into vector pBBR1p264 also restricted with EcoRI/HindIII. These plasmids later served for construction of pAJ63a derivatives.

2.5. Genomic integration of sdhCDABE, sucCD and *ndh*

For construction of the integration plasmid pAJ63a-sdhCDAB-Pnat-sdhE-gdhS the upstream and downstream regions (500 bp each) of the *gdhS* gene (cytoplasmic glucose dehydrogenase, GOX2015) were amplified with the oligonucleotide pairs gdhS-forw-FlA/gdhS-rev-FlA and gdhS-forw-FlB/gdhS-rev-FlB and fused by overlap extension PCR with the oligonucleotide pair gdhS-forw-FlA/gdhS-rev-FlB. Subsequently, the DNA fragment

(FlAB) was cloned into the SmaI-restricted vector pAJ63a. The resulting plasmid pAJ63a-FlAB-gdhS was restricted via a SmaI site introduced between the *gdhS* upstream and downstream regions. Plasmid pBBR1p264-sdh-Pnat-sdhE served as template for amplification of the insert p264-sdh-Pnat-sdhE via PCR using the oligonucleotide pair p264-forw/p264-seq1-rev. The PCR fragment was phosphorylated with T4 polynucleotide kinase (Roche Diagnostics) and ligated into the SmaI-linearized and shrimp alkaline phosphatase-dephosphorylated plasmid pAJ63a-FlAB-ghdS. The resulting plasmid pAJ63a-sdhCDAB-Pnat-sdhE-gdhS was checked by DNA sequencing and transferred into *G. oxydans* 621H Δ*upp* via conjugation using *E. coli* S17-1 as donor strain. Exconjugants showing a kanamycin-resistant phenotype were tested by colony PCR with the oligonucleotide pair gdhS_mut_forw_2/gdhS_mut_rev_2 for integration of the plasmid into the genome. Identified integrants were subjected to excision enforcement in recombination medium and subsequently plated on 5`-fluorouracil-containing mannitol plates as described previously (Peters et al. 2013a). Kanamycin-sensitive clones were tested via colony PCR for genomic integration of the *sdhCDABE* genes and simultaneous deletion of the *gdhS* gene using the oligonucleotide pairs gdhS_mut_forw_2/gdhS_mut_rev_2 for amplification of integrated *sdhCDABE* genes and gdhS-forw/gdhS-rev for showing that an internal part of the *gdhS* gene cannot be amplified anymore. Sequencing of the *gdhS* region (gdhS_mut_forw_2/gdhS_mut_rev_2) amplified from genomic DNA using Phusion polymerase also verified the genomic integration of *sdhCDABE* in *G. oxydans*. The resulting strain was termed IK001.

For construction of the integration plasmid pAJ63a-Pnat-ndh-pdc, 500 bp upstream and downstream of the *pdc* gene encoding pyruvate decarboxylase (GOX1081) were amplified with the oligonucleotide pairs pdc-forw-FlA/pdc-rev-FlA and pdc-forw-FlB/pdc-rev-FlB using genomic DNA of *G. oxydans* 621H Δ*upp* as template. The two PCR fragments were then fused via overlap extension-PCR with the oligonucleotide pair pdc-forw-FlA/pdc-rev-FlB. After phosphorylation of the fusion product with T4 polynucleotide kinase, it was cloned into the SmaI-dephosphorylated vector pAJ63a vector, resulting in plasmid pAJ63a-FlAB-pdc. The *ndh* (GLS_c05650) gene with its native promoter was amplified with the oligonucleotide pair GLS-pnatc05650-forw/GLS-c05650-rev-KpnI using genomic DNA of *G. oxydans* DSM3504 as template. After phosphoryation of the *ndh* PCR product it was cloned into pAJ63a-FlAB-pdc that had been restricted with SmaI and dephosphorylated. Genomic integration of the *ndh* gene into the *pdc* locus of strain IK001 was performed as described above and the selected clones were checked by colony PCR with the oligonucleotide pairs pdc-mut-forw/pdc-mut-rev and pdc-for_2/pdc-rev_2 and DNA sequencing of a fragment obtained with oligonicleotides pdc-mut-forw/pdc-mut-rev. The resulting strain was named IK002.1.

Integration plasmid pAJ63a-sucCD-gdhM was constructed by amplification of 500 bp upstream and downstream of the *gdhM* gene encoding the membrane-bound glucose dehydrogenase (GOX0265) using the oligonucleotide pairs gdhM-forw-FlA/gdhM-rev-FlA-EcoRV and gdhM-forw-FlB-EcoRV/gdhM-rev-FlB. The two PCR products were fused by overlap extension-PCR with the oligonucleotide pair gdhM-forw-FlA/gdhM-rev-FlB. The fusion product was cloned into the SmaI-linearized vector pAJ63a resulting in pAJ63a-FlAB-gdhM. Insert p264-sucCD was amplified from the expression plasmid pBBR1p264-sucCD by PCR with the oligonucleotide pair p264-forw/sucCD-rev-HindIII_2 and phosphorylated with T4 polynucleotide kinase. Subsequently, the insert was ligated into dephosphorylated pAJ63a-FlAB-gdhM, which had been linearized via an introduced EcoRV restriction site between the up- and downstream *gdhM* regions. Genomic integration of the *sucCD* genes into the *gdhM* locus of the *G. oxydans* strain IK002.1 was performed as described above and the selected clones were checked by colony PCR with the oligonucleotide pairs gdhM-mut-forw_2/gdhM-mut-rev_2 and gdhM-forw/ghdM-rev and sequencing of a DNA fragment amplified with oligonucleotide pair gdhM-mut-forw_2/gdhM-mut-rev_2. The resulting strain was named IK003.1.

2.6. Preparation of cell extracts and membranes for enzyme assays

For the measurement of citrate synthase, aconitase, isocitrate dehydrogenase, 2-oxoglutarate dehydrogenase, succinyl-CoA synthetase and fumarase activies, *G. oxydans* strains were cultivated in 50 mL mannitol medium at 30 °C and 140 rpm and *E. coli* in 50 mL LB medium at 37 °C and 130 rpm (Infors shaker, Basel, Switzerland) for 10 h. The cells were harvested (10,414 x *g*, 3 min, 4 °C) and resuspended in 300 µL of the buffers used in the corresponding enzyme assay (see below). The cell suspension was mixed with 250 mg zirconia/silica beads (0.1-mm diameter; Biospec, Bartlesville, USA) in a 1.5 mL Eppendorf tube, and the cells were mechanically disrupted by 3 x 20 sec bead-beating in a Silamat S5 (Ivoclar Vivadent, Ellwangen, Germany). Cell debris and unbroken cells were sedimented by 30 min centrifugation at 16,100 x *g* at 4 °C. The resulting supernatant was used as cell extract and kept on ice until it was used for the assay. Membrane preparations for the determination of the activities of succinate dehydrogenase, malate:quinone oxidoreductase, and NADH dehydrogenase were performed as described by Kiefler et al. (Kiefler et al. 2015).

The protein concentration of cell extracts was determined according to Bradford using bovine serum albumin as standard (Bradford 1976). The protein concentration of membranes was determined with the bicinchoninic acid (BCA) protein assay (Interchim, Montluçon, France) using bovine serum albumin (BSA) as standard.

2.7. Enzyme assays

The determination of citrate synthase activity was based on the reaction of coenzyme A with 5,5-dithiobis(2-nitrobenzoic acid) (Ellman's reagent). The absorbance of the resulting yellow 2-nitro-5-thiobenzoate dianion was measured spectrophotometrically at 412 nm as described previously (Radmacher and Eggeling 2007). Aconitase activity was assayed by a coupled assay with isocitrate dehydrogenase in which the formation of NADPH at 340 nm was monitored. The reaction mixture contained 100 mM Tris-HCl pH 8.0, 20 mM trisodium citrate, 1 mM $NADP^+$, 1 mM $MnSO_4$ and 1.6 U isocitrate dehydrogenase (USB Corporation, Cleveland, OH, USA) (Baumgart and Bott 2011). Isocitrate dehydrogenase was assayed as described by measuring the formation of NADPH (Eikmanns et al. 1995; Nachlas et al. 1963). 2-Oxoglutarate dehydrogenase activity was measured at 30 °C in a photometric assay by following the initial increase in absorbance of NADH at 340 nm (Niebisch et al. 2006). The succinyl-CoA synthetase activity measurement was based on the reaction of CoASH with Ellman's reagent (Kersters and De Ley 1968) resulting in CoA formation monitored at 412 nm (Hauge et al. 1955). The fumarase assay was conducted with malate as substrate measuring fumarate concentration at 250 nm nm (Genda et al. 2006). For measurement of the activity of the pyruvate dehydrogenase complex (Niebisch et al. 2006) a cell-free extract of a *G. oxydans pdc* deletion mutant was used, since the presence of pyruvate decarboxylase impedes this activity determination (Bringer-Meyer and Sahm 1993). NADH dehydrogenase activity measurment was performed with the membrane fraction following the NADH oxidation at 385 nm (Bringer et al. 1984). For all enzymes mentioned above, one unit (U) of enzyme activity is defined as 1 nmol of product formed per minute.

Succinate:DCPIP reductase and malate:DCPIP reductase activities were determined with the membrane protein fraction as described previously (Kiefler et al. 2015). One molecule DCPIP is reduced by one molecule succinate or malate. One unit (U) is defined as 1 nmol DCPIP reduced per min.

2.8. Determination of substrates and products by HPLC analysis

One mL culture was centrifuged for 2 min at 13,000 x *g* and the supernatant was filtered through a 0.2 µm filter (Millipore, MA, USA) prior to HPLC analysis. Gluconate, 2-ketogluconate and 5-ketogluconate were quantified by method A with a Shodex RSpak DE-413L 250 × 4.6 mm ID column (CS Chromatographie Service GmbH, Langerwehe, Germany) at 40 °C using 2 mM $HClO_4$ as the eluent at a flow rate of 0.5 mL min^{-1}. Gluconate, 2-ketogluconate, and 5-ketogluconate were detected by an UV detector at 190 nm. Retention times for 2-ketogluconate, gluconate and 5-ketogluconate were 5.5, 6.0 and 6.5 min, respectively (Richhardt et al. 2013a). Since separation of pyruvate and 5-ketogluconate was not possible by method A, method B was applied for further quantification of gluconate, 2-

ketogluconate, and 5-ketogluconate. Method B was carried out with a Rezex organic acid HPLC column (300 x 7.8 mm, Phenomenex, Aschaffenburg, Germany) at 65 °C by an isocratic separation with 92 % 1 mM H_2SO_4 and 8 % 100 mM H_2SO_4 as eluent at a flow rate of 0.3 mL min^{-1}. Gluconate, 2-ketogluconate and 5-ketogluconate were detected by an UV detector at 215 nm. Retention times for 2-ketogluconate, 5-ketogluconate and gluconate were 20.3 min, 21 min and 22.6 min, respectively. Calibration curves were prepared using concentration series ranging from 0-20.4 mM gluconate, 0-20.6 mM 2-ketogluconate and 0-20.6 mM 5-ketogluconate. Pyruvate, succinate, acetate and fumarate concentrations were measured with an Organic Acid Resin 300 × 8 mm column (CS Chromatographie Service, Langerwehe, Germany) at 25 °C using 8 mM H_2SO_4 as the eluent at a flow rate of 0.6 mL min^{-1}. Pyruvate, succinate, acetate and fumarate were detected with an UV detector at 215 nm, and the retention times were 11.5, 14.6, 18.15 and 20.42 min, respectively. Calibration curves were made using a series of standards ranging from 1 to 10 mM of the corresponding acid.

2.9 Enzymatic determination of glucose concentrations

One mL culture was centrifuged 2 min at 13,000 x *g* and the supernatant was filtered through a 0.2 µm filter (Millipore, MA, USA) prior to the glucose assay. Glucose concentrations were determined by a coupled enzymatic assay with hexokinase and glucose 6-phosphate dehydrogenase by measuring NADPH formation spectrophotometrically at 340 nm using suitable dilutions of the supernatant according to the method described previously (Richhardt et al. 2013a).

2.10. Determination of cell dry weight and calculation of cell yield

At different time points during growth of the *G. oxydans* strains in a bioreactor system with four vessels, the optical densities at 600 nm were determined and the cell dry weight was determined as described (Richhardt et al. 2012). A linear correlation between cell dry weight and OD_{600} was obtained with an OD_{600} of 1 corresponding to 0.36 g of cell dry weight per liter. The cell yield $Y_{X/S}$ represents g cell dry weight formed per g glucose consumed.

Results

3.1 Metabolic engineering of G. oxydans strains for improved growth yield on glucose

The strategy to engineer a *G. oxydans* strain with improved biomass yield on glucose (Fig. 1A) involved (i) the completion of the disrupted TCA cycle by genomic integration of the *A. pasteurianus* succinate dehydrogenase genes (*sdhCDAB*) and the assembly factor gene *sdhE* and of the succinyl-CoA synthetase genes (*sucCD*) from *Ga. diazotrophicus*, (ii) the

chromosomal integration of a second NADH dehydrogenase gene (*ndh*) from the *G. oxydans* strain DSM3504 (Kostner et al. 2015) to allow for increased NADH oxidation capacity, (iii) the elimination of gluconate formation from glucose by deletion of the genes *gdhS* and *gdhM* for the soluble and the membrane-bound glucose dehydrogenase, respectively, thereby enforcing cytosolic glucose catabolism, and (iv) elimination of acetaldehyde and acetate formation from pyruvate by deletion of the pyruvate decarboxylase gene (*pdc*). The task of genomic integration of heterologous genes and deletion of undesired genes was combined by simultaneous insertion and deletion. For the expression of the genes, either the native promoters (*sdhE*, *ndh*) or promoters of genes encoding the ribosomal proteins L35 (GOX0264, P264), L13 (GOX0452, P452), or S12 (GOX0384, P384) were used (Kallnik et al. 2010). P384, P452, and P264 represent weak, moderate, and strong promoters, respectively.

Fig. 1B shows the seven strains with genomic modifications constructed in this work. The first series of strains, named IK-A, IK-B, and IK-C, included the weak promoter P384 in front of *sdhCDAB* and the native promoter in front of *sdhE* replacing the *gdhS* gene, the moderate promoter P452 in front of *sucCD* replacing the *gdhM* gene, and P384 in front of the *Zymonomas mobilis glf* gene and *glk* gene replacing the *pdc* gene. The glucose facilitator gene *glf* and glucokinase gene *glk* were introduced in order to increase glucose uptake and catabolism. Cultivation on glucose in a bioreactor system revealed retarded and unreproducible growth of strain IK-B (Fig. S1 A). Strain IK-C showed a retarded growth, but reached a higher final OD_{600} than the reference strain (Fig. S1 B). However, these genomic changes did not result in enhanced cell yields and only minimal *in vitro* activities of the introduced enzymes (succinate dehydrogenase, succinyl-CoA synthetase, glucose kinase) were detectable (data not shown). A second series of strains was initiated by placing the strong promoter P264 in front of *sdhCDAB* and again the native promoter in front of *sdhE*, these genes replacing the *gdhS* gene (IK001). In the second step, the *sucCD* genes under control of P264 replaced the *pdc* gene in IK001, resulting in strain IK002.0. Due to the fact that the integration of a *ndh* gene into the *gdhM* locus was not possible, it was not used for further strain development (Supplement). Consequently, instead of *sucCD*, the *ndh* gene (GLS_c05650) of *G. oxydans* DSM3504 under control of its native promoter was used to replace the chromosomal *pdc* gene, resulting in strain IK002.1. In the third step, the *sucCD* genes under control of P264 were used to replace the *gdhM* gene in IK002.1, resulting in strain IK003.1. These experiments suggested that the type of promoter used, the locus of the integration, and the order of the metabolic engineering steps influence strain stability. The genomic integrations and deletions were confirmed by colony PCR and sequencing of the resulting DNA fragments.

3.2 Growth parameters of the G. oxydans strains IK001, IK002.1, and IK003.1

The growth behavior of strains IK001, IK002.1, and IK003.1 on glucose (110 mM) was studied in a bioreactor system under constant conditions of pH 6 and 15 % dissolved oxygen. *G. oxydans* 621H Δ*upp* was used as reference strain. The growth parameters of the three recombinant strains and the reference strain are summarized in Table 2 and the kinetics of growth, glucose consumption, and product formation are shown in Figs. 2 and 3. The calculations of the carbon balances are summarized in Table S1.

Strain IK001 (Δ*gdhS*::*sdhCDABE*) containing succinate dehydrogenase and lacking the soluble glucose dehydrogenase showed a slightly faster growth rate (0.3699 ± 0.0090 h^{-1}) than the reference strain (0.3634 ± 0.0341 h^{-1}) (Fig. 2A) and the cell yield was not changed (Table 2). The kinetics of glucose consumption and product formation were comparable for IK001 and the reference strain (Fig. 2B and 2C), but IK001 formed slightly more 2-ketogluconate (10 mM) and less CO_2 (38 mM). 2-Ketogluconate is formed by the membrane-bound flavoprotein gluconate 2-dehydrogenase (GOX1230-1232) (Weenk et al., 1984; Prust et al., 2005). With 104 % the carbon balance, which does not include carbon derived from the yeast extract, was almost closed for both strains (Table 2 and Table S1). The succinate:DCPIP reductase activity of the membrane fraction of strain IK001 was 75 nmol min^{-1} (mg protein)$^{-1}$ and thus far above the background activity of 4 nmol min^{-1} (mg protein)$^{-1}$ of the reference strain, indicating the presence of a functional succinate dehydrogenase (Table 3). The inconspicuous growth phenotype of strain IK001 compared to the reference strain is in accordance with the minor role of the soluble glucose dehydrogenase in gluconate formation (Pronk et al. 1989; Rauch et al. 2010).

Strain IK002.1 (Δ*gdhS*::*sdhCDABE* Δ*pdc*::*ndh*), which contained in addition to IK001 a second *ndh* gene and lacked pyruvate decarboxylase, showed a decreased growth rate of 0.2478 ± 0.0113 h^{-1}, but the cell yield was increased by 12 % (Fig. 3A, Table 2). Whereas formation of 2-ketogluconate was somewhat decreased compared to the reference strain (31 mM vs. 39 mM), IK002.1 accumulated 21 mM 5-ketogluconate in the supernatant, which was not detected in the supernatant of the reference strain (Fig. 3B). Caused by the absence of pyruvate decarboxylase, acetate formation was almost completely abolished and instead of acetate strain IK002.1 excreted comparable concentrations of pyruvate (35 mM) (Fig. 3C). The NADH dehydrogenase activity determined with the membrane fraction of IK002.1 was 9630 ± 2620 nmol min^{-1} (mg protein)$^{-1}$ and thus only 11 % higher than the activity of the reference strain (8670 ± 1590 nmol min^{-1} (mg protein)$^{-1}$). This might be due to a low activity of the native promoter of the *ndh* gene from *G. oxydans* strain DSM3504. The carbon balance of IK002.1 (120 %) revealed a 20 % surplus in the products, which must be caused by an increased usage of compounds of the yeast extract.

Strain IK003.1 (Δ*gdhS*::*sdhCDABE* Δ*pdc*::*ndh* Δ*gdhM*::*sucCD*) contains in addition to IK002.1 the succinyl-CoA synthetase genes, but lacks the membrane-bound PQQ-dependent glucose dehydrogenase, which is the key enzyme for the rapid initial oxidation of glucose to gluconate. The deletion of *gdhM* had noticeable consequences for growth and product formation (Fig. 3). IK003.1 exhibited retarded growth (0.1678 ± 0.0014 h^{-1}) in line with retarded glucose consumption. Glucose was completely metabolized after 28 h, whereas it required only 6 h in the reference strain (Fig. 2E). The OD_{600} of IK003.1 increased until the cultivation was terminated after 28 h and reached a value of 7.9, whereas in the reference strain the OD_{600} reached its maximum of 4.6 after about 12 h. Most importantly, the cell yield of IK003.1 was increased by 60 % compared to the reference strain (Fig. 3D, Table 2). As expected from the deletion of *gdhM* and *gdhS*, neither gluconate nor 2-ketogluconate were formed by strain IK003.1 (Fig. 3E). Surprisingly, like IK002.1 also strain IK003.1 formed up to 20 mM 5-ketogluconate. The succinyl-CoA synthetase activity measured in cell-free extracts of IK003.1 was 3.2 ± 1.2 nmol min^{-1} (mg protein)$^{-1}$, which is 4.5-fold above the background level of 0.7 ± 1.7 nmol min^{-1} (mg protein)$^{-1}$ measured in the reference strain. This suggests that the *sucCD* genes are functionally expressed, but allow only for a very low succinyl-CoA synthetase activity. Similar to strain IK002.1, IK003.1 produced 38 mM pyruvate instead of acetate (Table 2), suggesting a bottleneck in pyruvate dissimilation despite the potential presence of a functional TCA cycle. A distinctive characteristic of IK003.1 was an increased formation of CO_2, the amount being more than twice as high than in the reference strain or IK001 and IK002.1 (Table 2). The calculation of the carbon balance for IK003.1 revealed a surplus of 30 % in the products formed compared to the glucose consumed, in line with an increased utilization of yeast extract components for biomass formation.

3.3 In vitro activities of the endogenous TCA cycle enzymes and the pyruvate dehydrogenase complex

As described above, IK003.1 produced 38 mM pyruvate despite the introduction of heterologous succinyl-CoA synthetase and succinate dehydrogenase that should enable a functional TCA cycle. Even if the activity of the TCA cycle would be low, at least partial dissimilation of pyruvate should be possible. In order to find the reason(s) for the bottleneck in pyruvate dissimilation, we measured the activities of the pyruvate dehydrogenase complex and of the endogenous TCA cycle enzymes citrate synthase, aconitase, isocitrate dehydrogenase, 2-oxoglutarate dehydrogenase, fumarase, and malate:quinone oxidoreductase in cell-free extracts or the membrane fraction. As shown in Table 3, no pyruvate dehydrogenase complex activity could be detected, although *G. oxydans* possesses the corresponding genes *aceEα-aceEβ-aceF-lpd* (GOX2289-2292). In order to

exclude technical reasons for the inability to measure pyruvate dehydrogenase complex activity, we transformed IK003.1 with plasmid pBBR1p452-pdhC expressing the genes *aceEα-aceEβ-aceF-lpd* under the control of promoter P452. Growth of the recombinant strain was significantly inhibited compared to the reference strain IK003.1 carrying the vector pBBR1p452 (data not shown), but in cell-free extracts a pyruvate dehydrogenase complex activity of 95 nmol min^{-1} (mg protein)$^{-1}$ was measured, showing that the assay conditions were suitable. The apparent absence of pyruvate dehydrogenase complex activity might explain the inability for pyruvate dissimilation in strain IK003.1.

For citrate synthase, oxoglutarate dehydrogenase, fumarase, and malate:quinone oxidoreductase, activities between 10 and 20 nmol min^{-1} (mg protein)$^{-1}$ were determined in the *G. oxydans* reference strain. The activities measured for aconitase and isocitrate dehydrogenase were much lower, for the latter enzyme even below 1 nmol min^{-1} (mg protein)$^{-1}$. Therefore, despite the functional expression of heterologous succinate dehydrogenase and succinyl-CoA synthetase in strain IK003.1, the activity of the TCA cycle is likely to be very limited.

Discussion

With 0.1 or even less g cell dry weight per g glucose consumed, the cell yield of *G. oxydans* 621H is 60-80 % lower than that of many other industrially relevant bacteria cultivated aerobically with glucose as carbon source, such as *E. coli* (Ng 1969), even though the medium contains also yeast extract. The reasons for this low cell yield have been described in the introduction. As the industrial applications of *G. oxydans* are typically oxidative biotranformations (Pappenberger and Hohmann 2014) that require the initial production of *G. oxydans* biomass, a better cell yield would lower the production costs. Therefore, this study aimed at an increase of the cell yield of *G. oxydans* 621H on glucose by metabolic engineering. Glucose represents a comparably cheap carbon source and the metabolic alterations for an improved cell yield should not interfere with the activity of the membrane-bound dehydrogenases involved in industrial applications.

The strategy applied involved the elimination of periplasmic and cytoplasmic oxidation of glucose to gluconate, the elimination of pyruvate decarboxylation, the establishment of a functional TCA cycle by introduction of heterologous succinate dehydrogenase and succinyl-CoA synthetase, and the improvement of the NADH oxidation capacity by introduction of a second NADH dehydrogenase gene. The introduction of the heterologous genes (*sdhCDAB-sdhE, ndh, sucCD*) was combined with the simultaneous deletion of the undesired genes (*gdhS*, *pdc*, *gdhM*), resulting in strains IK001, IK002.1, and IK003.1 (Fig. 1B). The replacement of *gdhS* by the *sdh* genes of *A. pasteurianus* in IK001 led to an active succinate

dehydrogenase, but had no influence on the growth yield. The subsequent replacement of *pdc* by *ndh* in strain IK002.1 prevented acetate formation, but led to the secretion of equivalent amounts of pyruvate.

In contrast to IK001, IK002.1 produced significant amounts 5-ketogluconate, which were not metabolized further. At the pH of 6 used during cultivation, 5-ketogluconate synthesis is presumably catalyzed by the NADP-dependent gluconate 5-dehydrogenase (GOX2187, Gno) (Fig. 1) (Hanke et al. 2013). As NADPH can presumably be converted to NADH by the transhydrogenase PntA1A2B, possibly coupled to proton extrusion, the increased NADH oxidation capacity provided by the *ndh* gene in strain IK002.1 might be responsible for 5-ketogluconate formation and reduced 2-ketogluconate synthesis, the latter being formed by the membrane-bound flavoprotein gluconate 2-dehydrogenase (GOX1230-1232) (Weenk et al. 1984; Prust et al. 2005). In a recent study, overexpression of the *ndh* gene from *G. oxydans* DSM3504 in *G. oxydans* 621H using plasmid pAJ78 stimulated growth on mannitol and prevented intermediate accumulation of fructose (Kostner et al. 2015). The authors explained the positive effect of *ndh* overexpression by a competition of the membrane-bound substrate dehydrogenases and NADH dehydrogenase for delivering electrons into the electron transport chain. In the case of IK002.1, the additional chromosomal copy of *ndh* under control of its native promoter caused an increase of the NADH dehydrogenase activity of 960 nmol min^{-1} (mg protein)$^{-1}$, which did not prevent the accumulation of gluconate from glucose. The NADH dehydrogenase activity provided by plasmid pAJ78 was not reported (Kostner et al. 2015), but assuming a copy number of around 10 for pAJ78, the resulting NADH dehydrogenase activity is estimated to be in the range of 10 µmol min^{-1} (mg protein)$^{-1}$. Combined with the native NADH dehydrogenase activity of *G. oxydans* 621H of 8.7 µmol min^{-1} (mg protein)$^{-1}$, the total activity of *G. oxydans* 621H with pAJ78 would be around 20 µmol min^{-1} (mg protein)$^{-1}$. Further studies are required to test if plasmid-based overexpression of *ndh* can stimulate growth with glucose to a larger extent than the single-copy chromosomal expression in strain IK002.1.

The growth yield of IK002.1 was increased by 12 % and the carbon balance of 120 % showed that the increased growth yield was caused by an increased utilization of compounds of the yeast extract. Besides the slightly increased NADH oxidation capacity of IK002.1, the replacement of acetate formation by pyruvate formation may play a role in this context. Acetate with a pK_a of 4.78 is known to act as an uncoupler (Axe and Bailey 1995), whereas pyruvate does not act in this way due to a pK_a of 2.49. Prevention of acetate formation thus could increase the energetic efficiency of strain IK002.1, allowing for an increased utilization of yeast extract components for biomass synthesis.

Strain IK003.1 formed up to 20 mM 5-ketogluconate, although both the membrane-bound and the soluble glucose dehydrogenase are absent. Two possible explanations are the

presence of another glucose dehydrogenase that has not yet been identified or the presence of a 6-phosphogluconate phosphatase that hydrolyses 6-phosphogluconate to gluconate and P_i. In *E. coli*, the protein encoded by *yieH* was shown to catalyze this reaction with a K_m value of 2.2 mM for 6-phosphogluconate and a k_{cat} of 16 s^{-1} (Kuznetsova et al. 2006). A BLAST search revealed that GOX1036 of *G. oxydans* 621H, annotated as a putative phosphatase (Prust et al. 2005), displays 32 % sequence identity to YieH and might function as 6-phosphogluconate phosphatase. The specific glucose 6-phosphate dehydrogenase activity in cell extracts of *G. oxydans* 621H was found to be about five times higher than the 6-phosphogluconate dehydrogenase activity (Richhardt et al. 2012), which might cause an accumulation of 6-phosphogluconate. Such an accumulation was reported to be toxic for several bacteria (Richhardt et al. 2012; Fuhrman et al. 1998) and a 6-phosphogluconate phosphatase might serve to protect the cell from this situation.

A striking feature of strain IK003.1 was the 2.2-fold increased carbon dioxide formation (Table 2). In the absence of pyruvate decarboxylase, the enhanced CO_2 formation is likely caused to a significant extent by the oxidative pentose phosphate cycle, which is the major pathway of sugar degradation in *G. oxydans* (Richhardt et al. 2012; Hanke et al. 2013; Richhardt et al. 2013a). Glucose is completely catabolized in the cytoplasm in IK003.1 and a significant fraction via the pentose phosphate pathway, which can operate in cyclic way in *G. oxydans* (Hanke et al. 2013). If the 2-ketogluconate formed in the reference strain (38 mM) would be completely oxidized to CO_2 via a cyclic PPP in IK003.1, the difference in CO_2 formation could be explained to a large extent. A second possible explanation for the increased CO_2 level formed by IK003.1 could be the activity of a functional TCA cycle. However, as we did not detect pyruvate dehydrogenase complex activity in *G. oxydans* 621H despite the presence of the corresponding genes, a flux of glucose-derived carbon into the TCA cycle might only be possible by carboxylation of PEP to oxaloacetate via PEP carboxylase (GOX0102). The next problem would be the provision of acetyl-CoA, where the only source might be the oxidation of fatty acids or other components of the yeast extract. If acetyl-CoA would be available, also other constituents of the yeast extract, such as aspartate or glutamate could be oxidized in the TCA cycle after conversion to the corresponding 2-ketoacids.

Besides the apparent absence of pyruvate dehydrogenase complex activity, also aconitase and isocitrate dehydrogenase showed very low specific activities in *G. oxydans*, suggesting that despite the successfull introduction of succinate dehydrogenase and succinyl-CoA synthetase the activity of the TCA cycle appears to be very limited and a major contribution to growth may be doubted for strain IK003.1. The generally low activities of the TCA cycle enzymes in *G. oxydans* wild type are not surprising in view of the absence of succinyl-CoA synthetase and succinate dehydrogenase and probably result from the

evolutionary metabolic adaptation to sugar-rich ecological niches in association with plants, which favored incomplete periplasmic oxidations rather than cytoplasmic catabolism. Formation of sugar acids may support the nutrition of the plants by solubilization of phosphorus and zinc (Intorne et al. 2009), thereby also ensuring the provision of substrates for *Gluconobacter*.

The present study has demonstrated that the conversion of the special catabolism of *G. oxydans* with a predominantly periplasmic oxidation of glucose to a more standard-type cytoplasmic catabolism with a functional TCA cycle cannot be achieved simply by provision of the missing enzymes. Rather, the activities of several other enzymes, in particular pyruvate dehydrogenase complex, aconitase, and isocitrate dehydrogenase need to be increased to allow a significant flux through the TCA cycle. Strain IK003.1 presents a suitable parent for these following metabolic approaches aiming at a growth yield in the range of 0.4 – 0.5 g cell dry weigth per g glucose.

Acknowledgements

The scientific activities of the Bioeconomy Science Center were financially supported by the Ministry of Innovation, Science and Research within the framework of the NRW Strategieprojekt BioSC (No. 313/323-400-002 13). We are most grateful to Uwe Deppenmeier (Universität Bonn) for providing plasmids pBBR1p452 and pBBR1p264.

Appendix A. Supplementary materials

Supplementary data associated with this article can be found in the online version at http://dx.doi.org/

References

Adachi, O., Moonmangmee, D., Toyama, H., Yamada, M., Shinagawa, E., Matsushita, K., 2003. New developments in oxidative fermentation. Appl. Microbiol. Biotechnol. 60**,** 643-653.

Axe, D. D., Bailey, J. E., 1995. Transport of lactate and acetate through the energized cytoplasmic membrane of *Escherichia coli*. Biotechnol Bioeng. 47**,** 8-19.

Azuma, Y., Hosoyama, A., Matsutani, M., Furuya, N., Horikawa, H., Harada, T., Hirakawa, H., Kuhara, S., Matsushita, K., Fujita, N., Shirai, M., 2009. Whole-genome analyses reveal genetic instability of *Acetobacter pasteurianus*. Nucleic Acids Res. 37**,** 5768-5783.

Baumgart, M., Bott, M., 2011. Biochemical characterisation of aconitase from *Corynebacterium glutamicum*. J. Biotechnol. 154**,** 163-170.

Bertani, G., 1951. Studies on lysogenesis. I. The mode of phage liberation by lysogenic *Escherichia coli*. J. Bacteriol. 62**,** 293-300.

Bertani, G., 2004. Lysogeny at mid-twentieth century: P1, P2, and other experimental systems. J. Bacteriol. 186**,** 595-600.

Bradford, M. M., 1976. A rapid and sensitive method for the quantitation of microgram quantities of protein utilizing the principle of protein-dye binding. Anal. Biochem. 72**,** 248-254.

Bringer-Meyer, S., Sahm, H., 1993. Formation of acetyl-CoA in *Zymomonas mobilis* by a pyruvate dehydrogenase complex. Arch. Microbiol. 159**,** 197-199.

Bringer, S., Finn, R. K., Sahm, H., 1984. Effect of oxygen on the metabolism of *Zymomonas mobilis*. Arch. Microbiol. 139**,** 376-381.

Deppenmeier, U., Hoffmeister, M., Prust, C., 2002. Biochemistry and biotechnological applications of *Gluconobacter* strains. Appl. Microbiol. Biotechnol. 60**,** 233-242.

Eikmanns, B. J., Rittmann, D., Sahm, H., 1995. Cloning, sequence analysis, expression, and inactivation of the *Corynebacterium glutamicum icd* gene encoding isocitrate dehydrogenase and biochemical characterization of the enzyme. J. Bacteriol. 177**,** 774-782.

Fuhrman, L. K., Wanken, A., Nickerson, K. W., Conway, T., 1998. Rapid accumulation of intracellular 2-keto-3-deoxy-6-phosphogluconate in an Entner-Doudoroff aldolase mutant results in bacteriostasis. FEMS Microbiol. Lett. 159**,** 261-266.

Genda, T., Watabe, S., Ozaki, H., 2006. Purification and characterization of fumarase from *Corynebacterium glutamicum*. Biosci. Biotechnol. Biochem. 70**,** 1102-1109.

Green, M. S., Sambrook, J., 2012. Molecular Cloning: A Laboratory Manual (Fourth Edition), Cold Spring Harbor Laboratory Press, www.molecularcloning.org.

Hanahan, D., Jessee, J., Bloom, F. R., 1991. Plasmid transformation of *Escherichia coli* and other bacteria. Meth. Enzymol. 204**,** 63-113.

Hanke, T., Nöh, K., Noack, S., Polen, T., Bringer, S., Sahm, H., Wiechert, W., Bott, M., 2013. Combined fluxomics and transcriptomics analysis of glucose catabolism via a partially cyclic pentose phosphate pathway in *Gluconobacter oxydans* 621H. Appl. Environ. Microbiol. 79**,** 2336-2348.

Hauge, J. G., King, T. E., Cheldelin, V. H., 1955. Oxidation of dihydroxyacetone via the pentose cycle in *Acetobacter suboxydans*. J Biol Chem. 214**,** 11-26.

Intorne, A. C., de Oliveira, M. V., Lima, M. L., da Silva, J. F., Olivares, F. L., de Souza Filho, G. A., 2009. Identification and characterization of *Gluconacetobacter diazotrophicus* mutants defective in the solubilization of phosphorus and zinc. Arch Microbiol. 191**,** 477-483.

Katzen, F., Becker, A., Ielmini, M. V., Oddo, C. G., Ielpi, L., 1999. New mobilizable vectors suitable for gene replacement in gram-negative bacteria and their use in mapping of the 3' end of the *Xanthomonas campestris* pv. campestris *gum* operon. Appl. Environ. Microbiol. 65**,** 278-282.

Kersters, K., De Ley, J., 1968. An easy screening assay for the enzymes of the Entner-Doudoroff pathway. Antonie Van Leeuwenhoek. 34**,** 388-392.

Kiefler, I., Bringer, S., Bott, M., 2015. SdhE-dependent formation of a functional *Acetobacter pasteurianus* succinate dehydrogenase in *Gluconobacter oxydans*-a first step toward a complete tricarboxylic acid cycle. Appl. Microbiol. Biotechnol. 99**,** 9147-9160.

Kostner, D., Luchterhand, B., Junker, A., Volland, S., Daniel, R., Büchs, J., Liebl, W., Ehrenreich, A., 2015. The consequence of an additional NADH dehydrogenase paralog on the growth of *Gluconobacter oxydans* DSM3504. Appl. Microbiol. Biotechnol. 99**,** 375-386.

Krajewski, V., Simić, P., Mouncey, N. J., Bringer, S., Sahm, H., Bott, M., 2010. Metabolic engineering of *Gluconobacter oxydans* for improved growth rate and growth yield on glucose by elimination of gluconate formation. Appl. Environ. Microbiol. 76**,** 4369-4376.

Kuznetsova, E., Proudfoot, M., Gonzalez, C. F., Brown, G., Omelchenko, M. V., Borozan, I., Carmel, L., Wolf, Y. I., Mori, H., Savchenko, A. V., Arrowsmith, C. H., Koonin, E. V., Edwards, A. M., Yakunin, A. F., 2006. Genome-wide analysis of substrate specificities of the *Escherichia coli* haloacid dehalogenase-like phosphatase family. J Biol Chem. 281**,** 36149-36161.

Macauley, S., McNeil, B., Harvey, L. M., 2001. The genus *Gluconobacter* and its applications in biotechnology. Crit. Rev. Biotechnol. 21**,** 1-25.

Mamlouk, D., Gullo, M., 2013. Acetic Acid bacteria: physiology and carbon sources oxidation. Indian J. Microbiol. 53**,** 377-384.

Matsushita, K., Shinagawa, E., Adachi, O., Ameyama, M., 1987. Purification, characterization and reconstitution of cytochrome *o*-type oxidase from *Gluconobacter suboxydans*. Biochim. Biophys. Acta. 894**,** 304-312.

Miura, H., Mogi, T., Ano, Y., Migita, C. T., Matsutani, M., Yakushi, T., Kita, K., Matsushita, K., 2013. Cyanide-insensitive quinol oxidase (CIO) from *Gluconobacter oxydans* is a unique terminal oxidase subfamily of cytochrome *bd*. J. Biochem. 153**,** 535-545.

Nachlas, M. M., Davidson, M. B., Goldberg, J. D., Seligman, A. M., 1963. Colorimetric method for the measurement of isocitric dehydrogenase activity. J. Lab. Clin. Med. 62**,** 148-158.

Ng, H., 1969. Effect of decreasing growth temperature on cell yield of *Escherichia coli*. J Bacteriol. 98**,** 232-237.

Niebisch, A., Kabus, A., Schultz, C., Weil, B., Bott, M., 2006. Corynebacterial protein kinase G controls 2-oxoglutarate dehydrogenase activity via the phosphorylation status of the OdhI protein. J. Biol. Chem. 281**,** 12300-12307.

Nishikura-Imamura, S., Matsutani, M., Insomphun, C., Vangnai, A. S., Toyama, H., Yakushi, T., Abe, T., Adachi, O., Matsushita, K., 2014. Overexpression of a type II 3-dehydroquinate dehydratase enhances the biotransformation of quinate to 3-dehydroshikimate in *Gluconobacter oxydans*. Appl. Microbiol. Biotechnol. 98**,** 2955-2963.

Pappenberger, G., Hohmann, H. P., 2014. Industrial production of L-ascorbic Acid (vitamin C) and D-isoascorbic acid. Adv. Biochem. Eng. Biotechnol. 143**,** 143-188.

Peters, B., Junker, A., Brauer, K., Mühlthaler, B., Kostner, D., Mientus, M., Liebl, W., Ehrenreich, A., 2013. Deletion of pyruvate decarboxylase by a new method for efficient markerless gene deletions in *Gluconobacter oxydans*. Appl. Microbiol. Biotechnol. 97**,** 2521-2530.

Pronk, J. T., Levering, P. R., Oiijve, W., van Dijken, J. P., 1989. Role of NADP dependent and quinoprotein glucose dehydrogenases in gluconic acid production by *Gluconobacter oxydans*. Enzyme Microb Tech. 11**,** 160-164.

Prust, C., Hoffmeister, M., Liesegang, H., Wiezer, A., Fricke, W. F., Ehrenreich, A., Gottschalk, G., Deppenmeier, U., 2005. Complete genome sequence of the acetic acid bacterium *Gluconobacter oxydans*. Nat. Biotechnol. 23**,** 195-200.

Radmacher, E., Eggeling, L., 2007. The three tricarboxylate synthase activities of *Corynebacterium glutamicum* and increase of L-lysine synthesis. Appl. Microbiol. Biotechnol. 76**,** 587-595.

Raspor, P., Goranovič, D., 2008. Biotechnological applications of acetic acid bacteria. Crit. Rev. Biotechnol. 28**,** 101-124.

Rauch, B., Pahlke, J., Schweiger, P., Deppenmeier, U., 2010. Characterization of enzymes involved in glucose and gluconate utilization in the central metabolism of *Gluconobacter oxydans*. Appl. Microbiol. Biotechnol. 88**,** 711-718.

Richhardt, J., Bringer, S., Bott, M., 2012. Mutational analysis of the pentose phosphate and Entner-Doudoroff pathways in *Gluconobacter oxydans* reveals improved growth of a Δ*edd* Δ*eda* mutant on mannitol. Appl. Environ. Microbiol. 78**,** 6975-6986.

Richhardt, J., Bringer, S., Bott, M., 2013a. Role of the pentose phosphate pathway and the Entner-Doudoroff pathway in glucose metabolism of *Gluconobacter oxydans* 621H. Appl. Microbiol. Biotechnol. 97**,** 4315-4323.

Richhardt, J., Luchterhand, B., Bringer, S., Büchs, J., Bott, M., 2013b. Evidence for a key role of cytochrome bo_3 oxidase in respiratory energy metabolism of *Gluconobacter oxydans*. J. Bacteriol. 195**,** 4210-4220.

Simon, R., Priefer, U., Pühler, A., 1983. A broad host range mobilization system for *in vivo* genetic-engineering-transposon mutagenesis in Gram-negative bacteria. Bio-Technol. 1**,** 784-791.

Weenk, G., Olijve, W., Harder, W., 1984. Ketogluconate formation by *Gluconobacter* species. Appl. Microbiol. Biotechnol. 20**,** 400-405.

Table 1
Bacterial strains, plasmids and oligonucleotides used in this work.

Strain or plasmid or oligonucleotide	Description or oligonucleotide sequence (5'→3')	Source or added restriction site[a] or purpose of use
Strain		
E. coli DH10B	F⁻ *mcr*A Δ (*mrr-hsd*RMS-*mcr*BC) Φ80*lac*ZΔM15 Δ*lac*X74 *rec*A1 *end*A1 *ara*D139 Δ (*ara leu*) 7697 *gal*U *gal*K *rps*L *nup*G λ⁻	Invitrogen, Darmstadt, Germany
E. coli S17-1	Δ*rec*A, *end*A1, *hsd*R17, *sup*E44, *thi*-1, *tra*⁺	(Simon et al. 1983)
A. pasteurianus	*Acetobacter pasteurianus* DSM3509	DSMZ, Braunschweig, Germany
Ga. diazothrophicus	*Gluconacetobacter diazotrophicus* DSM5601	DSMZ, Braunschweig, Germany
Z. mobilis	*Zymomonas mobilis* ATCC10988	American Type Culture Collection
G. oxydans DSM3504	*G. oxydans* DSM3504	DSMZ, Braunschweig, Germany
G. oxydans (reference strain)	*G. oxydans* 621H derivative with a deletion of GOX0327 coding for uracil phosphoribosyl-transferase (Δ*upp*)	(Peters et al. 2013a)
IK-A	*G. oxydans* Δ*gdhS*::*sdhCDABE*; *sdhCDAB* (APA01_00310-00340) from *A. pasteurianus* with promoter P384 and *sdhE* (APA01_11050) from *A. pasteurianus* with its native promoter genomically integrated into the *gdhS* (GOX2015) locus of *G. oxydans*	This work
IK-B	*G. oxydans* Δ*gdhS*::*sdhCDABE* Δ*gdhM*::*sucCD*; strain IK-A with *sucCD* (GDI_2951-2952) from *Ga. diazotrophicus* genomically integrated with P452 promoter into the *gdhM* (GOX0265) locus of *G. oxydans*	This work
IK-C	*G. oxydans* Δ*gdhS*::*sdhCDABE* Δ*gdhM*::*sucCD* Δ*pdc*::*glf-glk*; strain IK-B with *glf* (Zmob_0907) and *glk* (Zmob_0910) genes from *Z. mobilis* under promoter P384 genomically integrated into the *pdc* (GOX1081) locus of *G. oxydans*	This work
IK001	*G. oxydans* Δ*gdhS*::*sdhCDABE*; *sdhCDAB* (APA01_00310-00340) from *A. pasteurianus* with promoter P264 and *sdhE* (APA01_11050) from *A. pasteurianus* with its native promoter genomically integrated into the *gdhS*	This work

	(GOX2015) locus of *G. oxydans*	
IK002.0	*G. oxydans* Δ*gdhS::sdhCDABE* Δ*pdc*::*sucCD;* strain IK001 with with *sucCD* (GDI_2951-2952) genes from *Ga. diazotrophicus* genomically integrated with promoter P264 into the *pdc* (GOX1081) locus of *G. oxydans*	This work
IK002.1	*G. oxydans* Δ*gdhS::sdhCDABE* Δ*pdc*::*ndh*; strain IK001 with *ndh* from *G. oxydans* DSM3504 (GLS_c05650) genomically integrated with its native promoter into the *pdc* (GOX1081) locus of *G. oxydans*	This work
IK003.1	*G. oxydans* Δ*gdhS::sdhCDABE* Δ*pdc::ndh* Δ*gdhM::sucCD*; strain IK002.1 with *sucCD* (GDI_2951-2952) from *Ga. diazotrophicus* genomically integrated with promoter P264 into *gdhM* (GOX0265) locus of *G. oxydans*	This work
Plasmid		
pAJ63a	Kan^R; pK18mobGII derivative; *lacZ*, *mob*, *oriV*, GOX0327 and GOX0328	(Peters et al. 2013a; Katzen et al. 1999)
pAJ63a_sdhCDAB_ Pnat-sdhE-gdhS	Kan^R; plasmid for genomic integration of P264-*sdhCDAB* (APA01_00310-00340) and *sdhE* (APA01_11050) under control of its native promoter from *A. pasteurianus* DSM3509 into the *gdhS* (GOX2015) locus of the genome of *G. oxydans* 621H with simultaneous deletion of *gdhS*	This work
pAJ63a-Pnat-ndh-pdc	Kan^R; plasmid for genomic integration of *ndh* (GLS_c05650) gene from *G. oxydans* DSM3504 under control of its native promoter into the *pdc* (GOX1081) locus of the genome of *G. oxydans* 621H with simultaneous deletion of *pdc*	This work
pAJ63a-sucCD-gdhM	Kan^R; gene integration plasmid; integration of *sucCD* (Gdia_3398-3397) genes from *Ga. diazotrophicus* with promoter P264 into the *gdhM* (GOX0265) locus of the genome of *G. oxydans* 621H with simultaneous deletion of *gdhM*	This work
Oligonucleotide		
gdhS-forw-FlA	CGATATGGTACCTCCCGCTGGCCAAGGCCCGC	KpnI
gdhS-rev-FlA	GGCCCGGGTGTTTTCCATCTGGCCTCACCTCTC CTTGTGAATGCAGGTTT	SmaI
gdhS-forw-FlB	AGGTGAGGCCAGATGGAAAACACCCGGGCCTC GTAAACTTATATGGCCCC	SmaI
gdhS-rev-FlB	CTAACGTCTAGAGGCCAGGCGGCTGGCTGATG	XbaI
p264-forw	GTTGCGCCTGAATGAGAGGA	
p264-seq1-rev	TAACCCTCACTAAAGGGAAC	

gdhS_mut_forw_2	GGACGCGACCTTCAGGAACC	Colony PCR
gdhS_mut_rev_2	CAGGGCCGGGATTTCAGTCG	Colony PCR
gdhS-forw	GAAGCTGCCCAAGGTTTC	Colony PCR
gdhS-rev	GATGTAGGTGCTGTCCTC	Colony PCR
gdhM-forw-FlA	CGTATAAAGCTTCCTTACGAAAGCCCGTAGGG	
gdhM-rev-FlA-EcoRV	GAGGGTGATATCAGAGATGTTCCTGGATCTGTTGTTCTGATGCATCACGG	EcoRV
gdhM-forw-FlB-EcoRV	AGATCCAGGAACATCTCTGATATCACCCTCGGGGCCATGAAAAAGGGGAG	EcoRV
gdhM-rev-FlB	TATAATTCTAGAGTCAGGTCGGGCGAGGCATG	
gdhM-mut-forw_2	GCTCCAGGGCAATGCGATAG	Colony PCR
gdhM-mut-rev_2	TCGGCGGCTTCGGGATAATG	Colony PCR
gdhM-forw	GCTCGGACATCGTCATCATC	Colony PCR
gdhM-rev	AGTTGTGTCCGCCTGCATAG	Colony PCR
sucCD_forw_EcoRI	CGCGCGGAATTCACAAACGCGGATCAAACCGT	EcoRI
sucCD_rev_HindIII_2	CGTATAAAGCTTGGAACACGCTCTGCCACAGA	HindIII
pdc-forw-FlA	TCTAGACCGGCTGTATTCAATTCCC	
pdc-rev-FlA	GCTCTGCGGCTTGCGCATGATTTCAGTACCCCGGGAGCCATAGGGACGGT	SmaI
pdc-forw-FlB	GGTACTGAAATCATGCGCAAGCCGCAGAGCGTCTGAACAAAGCGTCTGAT	SmaI
pdc-rev-FlB	TCTAGAGGGTAGCATTGTCGGTAAGG	
pdc-mut-forw	CGCTTCAATCGAGCTGACATGG	Colony PCR
pdc-mut-rev	CGCAATCCCATTCCGGTTCTG	Colony PCR
pdc-for_2	TGCCGGTGACTATAACCTCG	Colony PCR
pdc-rev_2	AGTCCGTGCGATCGAGTTTG	Colony PCR
GLS-pnatc05650-forw	TATATAGGTACCGGACAGCAGGGATGTGCCGG	KpnI
GLS-c05650-rev-KpnI	GCAATTGGTACCGCGCACCCCGGATGTTCTTC	KpnI
seq-bc1-rev-3	TCCGGCTCGTATGTTGTG	Colony PCR
M13uni(-43)	AGGGTTTTCCCAGTCACGACGTT	Colony PCR
M13rev(-49)	GAGCGGATAACAATTTCACACAGG	Colony PCR

Table 2
Cultivation parameters, glucose consumption and product formation of the engineered *G. oxydans* strains and the reference strains[a]

Parameter[c] (conc. in mM)	Reference strain I[b]	IK001	Reference strain II[b]	IK002.1	Reference strain II[b]	IK003.1
OD_{600}	4.7 ± 0.1	4.8 ± 0.1	4.8 ± 0.2	5.4 ± 0.2	4.6 ± 0.2	7.9 ± 0.2
g_{cdw}[d]	1.673 ± 0.049	1.740 ± 0.036	1.718 ± 0.080	1.925 ± 0.064	1.663 ± 0.054	2.837 ± 0.068
$Y_{X/S}$ ($g_{cdw}/g_{glucose}$)	0.088 ± 0.000	0.090 ± 0.002	0.092 ± 0.004	0.103 ± 0.003	0.089 ± 0.004	0.142 ± 0.001
$Y_{X/S}$ (% of ref.)	100	100	100	112	100	160
Growth rate (h^{-1})	0.3634 ± 0.0341	0.3699 ± 0.0090	0.3510 ± 0.0474	0.2478 ± 0.0113	0.3510 ± 0.0474	0.1678 ± 0.0014
Glucose (consumed)	105.2 ± 2.9	107.2 ± 1.4	103.6 ± 1.3	103.7 ± 1.4	103.6 ± 1.3	110.7 ± 1.8
Gluconate	0.0 ± 0.0	0.0 ± 0.0	3.5 ± 2.0	1.1 ± 0.8	2.0 ± 1.3	0.0 ± 0.0
2-KGA	41.9 ± 5.0	51.1 ± 0.3	38.8 ± 2.9	31.2 ± 0.2	38.1 ± 2.9	1.5 ± 0.1
5-KGA	0.9 ± 0.9	0.0 ± 0.0	0.0 ± 0.0	20.9 ± 2.9	0.0 ± 0.0	17.1 ± 1.6
Acetate	38.1 ± 1.6	38.1 ± 1.2	34.7 ± 2.0	0.8 ± 0.1	33.7 ± 3.2	1.0 ± 0.1
Pyruvate	0.2 ± 0.1	0.3 ± 0.2	0.4 ± 0.2	34.6 ± 0.6	0.3 ± 0.2	37.6 ± 0.6
Succinate	1.8 ± 1.2	0.7 ± 0.2	1.9 ± 1.2	0.7 ± 0.1	1.6 ± 0.9	2.0 ± 0.1
Fumarate	0.01 ± 0.00	0.01 ± 0.00	0.0 ± 0.0	0.01 ± 0.0	0.01 ± 0.0	0.03 ± 0.01
CO_2	250.1 ± 13.3	212.2 ± 0.5	229.4 ± 6.0	240.3 ± 7.4	233.1 ± 6.6	517.4 ±12.6
Carbon balance	104 %	104 %	102 %	120 %	99 %	131 %
Acid demand (2 M HCl, mL)	1.7 ± 0.1	1.4 ± 0.0	1.7 ± 0.1	3.6 ± 0.3	1.7 ± 0.1	0.1 ± 0.1
Base demand (2 M NaOH, mL)	10.9 ± 0.1	11.3 ± 0.2	12.6 ± 1.2	13.9 ± 0.7	12.6 ± 1.2	5.8 ± 0.0

[a]Mean values and standard deviation from three biological replicates are given.
[b]Reference strain I and II correspond to *G. oxydans* 621H Δ*upp* of separate cultivations. Reference strain I compares to strain IK001; reference strain II compares to strains IK002.1 and IK003.1.
[c]Concentrations refer to end times for IK001 and IK002.1, 24 h; IK003.1, 28 h.
[d]cdw, cell dry weight. Calculation: OD_{600} x 0.36 = g_{cdw}.

Table 3
Activities of the pyruvate dehydrogenase complex and the TCA cycle enzymes[a]

Enzyme	*G. oxydans*	*E. coli* DH10B[b]	*G. oxydans* IK001	*G. oxydans* IK003.1[c]
	(nmol min^{-1} mg $protein^{-1}$)			
Pyruvate dehydrogenase complex	0.0 ± 0.0	n.d.	n.d.	n.d.
Citrate synthase	19.5 ± 3.5	31.8 ± 26.9	n.d.	n.d.
Aconitase	2.7 ± 1.9	14.9 ± 5.2	n.d.	n.d.
Isocitrate dehydrogenase	0.7 ± 0.6	369.5 ± 138.2	n.d.	n.d.
Oxoglutarate dehydrogenase	11.0 ± 6.1	127.9 ± 28.7	n.d.	n.d.
Succinyl-CoA synthetase	0.7 ± 1.7	18.4 ± 5.0	n.d.	3.2 ± 1.2
Succinate dehydrogenase	4.2 ± 3.7	339.0 ± 44.0	74.7 ± 22.9	n.d.
Fumarase	10.3 ± 8.3	n.d.	n.d.	n.d.
Malate::quinone oxidoreductase	20.4 ± 8.0	2.1 ± 0.9	n.d.	n.d.

[a]Mean values and standard deviation from three biological replicates are given.
[b]*E. coli* served as a positive control.
[c]nd, not determined.

A

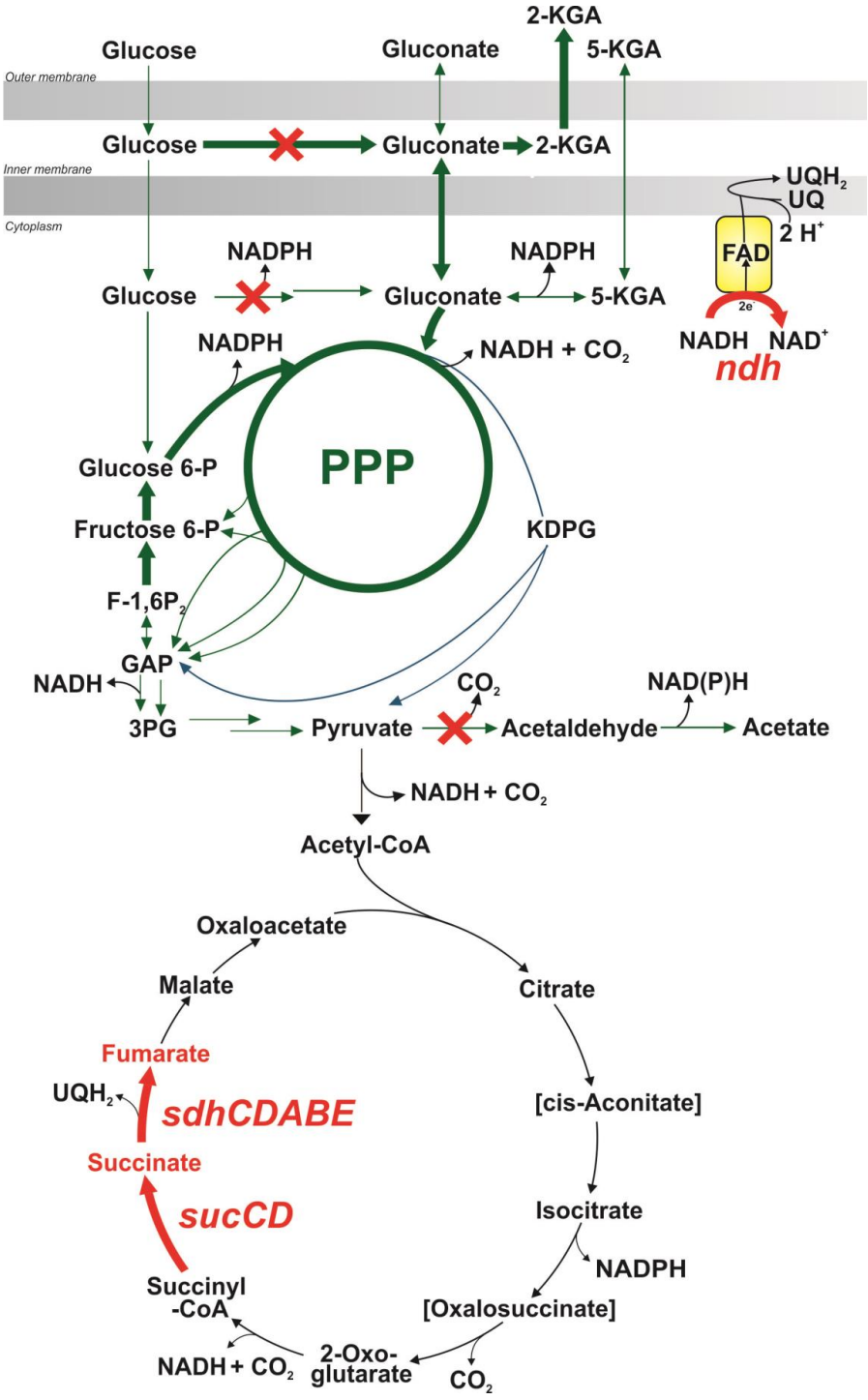
2-KGA
Glucose
Gluconate
5-KGA
Outer membrane
Glucose
Gluconate
2-KGA
Inner membrane
UQH2
UQ
2 H+
Cytoplasm
NADPH
NADPH
FAD
Glucose
Gluconate
5-KGA
2e-
NADPH
NADH + CO2
NADH NAD+
ndh
PPP
Glucose 6-P
Fructose 6-P
KDPG
F-1,6P2
GAP
NADH
CO2
NAD(P)H
3PG
Pyruvate
Acetaldehyde
Acetate
NADH + CO2
Acetyl-CoA
Oxaloacetate
Malate
Citrate
Fumarate
UQH2
sdhCDABE
[cis-Aconitate]
Succinate
sucCD
Isocitrate
NADPH
Succinyl
-CoA
[Oxalosuccinate]
NADH + CO2
2-Oxo-
glutarate
CO2

B

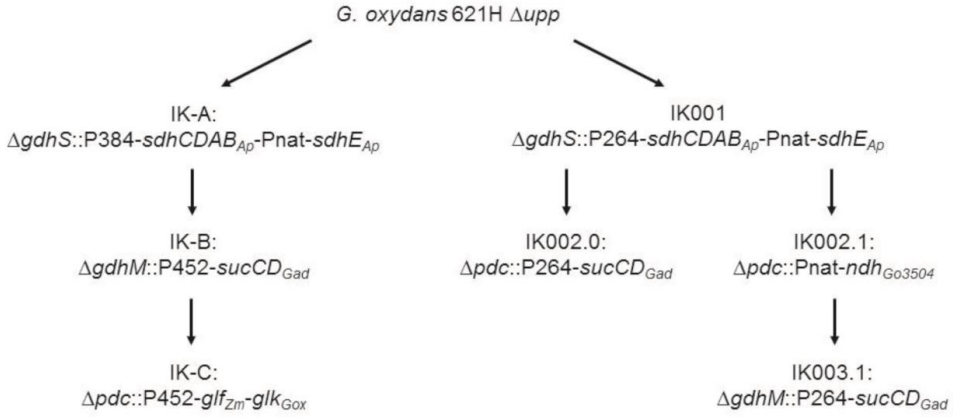

Figure 1. (A) Scheme of the central carbon metabolism of *G. oxydans* with the substrate glucose at a cultivation pH of 6. Green (bold) and blue (fine) arrows show the innate metabolism, red arrows (bold) denote reactions that were introduced by genomic integration of the respective genes from various sources and red crosses mark inactivated functions. 2-KGA, 2-ketogluconate; 5-KGA, 5-ketogluconate; UQ, ubiquinone; PPP, pentose phosphate pathway; glucose-6-P, glucose 6-phosphate; fructose 6-P, fructose 6-phosphate; F-1,6P_2, fructose 1,6-bisphosphate; GAP, glyceraldehyde 3-phosphate; 3PG, 3-phosphoglycerate; KDPG, 2-keto-3-deoxy-6-phosphogluconate. **(B)** Series of *G. oxydans* strains developed in this work.

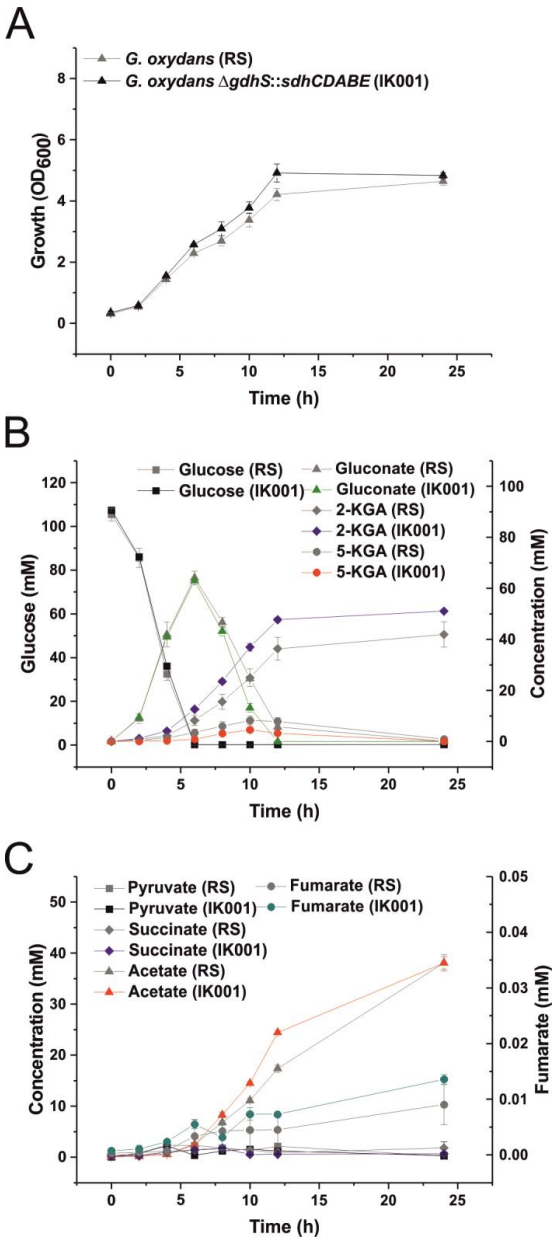

Figure 2. Growth **(A)**, substrate consumption and product formation **(B, C,)** of the *G. oxydans* reference strain I (RS, gray symbols), *G. oxydans* Δ*gdhS*::*sdhCDABE* (strain IK001, colored symbols). Gluconate, 2-ketogluconate (2-KGA), 5-ketogluconate (5-KGA), pyruvate, acetate succinate and fumarate concentrations were determined by HPLC. The cultures were grown in glucose (2 % w/v) medium at 15 % dissolved oxygen at pH 6 in a parallel bioreactor system (DASGIP, Juelich, Germany). Mean values and standard deviation from three biological replicates are shown.

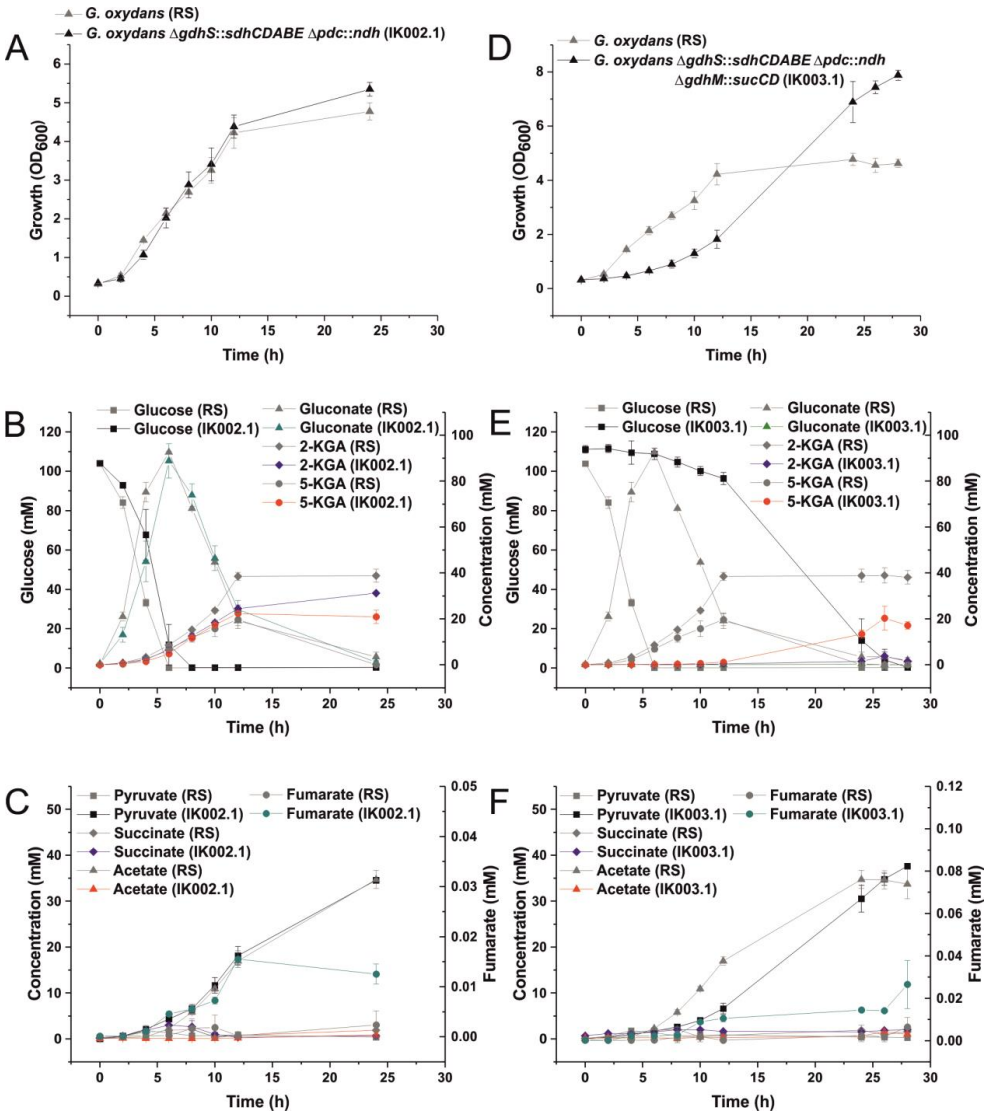

Figure 3. Growth **(A, D)**, substrate consumption and product formation **(B, C, E, F)** of the *G. oxydans* reference strain II (RS, gray symbols), *G. oxydans* Δ*gdhS*::*sdhCDABE* Δ*pdc*::*ndh* (strain IK002.1, colored symbols) and *G. oxydans* Δ*gdhS*::*sdhCDABE* Δ*pdc*::*ndh* Δ*gdhM*::*sucCD* (strain IK003.1, colored symbols). Gluconate, 2-ketogluconate (2-KGA), 5-ketogluconate (5-KGA), pyruvate, acetate, succinate and fumarate concentrations were determined by HPLC. The cultures were grown in glucose (2 % w/v) medium at 15 % dissolved oxygen at pH 6 in a parallel bioreactor system (DASGIP, Juelich, Germany). Mean values and standard deviation from three biological replicates are shown.

Table S1
Calculation of the carbon balances of engineered strains

Substrate/ Product ([C] mM)[c]	Ref. strain I[a]	(%)	IK001	(%)	Ref. strain II[a]	(%)	IK002.1	(%)	Ref. strain II[a]	(%)	IK003.1	(%)
Glucose (t_{0h})	632.7 ± 17.6	100	644.7 ± 8.1	100	623.3 ± 7.7	100	624.8 ± 8.2	100	623.3 ± 7.7	100	666.9 ± 11.0	100
Glucose (t_{end})	1.8 ± 0.1	0.3	1.7 ± 0.0	0.3	1.6 ± 0.1	0.3	2.40 ± 0.1	0.4	1.7 ± 0.0	0.3	2.5 ± 0.0	0.4
Biomass[b]	69.7 ± 21	11.0	72.5 ± 1.5	11.3	1.6 ± 3.3	11.5	80.2 ± 2.7	12.8	69.3 ± 2.2	11.1	118.2 ± 2.8	17.7
2-KGA	251.6 ± 29.9	39.8	306.4 ± 2.0	47.5	232.9 ± 17.1	37.4	187.3 ± 1.4	30.0	228.5 ± 17.4	36.7	9.2 ± 0.7	1.4
Gluconate	0.0	0.0	0.0	0.0	20.9 ± 12.3	3.4	6.3 ± 4.6	1.0	11.9 ± 7.8	1.9	0.0	0.0
5-KGA	0.0	0.0	0.0	0.0	0.0	0.0	125.2 ± 17.2	20.0	0.0	0.0	102.7 ± 9.9	15.4
Pyruvate	0.7 ± 0.4	0.1	1.0 ± 0.5	0.2	1.2 ± 0.6	0.2	103.7 ± 1.8	16.6	0.87 ± 0.5	0.1	112.9 ± 1.9	16.9
Succinate	7.3 ± 4.8	1.2	2.7 ± 0.7	0.4	7.5 ± 4.6	1.2	2.6 ± 0.2	0.4	6.4 ± 3.5	1.0	8.2 ± 0.3	1.2
Acetate	76.2 ± 3.2	12.0	76.1 ± 2.4	11.8	69.5 ± 4.0	11.2	1.7 ± 0.2	0.3	67.5 ± 6.4	10.8	2.0 ± 0.1	0.3
Fumarate	0.04 ± 0.01	0.0	0.04 ± 0.00	0.0	0.00	0.0	0.05 ± 0.02	0.0	0.03 ± 0.02	0.0	0.11± 0.05	0.0
CO_2	250.1 ± 13.3	39.5	212.2 ± 0.5	32.9	229.4 ± 5.9	36.8	240.3 ± 7.4	38.5	233.1 ± 6.6	37.4	517.4 ± 12.6	77.6
Balance	661.0	**104**	671.0	**104**	632.9	**102**	749.8	**120**	617.48	**99**	870.6	**131**

[a]Reference strain I and II correspond to *G. oxydans* 621H Δ*upp* of separate cultivations. Reference strain I compares to strain IK001; reference strain II compares to strains IK002.1 and IK003.1.
[b]Calculation: OD_{600} x 0.36 = gCDW l^{-1}; gCDW / 2 = carbon in cell dry weight (g l^{-1}) / 12 x 1000 = mmol C in biomass.
[c]The end times for calculation were: IK001and IK002.1, 24 h; IK003.1, 28 h.

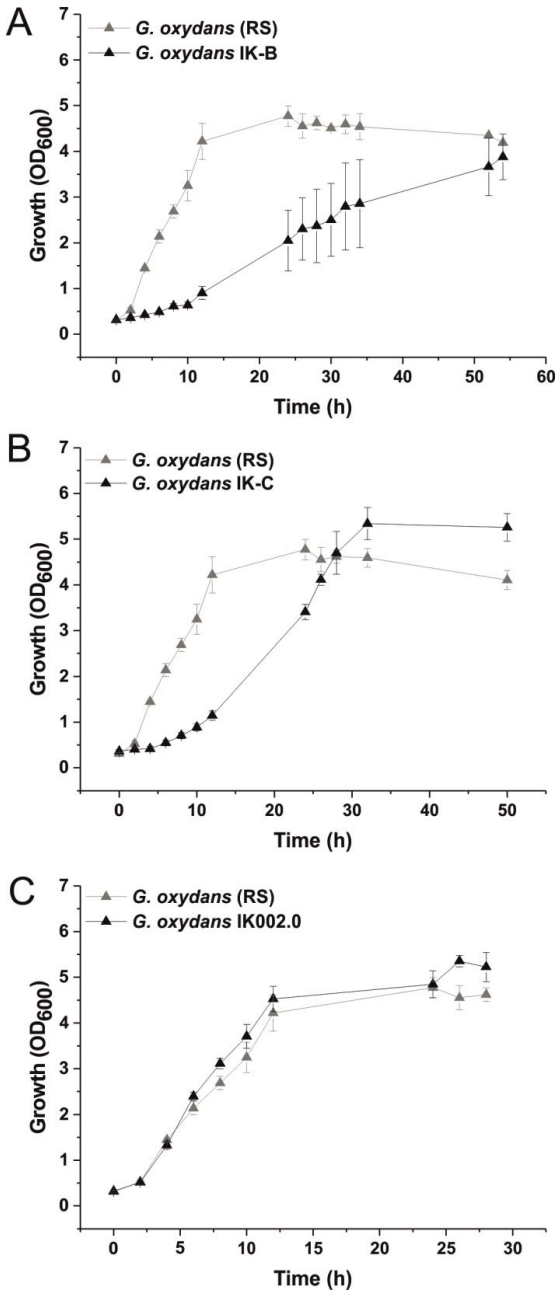

Figure S1. Growth of the *G. oxydans* reference strain *G. oxydans* Δ*upp* (RS, gray symbols), **(A)** *G. oxydans* Δ*gdhS*::P384-*sdhCDAB*-P_{nat}-*sdhE* Δ*gdhM*::P452-*sucCD* (strain IK-B, black symbols); **(B)** *G. oxydans* Δ*gdhS*::P384-*sdhCDAB*-P_{nat}-*sdhE* Δ*gdhM*::P452-*sucCD* Δ*pdc*::P384-*glf-glk* (strain IK-C, black symbols) and **(C)** *G. oxydans* Δ*gdhS*::P264-*sdhCDAB* P_{nat}-*sdhE* Δ*pdc*::P264-*sucCD* (strain IK002.0, black symbols). The cultures were grown in glucose (2 % w/v) medium at 15 % dissolved oxygen at pH 6 in a parallel bioreactor system (DASGIP, Juelich, Germany). Mean values and standard deviation from three biological replicates are shown.

3.3 Impact of expression of functions for glucose uptake and intracellular carbon flux on growth of *G. oxydans*

Own contribution to this publication: about 70 %. I performed all experimental work described in the publication and wrote a draft of the manuscript. I am first author of the publication.

To be submitted

Impact of plasmid-based expression of functions for glucose uptake and phosphorylation, glycolysis, and pyruvate oxidation to acetyl-CoA on growth of *Gluconobacter oxydans* IK003.1

Abstract

The obligatory aerobic acetic acid bacterium *Gluconobacter oxydans* is used in oxidative biotransformations due to its ability of rapid regio- and stereoselective oxidations of diverse carbohydrates in the periplasm. However, industrial applications are handicaped by the low cell yield, caused by the incomplete oxidation of the substrates and limitations in cytoplasmic catabolism such as the absence of glycolysis and the tricarboxylic acid (TCA) cycle. In a recent study aimed at an improved cell yield on glucose, we replaced the genes *gdhS* and *gdhM* for cytoplasmic and membrane-bound glucose dehydrogenase by heterologous genes for succinate dehydrogenase and succinyl-CoA synthetase, thereby preventing glucose oxidation to gluconate and introducing the missing enzymes of the TCA cycle. In addition, the *pdc* gene for pyruvate decarboxylase was replaced by a *ndh* gene for a second NADH dehydrogenase, thereby eliminating acetate formation from pyruvate and increasing the NADH oxidation capacity. The resulting strain IK003.1 showed retarded growth, but the cell yield on glucose was improved by 60 %. In the present study, attempts were made to further improve strain IK003.1 by (i) enhancing glucose uptake and phosphorylation by overexpression of the genes *glf* and *glk* for a glucose facilitator from *Zymomonas mobilis* and glucose kinase, (ii) allowing for glycolysis by overexpression of the phosphofructokinase gene *pfkA* from *E. coli*, and (iii) stimulating pyruvate conversion to acetyl-CoA by overexpression of the genes *aceEα-aceEβ-aceF-lpd* for the pyruvate dehydrogenase complex. Unfortunately, neither the individual nor the combined plasmid-based overexpression of these genes improved growth and cell yield of strain IK003.1, although the functional synthesis of phosphofructokinase and the pyruvate dehydrogenase complex were confirmed by enzymatic assays. We assume that imbalances of enzymatic activities could be responsible for the absence of a growth enhancement, which need to be addressed in future studies.

Introduction

The Gram-negative, strictly aerobic, rod-shaped α-proteobacterium *Gluconobacter oxydans* belongs to the family of acetic acid bacteria. Its industrial application is in vitamin C production and several other oxidative biotransformations. Due to a versatile set of membrane-bound dehydrogenases the organism has the ability to rapidly oxidize monosaccharides and alcohols regio- and stereoselectively in the periplasm (Deppenmeier et al. 2002; Adachi et al. 2003b; Mamlouk and Gullo 2013; Nishikura-Imamura et al. 2014; Macauley et al. 2001; Raspor and Goranovič 2008).

G. oxydans lacks genes of the central metabolism, such as succinyl-CoA synthetase and succinate dehydrogenase resulting in an incomplete tricarboxylic acid (TCA) cycle and phosphofructokinase causing an interrupted glycolysis (Prust et al. 2005). Furthermore, the PEP: carbohydrate phosphotransferase system (PTS) is incomplete due to the absence of EIIC and EIIB components, suggesting a regulatory rather than a transporter function (Prust et al. 2005).

Cultivation of *G. oxydans* on the carbon source glucose results in the oxidation of 90 % glucose to gluconate by the membrane-bound PQQ-dependent glucose dehydrogenase. Intracelluar glucose is oxidized to lesser extent by the by the cytoplasmic NADP-dependent glucose dehydrogenase (Hanke et al. 2013). So far, the transport system for glucose uptake is not known for *G. oxydans*. The incomplete glucose oxidation to gluconate and ketogluconates and the restriction of intracellular catabolism result in very low cell yields of *G. oxydans* causing high costs for the production of biomass to be used in whole-cell biotransformations.

In a recent study we increased the cell yield of *G. oxydans* by 60 % by metabolic engineering via (i) the prevention of periplasmic and cytoplasmic glucose oxidation to gluconate, (ii) elimination of pyruvate decarboxylation to acetaldehyde, (iii) complementation of the TCA cycle, and (iv) integration of a second NADH dehydrogenase gene (Kiefler et al., to be submitted). The resulting strain IK003.1 did not excrete gluconate, 2-ketogluconate, and acetate anymore, but formed some 5-ketogluconate, and pyruvate instead of acetate. Measurement of enzyme activities revealed that a major reason for pyruvate accumulation was the apparent absence of pyruvate dehydrogenase activity despite the presence of the corresponding genes (*aceE*α-*aceE*β-*aceF-lpd*). In addition also several activities of TCA cycle enzymes were quite low, such as aconitase and isocitrate dehydrogenase.

In this work, attempts were made to improve the growth properties and the cell yield of *G. oxydans* IK003.1 by improving glucose uptake and phosphorylation by expression of the glucose facilitator Glf from *Zymomonas mobilis* and glucokinase, by provision of a complete glycolytic pathway via expression of phosphofructokinase PfkA of *Escherichia coli*, and by

allowing for pyruvate conversion to acetyl-CoA via expression of the *aceE*α-*aceE*β-*aceF-lpd* genes.

Materials and methods

2.1. Materials

Chemicals were obtained from Sigma-Aldrich (Taufkirchen, Germany), Qiagen (Hilden, Germany), Merck (Darmstadt, Germany) and Roche Diagnostics (Mannheim, Germany).

2.2. Bacterial strains, plasmids, media and growth conditions

The bacterial strains and plasmids used in this study are listed in Table 1. The *E. coli* strains were cultivated in lysogeny broth (LB) medium or on LB agar plates at 37 °C (Bertani 1951, 2004). When required, kanamycin was added to a final concentration of 50 µg mL^{-1}. *Z. mobilis* cells were obtained by cultivation on 10 g L^{-1} peptone, 10 g L^{-1} yeast extract and 20 g L^{-1} glucose at 30 °C and 140 rpm. *G. oxydans* ATCC 621H Δ*upp* (ATCC 621H is identical to DSM2343), which lacks the *upp* gene for uracil phosphoribosyltransferase, was obtained from Armin Ehrenreich (Technical University of Munich, Germany). *G. oxydans* was cultivated on medium containing 220 mM (4 % w/v) mannitol or 110 mM (2 % w/v) glucose, 5 g L^{-1} yeast extract, 2.5 g L^{-1} $MgSO_4$ x 7 H_20, 1 g L^{-1} $(NH_4)_2SO_4$, 1 g L^{-1} KH_2PO_4 and 10 µM thymidine. The initial pH value of the medium was 6.0. *G. oxydans* possesses a natural resistance towards cefoxitin; as a precaution to prevent bacterial contaminations, cefoxitin was added to the media at a concentration of 50 µg mL^{-1}. When required, kanamycin (50 µg mL^{-1}) was added. Precultures were grown in baffled shaking flasks at 30 °C and 140 rpm. Main cultures were grown in 500 mL baffled shaking flasks containing 100 mL medium with the carbon source indicated in the text. Incubation was at 140 rpm and 30 °C in an Infors shaker (Basel, Switzerland) (Kiefler et al. 2015).

For determination of growth parameters with glucose as the carbon source, cells were cultivated in 250 mL of the same medium in a bioreactor system (DASGIP, Jülich, Germany) as described previously (Kiefler et al. 2015).

For small-scale cultivations a BioLector cultivation system (m2plabs GmbH, Aachen, Germany) was used. Precultures of the *G. oxydans* strains were grown overnight in 20 mL mannitol medium (4 % mannitol) at 30 °C and 140 rpm. Per well of the 48 well microtiter Flowerplates, the strains were inoculated to an OD_{600} of 0.3 (end volume per well 1 mL). For that purpose the necessary volume of the preculture was centrifuged (3 min, 10,414 x *g*, 4 °C) and the pellet was resuspended in 1 mL 0.9 % NaCl and centrifuged again. The pellet was resuspended in glucose medium (2 % glucose) and incubated at 30 °C and 1,200 rpm

(shaking diameter 3 mm) in the BioLector. During cultivation biomass was measured as scattered light intensity (620 nm, signal gain factor of 20).

2.3. Cloning and DNA techniques

DNA manipulation was performed by standard methods as described by Green and Sambrook (Green and Sambrook 2012). For PCR reactions, genomic DNA served as template for amplification. Competent cells of *E. coli* were prepared with $CaCl_2$ and transformed as described by Hanahan (Hanahan et al. 1991). DNA sequencing was performed by Eurofins MWG Operon (Ebersberg, Germany). Oligonucleotides were synthesized by Biolegio (Nijmegen, Netherlands) and are listed in Table 1.

2.4. Plasmid construction for expression of pyruvate dehydrogenase complex, glucose facilitator, glucokinase and phosphofructokinase genes

For construction of expression plasmid pBBR1p452-pdhC genes encoding the pyruvate dehydrogenase complex (GOX2289-2292, *aceEα-aceEβ-aceF-lpd*) were amplified by PCR (pdhC-forw-XhoI/ pdhC-rev-KpnI) from genomic DNA of *G. oxydans* 621H. The KpnI/XhoI restricted insert was ligated into the KpnI/XhoI linearized empty vector pBBR1p452. Expression plasmid pBBR1p452-glf was designed via PCR amplification (glf-Zm-forw-EcoRI/ glf-Zm-rev-HindIII-pT) of the *glf* gene from *Z. mobilis*, followed by EcoRI/HindIII restriction and cloning into EcoRI/HindIII restricted pBBR1p452. Construction of pBBR1p264-glk was performed by the amplification (glk-forw/glk-rev) of the *glk* gene (GOX2419) from genomic DNA of *G. oxydans* 621H and KpnI/XhoI restriction. The insert was ligated into the KpnI/XhoI linearized empty vector pBBR1p264. The *glk* gene with promoter P264 was amplified (p264-forw/p264-seq1-rev) from pBBR1p264-glk and phosphorylated. Plasmid pBBR1p452-glf was digested with HindIII, filled up via Klenow reaction and dephosphorylated. Ligation of insert p264-glk into the linearized vector pBBR1p452-glf resulted in expression plasmid pBBR1p452-glf-p264-glk. The expression plasmid pBBR1p452-glf-p264-glk served as matrix for amplification of p452-glf-p264-glk via PCR (pBBR1p452-screen-forw/p264-seq1-rev). After linearization of plasmid pBBR1p452-pdhC with AgeI the ends were filled up by Klenow reaction. The phosphorylated insert p452-glf-p264-glk was ligated into the linearized and dephosphorylated vector pBBR1p452-pdhC. The resulting expression plasmid pBBR1p452-pdhC-p452-glf-p264-glk was digested with EcoR81I, filled up by Klenow reaction and dephosphorylated. Expression plasmid pBBR1p384-pfkA was constructed by the amplification (pfkA-forw-HindIII/pfkA-rev-XhoI) of the *pfkA* gene from genomic DNA of *E. coli* DH10B. After HindIII/XhoI restriction the insert was cloned into the HindIII/XhoI linearized vector pBBR1p384. Insert p384-pfkA amplified (p384-seq-forw/p384-seq-rev) from

expression plasmid pBBR1p384-pfkA via PCR, phosphorylated and ligated into pBBR1p452-pdhC-p452-glf-p264-glk resulting in expression plasmid pIK1.

2.5. Enzyme assays

G. oxydans strains were grown in 50 mL mannitol medium at 30 °C and 140 rpm and *E. coli* in 50 mL LB medium at 37 °C and 130 rpm (Infors shaker, Basel, Switzerland) for 10 h. The cells were centrifuged at 10,414 x *g* for 3 min at 4 °C and resuspended in the corresponding buffer. 300 µl of the cell suspension was mixed with 250 mg zirconia/silica beads (0.1-mm diameter; Biospec, Bartlesville, OK) in a 1.5 mL Eppendorf tube, and the cells were mechanically disrupted by three 20 sec shakings in a Silamat S5 (Ivoclar Vivadent, Ellwangen, Germany). Cell debris and unbroken cells were separated by 30 min centrifugation at 16,100 x *g* at 4 °C. The resulting cell extract was kept on ice until it was used for the assay (Kiefler et al., to be submitted).

Pyruvate dehydrogenase complex activity was determined as described previously using pyruvate as substrate measuring the absorbance of NADH at 340 nm (Niebisch et al. 2006). Activity of glucokinase was measured via a coupled assay with glucose-6-phosphate dehydrogenase monitoring the reduction of $NADP^+$ to NADPH + H^+ at 340 nm. The assay consisted of 50 mM TrisHCl pH 7.5, 10 mM $MgCl_2$, 2 mM ATP, 0.2 mM $NADP^+$, 1.5 U/mL glucose-6-phosphate dehydrogenase and cell extract. The reaction was started by the addition of 0.5 mM glucose. Phosphofructokinase activity was determined as described by Santamaría et al. (Santamaría et al. 2002) using an enzymatic coupled assay with pyruvate kinase and lactate dehydrogenase. One unit (U) of enzyme activity was defined as 1 nmol of product formed per minute.

2.6. Determination of substrates and products by HPLC analysis

One mL culture was centrifuged for 2 min at 13,000 x *g* and the supernatant was filtered through a 0.2 µm filter (Millipore, MA, USA) prior to HPLC analysis. Gluconate, 2-ketogluconate and 5-ketogluconate were quantified by a Rezex organic acid HPLC-column (300 x 7.8 mm, Phenomenex, Aschaffenburg, Germany) at 65 °C by an isocratic separation with 92 % 1 mM H_2SO_4 and 8 % 100 mM H_2SO_4 as eluent at a flow rate of 0.3 mL min^{-1}. Gluconate, 2-ketogluconate and 5-ketogluconate were detected by an UV detector at 215 nm. Retention times for 2-ketogluconate, 5-ketogluconate and gluconate were 20.3 min, 21 min and 22.6 min, respectively. Calibration curves were made using different metabolite concentrations, ranging from 0-20.4 mM gluconate, 0-20.6 mM 2-ketogluconate and 0-20.6 mM 5-ketogluconate (Kiefler et al., to be submitted). Pyruvate, succinate, acetate and fumarate concentrations were measured with an Organic Acid Resin 300 × 8 mm column (CS Chromatographie Service, Langerwehe, Germany) at 25 °C using 8 mM H_2SO_4 as the

eluent at a flow rate of 0.6 mL min^{-1}. Pyruvate, succinate, acetate and fumarate were detected with an UV detector at 215 nm, and the retention times were 11.5, 14.6, 18.15 and 20.42 min, respectively. Calibration curves were made using a series of standards ranging from 1 to 10 mM of the corresponding substrate (Kiefler et al. 2015).

2.7. Enzymatic determination of glucose concentrations

One mL culture was centrifuged 2 min at 13,000 x *g* and the supernatant was filtered through a 0.2 µm filter (Millipore, MA, USA) prior to the glucose assay. Glucose concentrations were determined photometrically at 340 nm using suitable dilutions of the supernatant according to the method described by Richhardt et al. (Richhardt et al. 2013a).

2.8. Determination of cell dry weight and calculation of cell yield

At three different time points during the growth of *G. oxydans* 621H strains on glucose in a bioreactor system with four vessels, the optical densities at 600 nm were determined and the cell dry weight was determined according to Richhardt et al. (Richhardt et al. 2012). A linear correlation between cell weight (dry weight) and OD_{600} was obtained, and an OD_{600} of 1 corresponded to 0.36 g of cells (dry weight) per liter. The cell yield $Y_{X/S}$ represents g cell dry weight formed per g glucose consumed (Kiefler et al., to be submitted).

Results

3.1 Potential metabolic bottlenecks of G. oxydans IK003.1

In a recent study (Kiefler et al., to be submitted) we constructed a derivative of the *G. oxydans* wild type strain 621H, termed IK003.1, in which the *gdhS* gene for the soluble NADP-dependent glucose dehydrogenase was replaced by the *A. pasteurianus* genes *sdhCDAB* and *sdhE* for succinate dehydrogenase and the assembly protein SdhE, the *pdc* gene for pyruvate decarboxlyase was replaced by the *ndh* gene for NADH dehydrogenase from *G. oxydans* DSM3504, and the *gdhM* gene for the membrane-bound glucose dehydrogenase was replaced by the *sucCD* genes of *Ga. diazotrophicus*. Strain IK003.1 showed a slowed glucose consumption and growth, some 5-ketogluconate formation possibly by dephosphorylation of 6-phosphogluconate and oxidation by gluconate 5-dehydrogenase, pyruvate formation instead of acetate, and strongly increased CO_2 formation. Importantly, the cell yield was increased by 60 % compared to the parental strain.

In this study, we addressed three potential metabolic bottlenecks of strain IK003.1 (Fig. 1). As the slowed glucose consumption might be due to limitations in glucose uptake and phosphorylation, we attempted to improve these functions by overexpression of the glucose facilitator gene *glf* of *Z. mobilis* (Parker et al. 1995 Mol Microbiol 15 795-802; Weisser et al.

1994 J Bacteriol. 177 3351-3354) and the endogenous glucokinase gene *glk* (GOX2419). The production of 5-ketogluconate and the slow glucose consumption might also be caused by limitations in the flux capacity of the pentose phosphate pathway (PPP) and the Entner-Doudoroff pathway (EDP) (Richhardt et al. 2012, 2013, Hanke et al. 2013). We therefore attempted to create a functional glycolysis by overexpression of the *E. coli pfkA* gene for phosphofructokinase, an enzyme that is absent in *G. oxydans*. The possibility of glycolytic breakdown in addition to the PPP and EDP might increase the metabolic flux capacity for conversion of glucose to pyruvate. The third bottleneck we addressed concerned the apparent absence of pyruvate dehydrogenase complex activity, explaining pyruvate formation by strain IK003.1. To provide this activity, the corresponding endogenous genes *aceEα-aceEβ-aceF-lpd* were overexpressed.

3.2 Influence of individual expression of glf-glk, pfkA, and aceEα-aceEβ-aceF-lpd on growth of G. oxydans IK003.1

For the investigation of the effects of individual expression of *glf-glk*, *pfkA*, and *aceEα-aceEβ-aceF-lpd*, the expression plasmids pBBR1p452-glf-p264-glk, pBBR1p384-pfkA, and pBBR1p452-pdhC (carrying *aceEα-aceEβ-aceF-lpd*) were constructed as described in Materials and Methods and transferred into the parent strain and IK003.1. The same strains transformed with the vector pBBR1p452 were used as reference strains. The eight strains were cultivated in a BioLector microcultivation system with 110 mM glucose as carbon source. As shown in Fig. 2, the three expression plasmids had a slightly (pBBR1p452-glf-p264-glk, pBBR1p384-pfkA) or moderately (pBBR1p452-pdhC) negative effect on the growth of the parent strain and IK003.1.

3.3 Influence of combined expression of glf-glk, pfkA, and aceEα-aceEβ-aceF-lpd on growth of G. oxydans IK003.1

In a next attempt, the influence of the combined overexpression of *glf-glk*, *pfkA*, and *aceEα-aceEβ-aceF-lpd* was tested. For this purpose, the 16-kb expression plasmid pIK1 was constructed as described in Materials and Methods and transferred into strain IK003.1. As reference strain, *G. oxydans* 621H Δ*upp* carrying pBBR1p452 was used. The two strains were cultivated in a bioreactor system under constant conditions of pH 6 and 15 % dissolved oxygen using 110 mM glucose as carbon source. In Fig. 3 and Table 2, the growth parameters, glucose consumption, and product formation of the two strains are displayed. In addition, the corresponding data for *G. oxydans* IK003.1 and 621H Δ*upp* reported before (Kiefler et al., to be submitted) are shown to allow for a direct comparison of the influence of plasmid pIK1 on the behaviour of strain IK003.1.

The growth rate of strain IK003.1/pIK1 (0.0638 ± 0.0091 h^{-1}) was reduced compared to IK003.1 (0.1678 ± 0.0014 h^{-1}), 621H Δ*upp* (0.3510 ± 0.0474 h^{-1}), and 621H Δ*upp*/pBBR1p452 (0.3253 ± 0.0110 h^{-1}). The final OD_{600} of IK003.1/pIK1 was 33 % higher than for 621H Δ*upp*/pBBR1p452, but 23 % lower than for IK003.1 without a plasmid. Similarly, the cell yield of IK003.1/pIK1 (0.116 ± 0.011 g_{cdw} $(g_{glucose})^{-1}$) was 51 % higher than for 621H Δ*upp*/pBBR1p452, but 18 % lower than for IK003.1. Thus, contrary to our aim, plasmid pIK1 did not improve the growth properties of strain IK003.1, but even had a negative influence. When comparing the products formed by IK003.1/pIK1 and IK003.1 without plasmid, no drastic changes were observed. The plasmid-carrying strain formed comparable amounts of pyruvate (36.2 mM vs. 37.2 mM), twice as much succinate (4.5 mM vs. 2.0 mM), and 3.8 % more carbon dioxide. With 135 %, also the carbon balance of IK003.1/pIK1 was close to that of IK003.1.

3.4 In vitro activities of homologous and heterologous expressed genes in G. oxydans

To test whether the plasmid-borne genes for glucokinase, phosphofructokinase, and pyruvate dehydrogenase complex were functionally expressed in *G. oxydans* IK003.1/pIK1, the corresponding enzyme activities were determined in cell-free extracts in comparison to the parental strain 621H Δ*upp*. In the case of glucokinase, the specific activity of IK003.1/pIK1 (6.7 ± 2.8 nmol min^{-1} (mg protein)$^{-1}$) was 47 % decreased rather than increased compared to the reference strain (12.6 ± 2.2 nmol min^{-1} (mg protein)$^{-1}$). Expression of the *E. coli pfkA* gene in *G. oxydans* IK003.1 with plasmid pIK1 resulted in a specific phosphofructokinase activity of 62 ± 23 nmol min^{-1} (mg protein)$^{-1}$. In the case of pyruvate dehydrogenase complex, expression of the endogeneous *aceEα-aceEβ-aceF-lpd* genes with plasmid pIK1 led to an activity of 95 nmol min^{-1} (mg protein)$^{-1}$. Thus, phosphofructokinase and pyruvate dehydrogenase complex were functionally synthesized in *G. oxydans* IK003.1/pIK1.

Discussion

In a recent study we metabolically engineered *G. oxydans* 621H to obtain strain IK003.1 with a 60 % increased cell yield on glucose, allowing to decrease the costs for biomass synthesis in industrial applications. Here, we tried to further improve IK003.1 by plasmid-based expression of genes considered as beneficial to eliminate metabolic bottlenecks. Therefore, the 16-kb plasmid pIK1 was constructed which contains genes for a glucose facilitator and glucokinase in order to improve glucose uptake and phosphorylation, for phosphofructokinase in order to provide a functional glycolysis, and for the pyruvate dehydrogenase complex in order to allow pyruvate oxidation to acetyl-CoA and its oxidation

in the TCA cycle. The presence of plasmid pIK1 in strain IK003.1 did, however, not improve the growth properties, but rather reduced the growth rate and the cell yield on glucose compared to the plasmid-free IK003.1 strain. Overexpression of the endogenous *glk* gene caused a two-fold reduction of the specific glucokinase activity in cell extracts rather than an increase. The functionality of the glucose facilitator Glf from *Z. mobilis* in *G. oxydans* was not tested. Expression of *E. coli pfkA* led to the synthesis of functional phosphofructokinase, which should allow a functional glycolysis. Further studies are required to confirm usage of the glycolytic pathway experimentally, e.g. by labelling studies with ^{13}C-glucose. Overexpression of the endogenous *aceEα-aceEβ-aceF-lpd* genes led to a specific pyruvate dehydrogenase complex activity of 95.0 ± 59.0 nmol min^{-1} (mg protein)$^{-1}$. Despite this high activity, strain IK003.1/pIK1 still accumulated pyruvate to a similar concentration as strain IK003.1 without detectable pyruvate dehydrogenase complex activity. The inability to oxidize pyruvate could be due to a deficiency in NAD^+ and coenzyme A, which are essential substrates of the pyruvate dehydrogenase complex reaction, or to a deficiency in the subsequent enzymatic steps of the TCA cycle, in particular citrate synthase. The specific activity of citrate synthase measured in cell-free extracts of *G. oxydans* was 20 nmol min^{-1} (mg protein)$^{-1}$ (Kiefler et al., to be submitted) and thus five-fold lower than the pyruvate dehydrogenase complex activity in IK003.1/pIK1. This might cause an accumulation of acetyl-CoA, which is known to be an allosteric inhibitor of pyruvate dehydrogenase complex. The measured activities of aconitase and isocitrate dehydrogenase in cell-free extracts of *G. oxydans* were much lower than that of citrate synthase (Kiefler et al., to be submitted), suggesting that even in the case of sufficient citrate synthase activity the TCA cycle flux would stagnate soon. In summary, these results show that overproduction of single enzymes cannot solve the problem of a weak TCA cycle activity. Thus, future work should aim at the provision of sufficient and balanced activities of all TCA cycle enzymes in order to allow a complete oxidation of pyruvate to CO_2 with a concomitant gain in energy via oxidative phosphorylation and in cell yield.

Acknowledgements

The scientific activities of the Bioeconomy Science Center were financially supported by the Ministry of Innovation, Science and Research within the framework of the NRW Strategieprojekt BioSC (No. 313/323-400-002 13). We are most grateful to Uwe Deppenmeier (Universität Bonn) for providing plasmids pBBR1p384, pBBR1p452 and pBBR1p264.

References

Adachi, O., Moonmangmee, D., Toyama, H., Yamada, M., Shinagawa, E., Matsushita, K., 2003. New developments in oxidative fermentation. Appl. Microbiol. Biotechnol. 60**,** 643-653.

Bertani, G., 1951. Studies on lysogenesis. I. The mode of phage liberation by lysogenic *Escherichia coli*. J. Bacteriol. 62**,** 293-300.

Bertani, G., 2004. Lysogeny at mid-twentieth century: P1, P2, and other experimental systems. J. Bacteriol. 186**,** 595-600.

Deppenmeier, U., Hoffmeister, M., Prust, C., 2002. Biochemistry and biotechnological applications of *Gluconobacter* strains. Appl. Microbiol. Biotechnol. 60**,** 233-242.

Green, M. S., Sambrook, J., 2012. Molecular Cloning: A Laboratory Manual (Fourth Edition), Cold Spring Harbor Laboratory Press, www.molecularcloning.org.

Hanahan, D., Jessee, J., Bloom, F. R., 1991. Plasmid transformation of *Escherichia coli* and other bacteria. Meth. Enzymol. 204**,** 63-113.

Hanke, T., Nöh, K., Noack, S., Polen, T., Bringer, S., Sahm, H., Wiechert, W., Bott, M., 2013. Combined fluxomics and transcriptomics analysis of glucose catabolism via a partially cyclic pentose phosphate pathway in *Gluconobacter oxydans* 621H. Appl. Environ. Microbiol. 79**,** 2336-2348.

Kallnik, V., Meyer, M., Deppenmeier, U., Schweiger, P., 2010. Construction of expression vectors for protein production in *Gluconobacter oxydans*. J. Biotechnol. 150**,** 460-465.

Kiefler, I., Bringer, S., Bott, M., 2015. SdhE-dependent formation of a functional *Acetobacter pasteurianus* succinate dehydrogenase in *Gluconobacter oxydans*-a first step toward a complete tricarboxylic acid cycle. Appl. Microbiol. Biotechnol. 99**,** 9147-9160.

Kovach, M. E., Elzer, P. H., Hill, D. S., Robertson, G. T., Farris, M. A., Roop, R. M., 2nd,, Peterson, K. M., 1995. Four new derivatives of the broad-host-range cloning vector pBBR1MCS, carrying different antibiotic-resistance cassettes. Gene. 166**,** 175-176.

Krajewski, V., 2008. Modifikation des Glucosestoffwechsels in *Gluconobacter oxydans*. Dissertation, University of Duesseldorf, Germany.

Krajewski, V., Simić, P., Mouncey, N. J., Bringer, S., Sahm, H., Bott, M., 2010. Metabolic engineering of *Gluconobacter oxydans* for improved growth rate and growth yield on glucose by elimination of gluconate formation. Appl. Environ. Microbiol. 76**,** 4369-4376.

Macauley, S., McNeil, B., Harvey, L. M., 2001. The genus *Gluconobacter* and its applications in biotechnology. Crit. Rev. Biotechnol. 21**,** 1-25.

Mamlouk, D., Gullo, M., 2013. Acetic Acid bacteria: physiology and carbon sources oxidation. Indian J. Microbiol. 53**,** 377-384.

Niebisch, A., Kabus, A., Schultz, C., Weil, B., Bott, M., 2006. Corynebacterial protein kinase G controls 2-oxoglutarate dehydrogenase activity via the phosphorylation status of the OdhI protein. J. Biol. Chem. 281**,** 12300-12307.

Nishikura-Imamura, S., Matsutani, M., Insomphun, C., Vangnai, A. S., Toyama, H., Yakushi, T., Abe, T., Adachi, O., Matsushita, K., 2014. Overexpression of a type II 3-dehydroquinate dehydratase enhances the biotransformation of quinate to 3-dehydroshikimate in *Gluconobacter oxydans*. Appl. Microbiol. Biotechnol. 98**,** 2955-2963.

Parker, C., Barnell, W. O., Snoep, J. L., Ingram, L. O., Conway, T., 1995. Characterization of the *Zymomonas mobilis* glucose facilitator gene product (*glf*) in recombinant *Escherichia coli*: examination of transport mechanism, kinetics and the role of glucokinase in glucose transport. Mol. Microbiol. 15**,** 795-802.

Peters, B., Junker, A., Brauer, K., Mühlthaler, B., Kostner, D., Mientus, M., Liebl, W., Ehrenreich, A., 2013. Deletion of pyruvate decarboxylase by a new method for efficient markerless gene deletions in *Gluconobacter oxydans*. Appl. Microbiol. Biotechnol. 97**,** 2521-2530.

Prust, C., Hoffmeister, M., Liesegang, H., Wiezer, A., Fricke, W. F., Ehrenreich, A., Gottschalk, G., Deppenmeier, U., 2005. Complete genome sequence of the acetic acid bacterium *Gluconobacter oxydans*. Nat. Biotechnol. 23**,** 195-200.

Raspor, P., Goranovič, D., 2008. Biotechnological applications of acetic acid bacteria. Crit. Rev. Biotechnol. 28**,** 101-124.

Richhardt, J., Bringer, S., Bott, M., 2012. Mutational analysis of the pentose phosphate and Entner-Doudoroff pathways in *Gluconobacter oxydans* reveals improved growth of a Δ*edd* Δ*eda* mutant on mannitol. Appl. Environ. Microbiol. 78**,** 6975-6986.

Richhardt, J., Bringer, S., Bott, M., 2013a. Role of the pentose phosphate pathway and the Entner-Doudoroff pathway in glucose metabolism of *Gluconobacter oxydans* 621H. Appl. Microbiol. Biotechnol. 97**,** 4315-4323.

Santamaría, B., Estevez, A. M., Martinez-Costa, O. H., Aragon, J. J., 2002. Creation of an allosteric phosphofructokinase starting with a nonallosteric enzyme. The case of *Dictyostelium discoideum* phosphofructokinase. J. Biol. Chem. 277**,** 1210-1216.

Simon, R., Priefer, U., Pühler, A., 1983. A broad host range mobilization system for *in vivo* genetic-engineering-transposon mutagenesis in Gram-negative bacteria. Bio-Technol. 1**,** 784-791.

Weisser, P., Krämer, R., Sahm, H., Sprenger, G. A., 1995. Functional expression of the glucose transporter of *Zymomonas mobilis* leads to restoration of glucose and fructose uptake in *Escherichia coli* mutants and provides evidence for its facilitator action. J. Bacteriol. 177**,** 3351-3354.

Table 1
Bacterial strains, plasmids and oligonucleotides used in this work

Strain or plasmid or oligonucleotide	**Description or oligonucleotide sequence (5'→3')**	**Source or added restriction site[a]**
Strain		
E. coli DH10B	F⁻ *mcr*A Δ (*mrr-hsd*RMS-*mcr*BC) Φ80*lac*ZΔM15 Δ*lac*X74 *rec*A1 *end*A1 *ara*D139 Δ (*ara leu*) 7697 *gal*U *gal*K *rps*L *nup*G λ⁻	Invitrogen, Darmstadt, Germany
E. coli S17-1	Δ*rec*A, *end*A1, *hsd*R17, *sup*E44, *thi*-1, *tra*⁺	(Simon et al. 1983)
Z. mobilis	ATCC29191, wild type strain	American Type Culture Collection
G. oxydans Δ*upp* (reference strain)	*G. oxydans* 621H derivative with a deletion of GOX0327 coding for uracil phosphoribosyl-transferase (Δ*upp*)	A. Ehrenreich (TU Munich), (Peters et al. 2013a)
G. oxydans Δ*upp*/ pBBR1p452	*G. oxydans* 621H derivative with a deletion of GOX0327 coding for uracil phosphoribosyl-transferase (*upp*) carrying plasmid pBBR1p452	This work
IK003.1	*G. oxydans* Δ*gdhS::sdhCDABE* Δ*pdc::ndh* Δ*gdhM::sucCD*; *sdhCDAB* (APA01_00310-00340) from *A. pasteurianus* with promoter P264 and *sdhE* (APA01_11050) from *A. pasteurianus* with its native promoter genomically integrated into the *gdhS* (GOX2015) locus of *G. oxydans*; *ndh* from *G. oxydans* DSM3504 (GLS_c05650) genomically integrated with its native promoter into the *pdc* (GOX1081) locus of *G. oxydans*; *sucCD* (GDI_2951-2952) from *Ga. diazotrophicus* genomically integrated with promoter P264 into *gdhM* (GOX0265) locus of *G. oxydans*	Kiefler et al., to be submitted
IK003.1/pIK1	*G. oxydans* Δ*gdhS::sdhCDABE* Δ*pdc::ndh* Δ*gdhM::sucCD* carrying plasmid pIK1, see below	This work
Plasmid		
pBBR1p264	Kan^R, pBBR1MCS-2 derivative containing the 5'-UTR of GOX0264	(Kallnik et al. 2010; Kovach et al. 1995)
pBBR1p452	Kan^R, pBBR1MCS-2 derivative containing the 5'-UTR of GOX0452	(Kallnik et al. 2010; Kovach et al. 1995)
pBBR1p384	Kan^R, pBBR1MCS-2 derivative containing the 5'-UTR of GOX0384	Uwe Deppenmeier, Bonn
pBBR1p452-pdhC	pBBR1p452 derivative expressing *pdhC* (GOX2289-2292)	This work
pBBR1p452-glf	pBBR1p452 derivative expressing *glf* (Zmob_0907)	This work
pBBR1p264-glk	pBBR1p264 derivative expressing *glk* (GOX2419)	This work
pBBR1p452-glf-p264-glk	pBBR1p452 derivative expressing *glf* (Zmob_0907) and *glk* (GOX2419)	This work
pBBR1p384-pfkA	pBBR1p384 derivative expressing *pfkA* (ECDH10B_4105)	This work
pIK1	pBBR1p452 derivative expressing *pdhC* (GOX2289-	This work

	2292) under promoter P452, *glf* (Zmob_0907) with promoter P452, *glk* (GOX2419) with promoter P264 and *pfkA* (ECDH10B_4105) with promoter P384	
Oligonucleotide		
p264-forw	GTTGCGCCTGAATGAGAGGA	
p264-seq1-rev	TAACCCTCACTAAAGGGAAC	
pdhC-forw-XhoI	GTTAACCTCGAGATTTCCATCAGGAGACCGTC	XhoI
pdhC-rev-KpnI	TATATAGGTACCCAGGACGGCTTGCGCTGGAT	KpnI
glf-Zm-forw-EcoRI	GATATAGAATTCAAGGCGGGAGAGGAATCGCC	EcoRI
glf-Zm-rev-HindIII-pT	CGCGCGAAGCTTCCTTTTAGCCTGTTTTTAGC	HindIII
glk-forw	GCTATACTCGAGGCCAGAGGATTTGAGGTGCC	XhoI
glk-rev	GCTATAGGTACCAAACGGCGGTTTCGTGTGAG	KpnI
pfkA-forw-HindIII	CGCGCGAAGCTTTCCAAAGTTCAGAGGTAGTC	HindIII
pfkA-rev-XhoI	CGCGCGCTCGAGAATTGCAGAATTCATGTAGG	XhoI
p384-seq-forw	AAGACGCAGCGGAATGAGAG	Colony PCR
p384-seq-rev	CTTCCGGCTCGTATGTTGTG	Colony PCR
pBBR1p452-screen-forw	CTCACTATAGGGCGAATTGG	Colony PCR
pBBR1p452-screen-rev	CACAGGAAACAGCTATGACC	Colony PCR
M13uni(-43)	AGGGTTTTCCCAGTCACGACGTT	Colony PCR
M13rev(-49)	GAGCGGATAACAATTTCACACAGG	Colony PCR

Table 2
Cultivation parameters, glucose consumption and product formation of the engineered *G. oxydans* strains and the reference strains[a].

Parameter[c] (conc. in mM)	Reference strain I[b]	IK003.1	Reference strain II[b]	IK003.1/ pIK1
OD_{600}	4.6 ± 0.2	7.9 ± 0.2	4.6 ± 0.2	6.1 ± 0.4
g_{cdw}[d]	1.663 ± 0.054	2.837 ± 0.068	1.656 ± 0.085	2.194 ± 0.126
$Y_{X/S}$ ($g_{cdw}/g_{glucose}$)	0.089 ± 0.004	0.142 ± 0.001	0.077 ± 0.003	0.116 ± 0.011
$Y_{X/S}$ (% of ref.)	100	160	100	151
Growth rate (h^{-1})	0.3510 ± 0.0474	0.1678 ± 0.0014	0.3253 ± 0.0110	0.0638 ± 0.0091
Glucose (consumed)	103.6 ± 1.3	110.7 ± 1.8	108.1 ± 1.7	105.8 ± 4.8
Gluconate	2.0 ± 1.3	0.0 ± 0.0	0.0 ± 0.0	0.2 ± 0.2
2-KGA	38.1 ± 2.9	1.5 ± 0.1	39.7 ± 2.5	1.7 ± 0.2
5-KGA	0.0 ± 0.0	17.1 ± 1.6	3.6 ± 2.6	14.4 ± 0.3
Acetate	33.7 ± 3.2	1.0 ± 0.1	30.3 ± 1.5	3.1 ± 0.3
Pyruvate	0.3 ± 0.2	37.6 ± 0.6	0.6 ± 0.2	36.2 ± 0.1
Succinate	1.6 ± 0.9	2.0 ± 0.1	1.9 ± 1.1	4.5 ± 0.0
Fumarate	0.01 ± 0.0	0.03 ± 0.01	0.0 ± 0.0	0.0 ± 0.0
CO_2	233.1 ± 6.6	517.4 ±12.6	228.5 ± 2.7	536.8 ± 9.3
Carbon balance	99 %	131 %	96 %	135 %
Acid demand (2 M HCl, mL)	1.7 ± 0.1	0.1 ± 0.1	2.0 ± 0.1	0.3 ± 0.0
Base demand (2 M NaOH, mL)	12.6 ± 1.2	5.8 ± 0.0	13.6 ± 0.4	5.5 ± 0.2

[a]Mean values and standard deviation from three biological replicates are given.
[b]Reference strain I (*G. oxydans* 621H Δ*upp*) compares to strain IK003.1; reference strain II (*G. oxydans* Δ*upp*/pBBR1p452) compares to strain IK003.1 pIK1.
[c]Concentrations refer to end times for IK003.1, 28 h; IK003.1/pIK1, 50 h.
[d]cdw, cell dry weight. Calculation: OD_{600} x 0.36 = g_{cdw}.

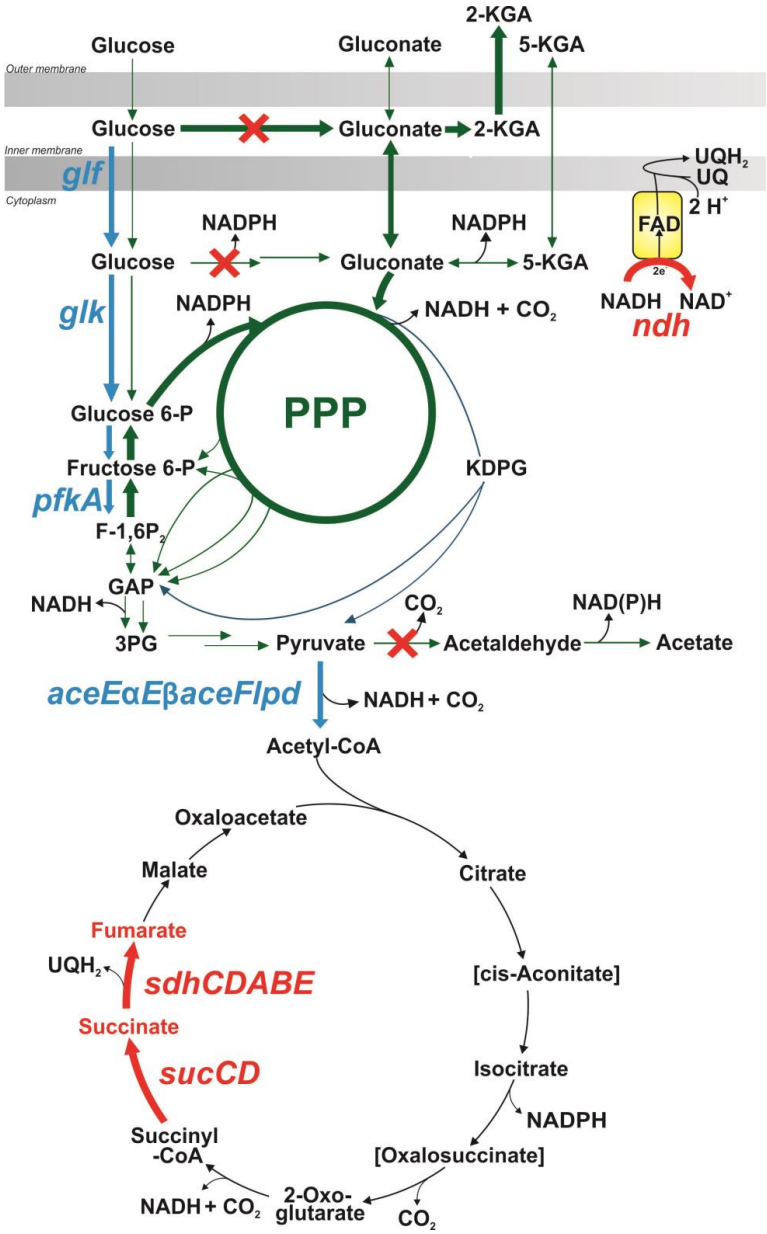

Figure 1. Scheme of the central carbon metabolism of *G. oxydans* with the substrate glucose at a cultivation pH of 6. 2-KGA, 2-ketogluconate; 5-KGA, 5-ketogluconate; UQ, ubiquinone; PPP, pentose phosphate pathway; glucose-6-P, glucose 6-phosphate; fructose 6-P, fructose 6-phosphate; F-1,6P_2, fructose 1,6-bisphosphate; GAP, glyceraldehyde 3-phosphate; 3PG, 3-phosphoglycerate; KDPG, 2-keto-3-deoxy-6-phosphogluconate. Green (bold) and blue (fine) arrows show the innate metabolism, red arrows (bold) denote reactions that were introduced by genomic integrations of the respective genes from various sources and red crosses mark inactivated functions. Blue arrows (bold) indicate reactions catalyzed by enzymes from plasmid-encoded genes.

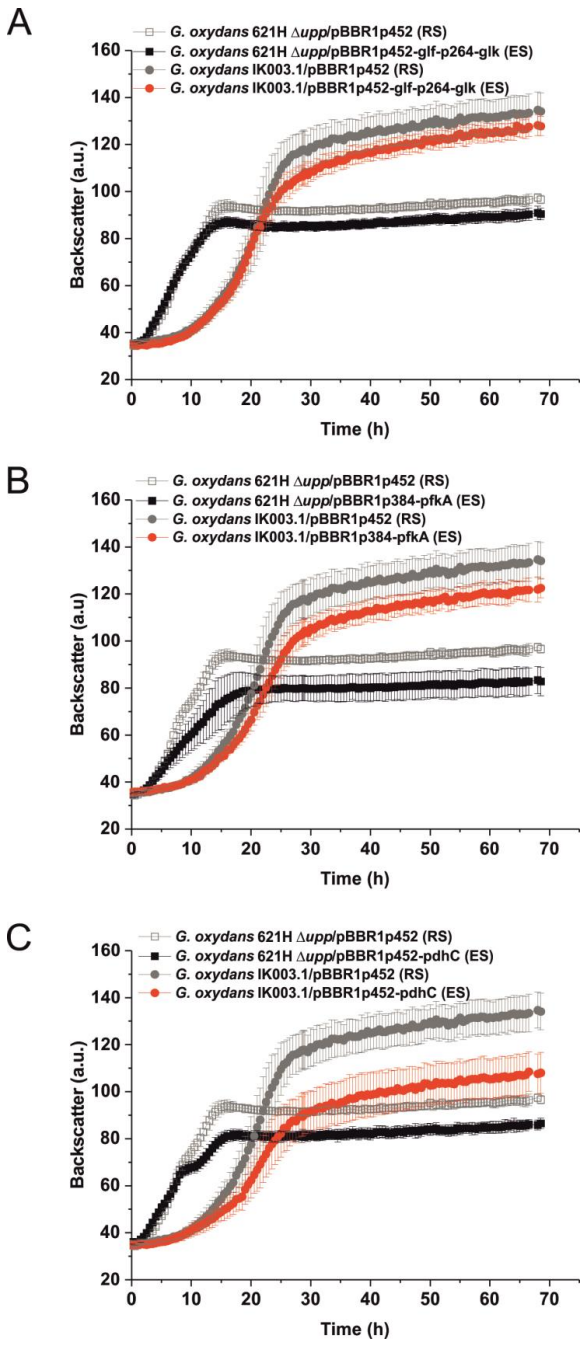

Figure 2. Growth of different *G. oxydans* reference (RS) and expression strains (ES) on glucose medium. The cultures were grown in a BioLector instrument (m2p-labs GmbH, Baesweiler, Germany) in glucose (2 %) medium and growth was followed by measuring the backscatter at 620 nm in arbitrary units (a.u.). Mean values and standard deviation from three replicates are given.

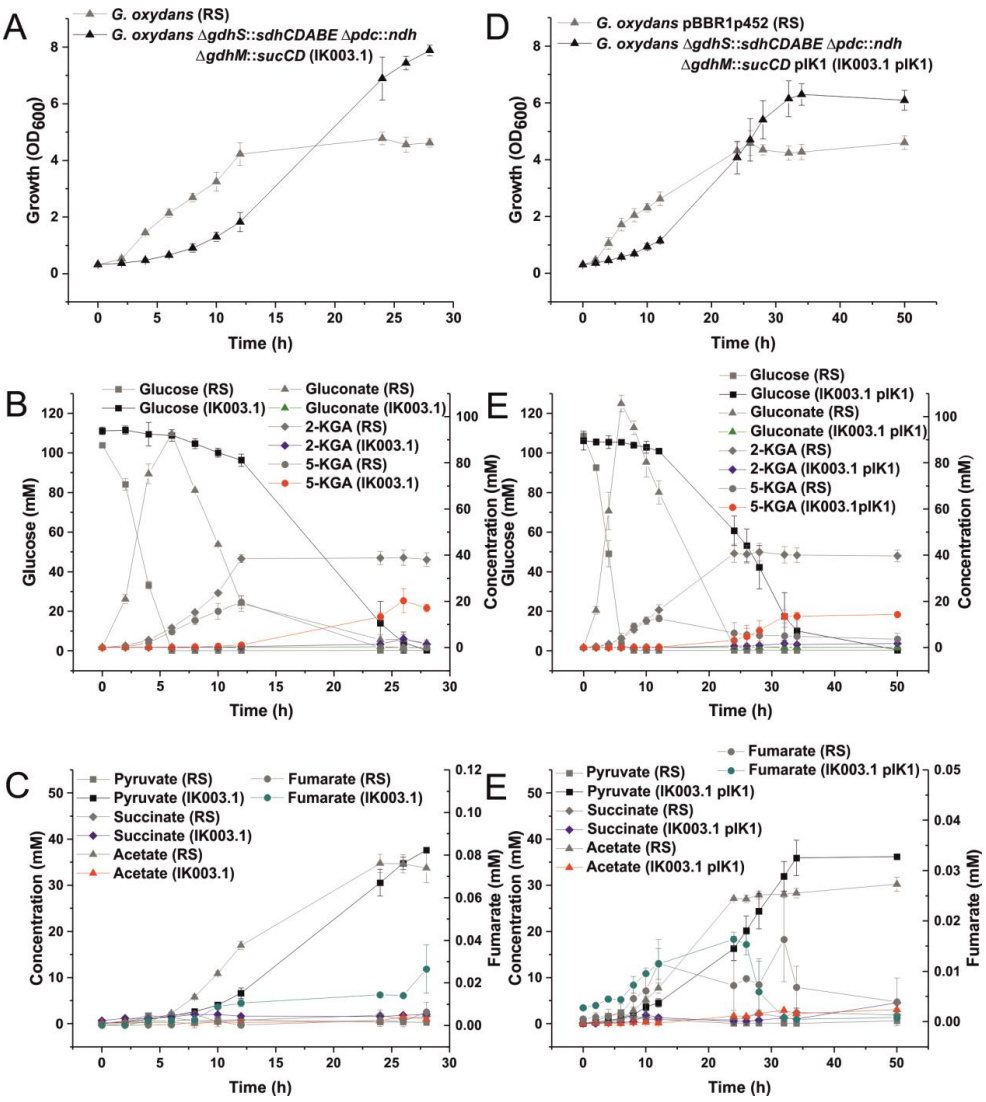

Figure 3. Growth **(A, D)**, substrate consumption and product formation **(B, C, E, F)** of the *G. oxydans* reference strain I (*G. oxydans* Δ*upp*; RS, gray symbols), *G. oxydans* Δ*gdhS*::*sdhCDABE* Δ*pdc*::*ndh* Δ*gdhM*::*sucCD* (strain IK003.1; colored symbols), reference strain II (*G. oxydans* Δ*upp*/pBBR1p452; RS, gray symbols) and *G. oxydans* Δ*gdhS*::*sdhCDABE* Δ*pdc*::*ndh* Δ*gdhM*::*sucCD*/pIK1 (strain IK003.1/pIK1; colored symbols). Gluconate, 2-ketogluconate (2-KGA), 5-ketogluconate (5-KGA), pyruvate, acetate, succinate and fumarate concentrations were determined by HPLC. The cultures were grown in glucose (2 % w/v) medium at 15 % dissolved oxygen at pH 6 in a parallel bioreactor system (DASGIP, Juelich, Germany). Mean values and standard deviation from three biological replicates are shown.

4. Discussion

The acetic acid bacterium *G. oxydans* is an organism of high biotechnological relevance due to a large set of membrane-bound dehydrogenases oxidizing a broad range of carbohydrates and alcohols in the periplasm stereo- and regioselectively. The corresponding products accumulate almost completely in the medium offering a great advantage to industrial applications. However, a handicap for further use of *G. oxydans* are very low cell yields caused by special metabolic features (De Ley et al. 1984; Deppenmeier and Ehrenreich 2009). The carbohydrates provided for energy and biomass formation are incompletely oxidized in the periplasm and the products remain unmetabolized in the medium. The mechanism of glucose uptake into the cell is not known so far. *G. oxydans* possesses an incomplete PEP: carbohydrate phosphotransferase system (PTS). Based on the absence of the EIIC and EIIB components a regulatory function rather than a transporter function is suggested. *G. oxydans* lacks genes for phosphofructokinase, succinyl-CoA synthetase, and succinate dehydrogenase resulting in an interrupted glycolysis and an incomplete TCA cycle (Prust et al. 2005). Intracellular carbon metabolism proceeds primarily via the PPP and to a minor part via the EDP (Hanke et al. 2013; Richhardt et al. 2012, 2013a). This study aimed at the improvement of the cell yield on glucose to increase the potential for industrial application in oxidative biotransformations. To this end, different strains of *G. oxydans* were constructed, which are unable to oxidize glucose to gluconate due to deletion of the genes coding for the membrane-bound glucose dehydrogenase (*gdhM*, GOX0265) and the cytosolic glucose dehydrogenase (*gdhS*, GOX2015). Heterologous expression of the glucose facilitator gene (*glf*) and overexpression of glucokinase (*glk*, GOX2419) should enhance the glucose consumption rate. Through the heterologous expression of the phosphofructokinase gene (*pfkA*), glucose degradation should be possible via the EMP pathway in addition to the PPP and EDP. The formation of acetate is prevented by deletion of the pyruvate decarboxylase gene (*pdc*, GOX1081) and an increased oxidative decarboxylation of pyruvate to acetyl-CoA should be possible by overexpression of the endogenous genes encoding the pyruvate dehydrogenase complex (GOX2289, *aceE*α; GOX2290, *aceE*β; GOX2291, *aceF*; GOX2292, *lpd*). *G. oxydans* strains constructed in this study theoretically possess a complete TCA cycle enabling a complete oxidation of acetyl-CoA due to the genomic integration of genes coding for succinate dehydrogenase (*sdhCDABE*) and succinyl-CoA synthetase (*sucCD*). Due to the complete intracellular glucose degradation the NADH formation rate should increase, leading to an enhanced demand for NADH dehydrogenase activity (Kostner et al. 2015). To avoid a NADH accumulation, a second gene for NADH dehydrogenase (*ndh*) was integrated into the

genome of *G. oxydans*. The four strains *G. oxydans* IK001, *G. oxydans* IK002.1, *G. oxydans* IK003.1 and *G. oxydans* IK003.1/pIK1 were characterized with respect to their growth behavior on glucose, substrate consumption and product formation. Furthermore, the enzyme activities resulting from expression of the corresponding homologous or heterologous genes and the TCA cycle genes were determined.

4.1. Synthesis of a heterologous succinate deyhdrogenase in *G.oxydans*

The TCA cycle is an amphibolic metabolic pathway providing energy in the form of reducing equivalents (NADH, NADPH, ubiquinol) and ATP and precursors (oxaloacetate, 2-oxoglutarate) for biosynthesis. In *G. oxydans* the generation of ATP via succinyl-CoA synthetase and ubiquinol formation by succinate dehydrogenase is not possible due to the absence of the corresponding genes (Prust et al. 2005). The first step in *G. oxydans* strain development was the introduction of a heterologous Sdh complex due to an assumed high risk for the functional synthesis of this membrane protein complex. As donor strain for the *sdh* genes the close relative *Acetobacter pasteurianus* was chosen. In Gram-negative bacteria Sdh is composed of a flavoprotein subunit SdhA containing a covalently linked flavin adenine dinucleotide (FAD) prosthetic group, an iron-sulfur protein subunit SdhB with three iron-sulfur clusters, and the membrane-integral subunits SdhC and SdhD containing a cytochrome *b* (Nishimura 1986; Park et al. 1997; Majumdar et al. 1991; Zhang et al. 2014; McNeil and Fineran 2013 a). The covalent binding of FAD to the SdhA subunit was reported to be essential for electron transfer from succinate due to an increase of the FAD redox potential (Cheng et al. 2015). McNeil and coworkers identified a protein required for the covalent attachment of FAD to the subunit SdhA in *Serratia* strain ATCC 39006 and named it SdhE (McNeil et al. 2012). Homologs of SdhE are present in α-, β-, and γ-proteobacteria and eukaryotes including humans (McNeil et al. 2012; McNeil and Fineran 2013 b, 2013 a; Van Vranken et al. 2015). SdhE of *Serratia* is a soluble protein of 88 amino acid residues with a highly conserved RGxxE motif (McNeil and Fineran 2013 b). In this study the SdhE homolog of *A. pasteurianus* was identified and shown to be required for synthesis of a functional Sdh of *A. pasteurianus* in the heterologous *G. oxydans* host. Thereby, the necessity of SdhE for activation of Sdh in α-proteobacteria was demonstrated. UV-induced fluorescence indicated flavinylation of the *A. pasteurianus* SdhA protein only in the presence of SdhE. In the absence of SdhE the residual Sdh activity was negligible quite in contrast to *Serratia*. Furthermore, it could be shown that the γ-proteobacterial *Serratia* SdhE protein is able to flavinylate the α-proteobacterial *A. pasteurianus* SdhA protein in *G. oxydans*. Co-expression of *sdhE* with the Sdh structural genes *sdhCDAB* was sufficient to achieve an active Sdh in *G. oxydans* with succinate/oxygen reductase activity, indicating the formation of a holo-

complex enabling the electron transfer from succinate via FAD in SdhA, the iron-sulfur clusters in SdhB to the ubiquinone binding site of SdhCD. Like *A. pasteurianus*, *G. oxydans* possesses the Suf and the Nif systems for iron-sulfur cluster biogenesis and repair (Roche et al. 2013; Prust et al. 2005) and the succinate/oxygen reductase activity indicates that these systems are sufficient for the correct insertion of [2Fe-2S], [3Fe-4S], and [4Fe-4S] into the heterologous apo-SdhB subunit. However, a functional Sdh complex in *G. oxydans* did not result in an improved growth on mannitol. On the contrary, for the *G. oxydans* strain exhibiting the highest Sdh activity (almost 4000 nmol min^{-1} mg $protein^{-1}$) even a decreased growth in the second growth phase was observed. An explanation might be the low energy availability in the second growth phase, where fructose is slowly oxidized to 5-ketofructose (Richhardt et al. 2012) and the strong metabolic burden of Sdh overexpression. Additionally, the Sdh-positive strain produced small amounts of fumarate implying the presence of a functional Sdh *in vivo* and at the same time a limiting fumarate hydratase activity.

The next critical step in *G. oxydans* strain development consisted in the genomic integration of the *sdhCDABE* genes with simultaneous deletion of the *gdhS* (GOX2015) gene for the cytosolic glucose dehydrogenase catalyzing the NADP-dependent oxidation of glucose to gluconate (Prust et al. 2005; Krajewski et al. 2010). The initial genomic integration of the insert p384-*sdhCDAB*-P_{nat}-*sdhE* resulted in a succinate/DCPIP reductase activity of 15.0 ± 0.5 nmol min^{-1} mg $protein^{-1}$. In order to achieve a higher Sdh activity the *sdhCDAB* genes were cloned under control of the strong promoter p264 and insert p264-*sdhCDAB*-P_{nat}-*sdhE* was used to replace the *gdhS* gene. The promoter change caused a five-fold increase of succinate/DCPIP reductase activity (74.7 ± 22.9 nmol min^{-1} $(mg\ protein)^{-1}$ of the resulting strain *G. oxydans* IK001. Cultivation of the *gdhS* negative/*sdhCDABE* positive strain *G. oxydans* IK001 with glucose as carbon source revealed a slightly faster growth, but no improvement of the cell yield in comparison to the reference strain *G. oxydans* Δ*upp*. It has previously been shown that a *G. oxydans gdhS* deletion mutant exhibited a minor growth inhibition in the second growth phase (Kiefler 2012) (Supplement, Fig. 1). This observation supports that the slightly enhanced growth of strain *G. oxydans* IK001 is caused by an active Sdh. Glucose consumption and product formation of strain IK001 and the reference strain were comparable. However, strain *G. oxydans* IK001 produced almost 10 mM more 2-KGA than the reference strain, which might be caused by an increased glucose oxidation in the periplasm as a consequence of the *gdhS* deletion. Furthermore, the mutant produced minute fumarate concentrations suggesting a Sdh *in vivo* activity. In *G. oxydans* carbon metabolism proceeds mainly via the PPP, however a decreased CO_2 production of 18 % during cultivation is presumably a hint on a preference of strain IK001 to metabolize glucose via the EDP instead of the PPP (Kruger and von Schaewen 2003; Richhardt et al. 2012).

4.2 Impact of an additional NADH dehydrogenase

G. oxydans strain IK001 was still able to oxidize the major part of glucose in the periplasm. In order to prevent this reaction and increase intracellular glucose metabolism, the next expected step would be the deletion of the membrane-bound glucose dehydrogenase gene (GOX0265, *gdhM*). Previous studies on glucose metabolism of *G. oxydans* strain N44-1 demonstrated the impact of the cytosolic and membrane-bound glucose dehydrogenase on growth. Disruption of the *gdhM* gene resulted in a growth yield increase of 110 %, whereas the growth rate raised about 271 % through deletion of *gdhM* and disruption of *gdhS* (Krajewski et al. 2010). However, the positive effect on growth by deletion of the *gdhM* and *gdhS* genes in strain *G. oxydans* 621 H was not observed revealing the large difference between these two strains (Kiefler 2012) (Supplement, Fig.2). Until now, we have no explanation for this effect. Genome sequencing of N44-1 has to be performed to have a closer look on the differences in carbon metabolism. Strain N44-1 might possess genes lacking in *G. oxydans* 621H and/or more copies of particular genes in the genome offering an advantage with respect to growth. For prevention of a negative effect of *gdhM* deletion on growth, we decided to delete the pyruvate decarboxylase gene (GOX1081, *pdc*) before *gdhM*. A positive effect on growth by deletion of the *pdc* gene was reported previously (Peters et al. 2013a; Kiefler 2012) (Supplement, Fig.3). Based on the incomplete TCA cycle of *G. oxydans*, a complete oxidation of pyruvate to CO_2 cannot occur via this pathway. Instead, a significant amount of pyruvate is converted to acetate by pyruvate decarboxylase and acetaldehyde dehydrogenase. Pyruvate decarboxylase, which is rarely found in bacteria, catalyzes the decarboxylation of pyruvate to the toxic intermediate acetaldehyde under CO_2 formation (Krajewski et al. 2010).

In a recent study, the plasmid-based expression of the *ndh* gene from *G. oxydans* DSM3504 in *G. oxydans* 621H led to a significantly increase of the growth rate (Kostner et al. 2015), indicating that a limited NADH oxidation capacity is in part responsible for the better growth of DSM3504 possessing an additional type II NADH dehydrogenase gene (*ndh*) compared to strain 621H with only a single *ndh* gene. As a consequence of the strongly elevated intracellular glucose metabolism caused by the *gdhS* deletion and planned *gdhM* deletion, the NADH and NADPH formation rate via glucose 6-phosphate dehydrogenase, 6-phosphogluconate dehydrogenase, and glyceraldehyde 3-phosphate dehydrogenase should also increase significantly. To support the reoxidation of NADH to NAD^+, the *ndh* gene of *G. oxydans* DSM3504 was used to replace the pyruvate decarboxylase gene in strain IK001, resulting in strain *G. oxydans* IK002.1. The mutant strain exhibited only an 11 % elevated NADH dehydrogenase activity compared to the reference strain, which might be caused by a low activity of the native promoter of the *ndh* gene from *G. oxydans* strain DSM3504. *G. oxydans* IK002.1 exhibited no significant differences in the first growth phase, but reached

a slightly higher final OD_{600} in comparison to the reference strain of about 12 %, when cultivated on glucose. The mutant strain produced less 2-KGA and significant amounts 5-KGA. At pH 6 used during cultivation, synthesis of 5-KGA is catalyzed by the NADP-dependent gluconate 5-dehydrogenase (GOX2187, Gno) in the cytoplasm and secreted into the medium. 5-KGA is taken up again by the reference strain, however the uptake mechanism is unknown (Rauch et al. 2010). Formation of 2-KGA occurs in the periplasm via the membrane-bound flavoprotein gluconate-2-dehydrogenase (GOX1230-1232, *gndSLC*). The transhydrogenase PntA1A2B presumably converted NADPH to NADH and is possibly coupled to proton extrusion. The increased NADH oxidation capacity provided by the introduced second *ndh* gene might be responsible for the 5-KGA formation and reduced 2-KGA production. Acetate formation was prevented in strain IK002.1, but equivalent amounts pyruvate were secreted caused by replacement of *pdc* by *ndh* (Peters et al. 2013a). Acetate (pK_a 4.78) act as an uncoupler in contrast to pyruvate (pK_a of 2.49) caused by a lower pK_a (Axe and Bailey 1995). Thus, prevention of acetate formation in strain IK002.1 might ensure an increase of energy efficiency leading to increased utilization component(s) of the yeast extract (carbon balance 120 %), and also might explain improved biomass formation.

4.3 Consequences of the absence of membrane-bound glucose dehydrogenase and introduction of a heterologous succinyl-CoA synthetase to provide all enzymes for a functional TCA cycle

The next step in *G. oxydans* strain development was the replacement of the *gdhM* gene (GOX0265) encoding the membrane-bound glucose dehydrogenase by the succinyl-CoA synthetase (Scs) genes *sucCD* from *Gluconacetobacter diazotrophicus* in strain IK002.1, resulting in strain *G. oxydans* IK003.1. *Ga. diazotrophicus* was chosen as donor strain, because *A. pasteurianus* lacks the *sucCD* genes. The close phylogenetic relationship of *G. oxydans* to *Ga. diazotrophicus* was promising with regard to a functional synthesis of Scs in the host *G. oxydans*. However, *G. oxydans* IK003.1 exhibited a very low *in vitro* Scs activity, although the *sucCD* genes were under control of the strong P264 promoter. The reason for this low activity is not known yet. Presumably the Scs activity is already very low in the host, which needs to be tested. As a consequence of the deletion of *gdhS* and *gdhM* in *G. oxydans* IK003.1, glucose was completely metabolized in the cytoplasm, providing more precursors for biomass formation, and neither gluconate nor 2-ketogluconate were formed. However, *G. oxydans* IK003.1 produced almost 20 mM 5-ketogluconate, which presumably is formed by dephosphorylation of 6-phosphogluconate to gluconate and subsequent oxidation via the NADP-dependent gluconate-5 dehydrogenase. Cultivation of *G. oxydans* IK003.1 on glucose revealed a retarded growth phenotype in the first 12 h. Nevertheless, the

mutant strain showed a significantly higher final OD_{600} of about 72 % and cell yield was increased by 60 % compared to the reference strain. Due to the *gdhM* deletion, degradation of the substrate glucose was also retarded, which might be due to limitations in glucose uptake and phosphorylation via glucokinases (GlkA, GlkB) (Rauch et al. 2010; Pronk et al. 1989). Like *G. oxydans* IK002.1, the mutant *G. oxydans* IK003.1 synthesized pyruvate in a growth-coupled manner (40 mM) instead of acetate due to the *pdc* deletion. The 2.2-fold increased CO_2 formation is a striking characteristic of strain IK003.1, although pyruvate decarboxylase is absent. Due to prevention of glucose oxidation the carbon source is completely catabolized in the cytoplasm in strain IK003.1 and to a large extent via the PPP. Thus, enhanced CO_2 formation might be caused by the cyclic PPP offering the major pathway of sugar degradation in *G. oxydans* (Richhardt et al. 2012; Hanke et al. 2013). Another possibility for the increased CO_2 level could be the activity of a functional TCA cycle. Although pyruvate dehydrogenase complex activity was not detectable in *G. oxydans*, carboxylation of PEP to oxaloacetate via PEP carboxylase (GOX0102) might enable a glucose-derived carbon flux into the TCA cycle. However, supply of acetyl-CoA offering a problem which could be derived from the oxidation of fatty acids and other components of the yeast extract.

4.4 Plasmid-based expression of genes encoding glucose facilitator, glucokinase, phosphofructokinase pyruvate dehydrogenase complex

The last step in *G. oxydans* strain development consisted in the plasmid-based expression of genes encoding glucose facilitator (*glf*) from *Zymomonas mobilis*, endogenous glucokinase (*glkB*), phosphofructokinase (*pfkA*) from *Escherichia coli* and endogenous pyruvate dehydrogenase complex (GOX2289, *aceE*α; GOX2290, *aceE*β; GOX2291, *aceF*; GOX2292, *lpd*) (plasmid pIK1) in the improved strain IK003.1. *In vitro* a PfkA activity of 62 nmol min^{-1} mg $protein^{-1}$ was obtained demonstrating a functional synthesis of *E. coli* PfkA in *G. oxydans*. The high amounts of pyruvate accumulating in the medium in the *pdc* negative strains indicate a low activity of the pyruvate dehydrogenase complex. The assumption was confirmed by an enzyme assay yielding no measurable pyruvate dehydrogenase complex activity in the reference strain. In contrast the expression strain *G. oxydans* IK003.1/pIK1 exhibited an active pyruvate dehydrogenase complex with 95 nmol min^{-1} $(mg\ protein)^{-1}$. However, *in vitro* glucokinase (Glk) activity decreased by 47 % in the expression strain. In a previous study it was observed that Glk activity in a *gdhS* deletion mutant was much less than in the wildtype (87 %) or in a *gdhM* disruption mutant (92 %) (Krajewski 2008). These data indicate a dependency of Glk activity (*in vitro*) on GdhS in *G. oxydans*. Cultivation of strain IK003.1/pIK1 on glucose showed a retarded growth. The final OD_{600} rose about 33 %

compared to the reference strain and a cell yield increase of 51 % was obtained. Nevertheless, the expression plasmid caused an impairment in comparison to strain IK003.1 without a plasmid. Previously, it has been shown that heterologous *pfkA* expression in *Neisseria meningitidis* resulted in a decrease of biomass yield caused by stress, protein turnover, or cycling with fructose bisphosphatase resulting in an ATP-consuming process. The enhanced ATP demand caused a higher oxygen consumption, CO_2 generation and biomass yield decrease (Baart et al. 2010). A slightly increased CO_2 formation was also observed in the *G. oxydans* IK003.1/pIK1 strain compared to IK003.1 without plasmid. Furthermore, the negative effect on cell yield might be due to a high protein burden and an imbalance of enzyme activities causing the accumulation of metabolic intermediates and redox cofactors. Another evidence for an enzyme activity imbalance is that pyruvate accumulation still occurred in the expression strain, although the pyruvate dehydrogenase complex is active. Most likely, pyruvate degradation is limited due to the very low activities of the TCA cycle enzymes measured *in vitro* and/or allosteric inhibiton of the pyruvate dehydrogenase complex by NADH and acetyl-CoA *in vivo*.

4.5 Conclusions and outlook

In this study different steps in synthetic biology were undertaken to obtain a *G. oxydans* strain generating improved cell yields for a broader industrial use. To this end, the genomic integration of genes in *G. oxydans* presents an essential method. In the present work the successful integration of genes was established offering possibilities for further investigations concerning this organism. The complementation of the TCA cycle by genomic integration of genes encoding the succinate dehydrogenase and succinyl-CoA synthetase revealed an important step in *G. oxydans* strain construction and is essential for further strain optimization. The constructed *G. oxydans* strain IK003.1 possesses the ability to metabolize glucose completely in the cytoplasm ensured by deletion of the cytosolic glucose dehydrogenase (*gdhS*) and the membrane-bound glucose dehydrogenase (*gdhM*) genes. Consequently, the energy and carbon source glucose can be used for the desired biomass formation. Furthermore, the additional support of NADH oxidation by a second gene for NADH dehydrogenase and the concurrent prevention of acetaldehyde formation through deletion of the pyruvate decarboxylase gene in the designed *G. oxydans* strain IK003.1 is ensured. Metabolic changes of the constructed strain resulted in an increased biomass formation on the favorable carbon source glucose. Consequently, the costs for biomass production of *G. oxydans* required for oxidative biotransformations with resting cells can be reduced offering a great advantage to industry.

The metabolic engineering steps undertaken in this work represent a good basis for further improvement of cell yields of *G. oxydans* and built a fundament for further strain optimization of *G. oxydans* for extended biotechnological applications.

Due to the low activities of the innate TCA cycle enzymes determined in this study, the increase of the activities is necessary to prevent pyruvate accumulation in the medium and to ensure the complete intracellular glucose metabolism. Therefore, in future attempts promoter exchanges of TCA cycle genes should be performed. As shown in the present work, pyruvate dehydrogenase complex exhibited no measurable *in vitro* activity. Thus, promoter exchange is also essential to improve pyruvate decarboxylation to acetyl-CoA and guarantee the entire oxidation of acetyl-CoA via the improved TCA cycle.

Richhardt et al. demonstrated a positive effect on growth caused by the overexpression of the cytochrome bo_3 oxidase genes in *G. oxydans* (Richhardt et al. 2013b). Consequently, a further optimization of the constructed *G. oxydans* strain in this study can be achieved by the improvement of the respiratory chain.

5. Literature

Adachi O, Moonmangmee D, Shinagawa E, Toyama H, Yamada M, Matsushita K (2003) New quinoproteins in oxidative fermentation. Biochim Biophys Acta 1647 (1-2):10-17

Adachi O, Toyama, H., Matsushita, K. (1999) Crystalline NADP-dependent D-mannitol dehydrogenase from *Gluconobacter suboxydans* Biosci Biotechnol Biochem 63 (2):402-407

Ameyama M, Matsushita K, Shinagawa E, Adachi O (1987) Sugar-oxidizing respiratory chain of *Gluconobacter suboxydans*. Evidence for a branched respiratory chain and characterization of respiratory chain-linked cytochromes. Agric Biol Chem 51 (11):2943-2950

Ano Y, Shinagawa E, Adachi O, Toyama H, Yakushi T, Matsushita K (2011) Selective, high conversion of D-glucose to 5-keto-D-gluconate by *Gluconobacter suboxydans*. Biosci Biotechnol Biochem 75 (3):586-589. doi:10.1271/bbb.100701

Asai T (1935) Taxonomic studies on acetic acid bacteria and allied oxidative bacteria isolated from fruits. A new classification of the oxidative bacteria. J Agr Chem Soc Jpn 11:499-513, 610-620, 674-708

Axe DD, Bailey JE (1995) Transport of lactate and acetate through the energized cytoplasmic membrane of *Escherichia coli*. Biotechnol Bioeng 47 (1):8-19. doi:10.1002/bit.260470103

Baart GJ, Langenhof M, van de Waterbeemd B, Hamstra HJ, Zomer B, van der Pol LA, Beuvery EC, Tramper J, Martens DE (2010) Expression of phosphofructokinase in *Neisseria meningitidis*. Microbiology 156 (Pt 2):530-542. doi:10.1099/mic.0.031641-0

Bassetti M, Pecori D, Sartor A, Londero A, Villa G, Cadeo B, Brillo F, Bongiorno D, Campanile F, Stefani S (2013) First report of endocarditis by *Gluconobacter* spp. in a patient with a history of intravenous-drug abuse. J Infect 66 (3):285-287. doi:10.1016/j.jinf.2012.05.006

Bizouarn T, Althage M, Pedersen A, Tigerstrom A, Karlsson J, Johansson C, Rydstrom J (2002) The organization of the membrane domain and its interaction with the NADP(H)-binding site in proton-translocating transhydrogenase from *E. coli*. Biochim Biophys Acta 1555 (1-3):122-127

Blangy D, Buc H, Monod J (1968) Kinetics of the allosteric interactions of phosphofructokinase from *Escherichia coli*. J Mol Biol 31 (1):13-35

Bridger WA (1971) Evidence for two types of subunits in succinyl coenzyme A synthetase. Biochem Biophys Res Commun 42 (5):948-954

Bridger WA (1974) Succinyl-CoA synthetase. In P D Boyer (ed), The enzymes, Academic Press, Inc, New York, NY 10:581-606

Cheng VW, Piragasam RS, Rothery RA, Maklashina E, Cecchini G, Weiner JH (2015) Redox state of flavin adenine dinucleotide drives substrate binding and product release in *Escherichia coli* succinate dehydrogenase. Biochemistry 54 (4):1043-1052. doi:10.1021/bi501350j

Cotton NP, White SA, Peake SJ, McSweeney S, Jackson JB (2001) The crystal structure of an asymmetric complex of the two nucleotide binding components of proton-translocating transhydrogenase. In: Structure, vol 9. vol 2, 2001/03/16 edn., pp 165-176

D'mello R, Hill S, Poole RK (1996) The cytochrome *bd* quinol oxidase in *Escherichia coli* has an extremely high oxygen affinity and two oxygen-binding haems: implications for regulation of activity *in vivo* by oxygen inhibition. Microbiology 142 (Pt 4):755-763

Dauner M, Sonderegger M, Hochuli M, Szyperski T, Wüthrich K, Hohmann HP, Sauer U, Bailey JE (2002) Intracellular carbon fluxes in riboflavin-producing *Bacillus subtilis* during growth on two-carbon substrate mixtures. Appl Environ Microbiol 68 (4):1760-1771

De Ley J, Gillis M, Swings J (1984) The genus *Gluconobacter*. Krieg NR, Holt JG (eds) Bergey's Manual of Systematic Bacteriology vol 1 (3):pp 267–278

Deppenmeier U, Ehrenreich A (2009) Physiology of acetic acid bacteria in light of the genome sequence of *Gluconobacter oxydans*. J Mol Microbiol Biotechnol 16 (1-2):69-80. doi:10.1159/000142895

Deppenmeier U, Hoffmeister M, Prust C (2002) Biochemistry and biotechnological applications of *Gluconobacter* strains. Appl Microbiol Biotechnol 60 (3):233-242. doi:10.1007/s00253-002-1114-5

Dibrova DV, Galperin M, Mulkidjanian A (2010) Characterization of the N-ATPase, a distinct, laterally transferred Na^+-translocating form of the bacterial F-type membrane ATPase. Bioinformatics 26:1473–1476. doi:10.1093/bioinformatics/btq234

Duckworth HW, Nguyen NT, Gao Y, Donald LJ, Maurus R, Ayed A, Bruneau B, Brayer GD (2013) Enzyme-substrate complexes of allosteric citrate synthase: evidence for a novel intermediate in substrate binding. Biochim Biophys Acta 1834 (12):2546-2553. doi:10.1016/j.bbapap.2013.07.019

Euzeby J (2005) Validation of publication of new names and new combinations previously effectively published outside the IJSEM. Int J Syst Evol Microbiol 55 (Pt 3):983-985. doi:10.1099/ijs.0.63767-0

Georgiou CD, Dueweke TJ, Gennis RB (1988) Beta-galactosidase gene fusions as probes for the cytoplasmic regions of subunits I and II of the membrane-bound cytochrome d terminal oxidase from *Escherichia coli*. J Biol Chem 263 (26):13130-13137

Gossele F, Van den Mooter M, Verdonck L, Swings J, De Ley J (1981) The nitrogen requirements of *Gluconobacter*, *Acetobacter* and *Frateuria*. Anton Leeuw 47 (4):289-296

Greenfield S, Claus GW (1972) Nonfunctional tricarboxylic acid cycle and the mechanism of glutamate biosynthesis in *Acetobacter suboxydans*. J Bacteriol 112 (3):1295-1301

Gupta A, Singh VK, Qazi GN, Kumar A (2001) *Gluconobacter oxydans*: its biotechnological applications. J Mol Microbiol Biotechnol 3 (3):445-456

Hägerhäll C (1997) Succinate: quinone oxidoreductases. Variations on a conserved theme. Biochim Biophys Acta 1320 (2):107-141

Hägerhäll C, Hederstedt L (1996) A structural model for the membrane-integral domain of succinate: quinone oxidoreductases. FEBS Lett 389 (1):25-31

Hanke T, Nöh K, Noack S, Polen T, Bringer S, Sahm H, Wiechert W, Bott M (2013) Combined fluxomics and transcriptomics analysis of glucose catabolism via a partially cyclic pentose phosphate pathway in *Gluconobacter oxydans* 621H. Appl Environ Microbiol 79 (7):2336-2348. doi:10.1128/AEM.03414-12

Hanke T, Richhardt J, Polen T, Sahm H, Bringer S, Bott M (2012) Influence of oxygen limitation, absence of the cytochrome bc_1 complex and low pH on global gene expression in *Gluconobacter oxydans* 621H using DNA microarray technology. J Biotechnol 157 (3):359-372. doi:10.1016/j.jbiotec.2011.12.020

Hauge JG, King TE, Cheldelin VH (1955) Oxidation of dihydroxyacetone via the pentose cycle in *Acetobacter suboxydans*. J Biol Chem 214 (1):11-26

Hederstedt L (1999) Respiration without O_2. Science 284 (5422):1941-1942

Hederstedt L (2003) Structural biology. Complex II is complex too. Science 299 (5607):671-672. doi:10.1126/science.1081821

Hölscher T, Schleyer U, Merfort M, Bringer-Meyer S, Görisch H, Sahm H (2009) Glucose oxidation and PQQ-dependent dehydrogenases in *Gluconobacter oxydans*. J Mol Microbiol Biotechnol 16 (1-2):6-13. doi:10.1159/000142890

Hutkins RW (2008) Microbiology and technology of fermented foods.402

Johnson JD, Mehus JG, Tews K, Milavetz BI, Lambeth DO (1998) Genetic evidence for the expression of ATP- and GTP-specific succinyl-CoA synthetases in multicellular eucaryotes. J Biol Chem 273 (42):27580-27586

Joyce MA, Fraser ME, Brownie ER, James MN, Bridger WA, Wolodko WT (1999) Probing the nucleotide-binding site of *Escherichia coli* succinyl-CoA synthetase. Biochemistry 38 (22):7273-7283. doi:10.1021/bi990527s

Kawai S, Goda-Tsutsumi M, Yakushi T, Kano K, Matsushita K (2013) Heterologous overexpression and characterization of a flavoprotein-cytochrome *c* complex fructose dehydrogenase of *Gluconobacter japonicus* NBRC3260. Appl Environ Microbiol 79 (5):1654-1660. doi:10.1128/AEM.03152-12

Kersters K, De Ley J (1968) An easy screening assay for the enzymes of the Entner-Doudoroff pathway. Antonie Van Leeuwenhoek 34 (4):388-392

Kersters K, Lisdiyanti P, Komagata K, Swings J (2006) The family *Acetobacteriaceae*: The genera *Acetobacter*, *Acidomonas*, *Asaia*, *Gluconacetobacter*, *Gluconobacter* and *Kozakia*. In: Dworkin M, Falkow S, Rosenberg E, Schleifer K-H, Stackebrandt E (eds) The Prokaryotes Vol 5, 3rd edition Springer-Verlag GmbH, Heidelberg p. 163-200. doi:10.1007/0-387-30745-1-9

Kiefler I (2012) Optimierung des Glucose-Stoffwechsels von *Gluconobacter oxydans* 621H Δ*upp* durch Metabolic Engineering. Master thesis, University of Düsseldorf

Klasen R, Bringer-Meyer S, Sahm H (1995) Biochemical characterization and sequence analysis of the gluconate:NADP 5-oxidoreductase gene from *Gluconobacter oxydans*. J Bacteriol 177 (10):2637-2643

Kondo K, Horinouchi S (1997) Characterization of an insertion sequence, IS12528, from *Gluconobacter suboxydans*. Appl Environ Microbiol 63 (3):1139-1142

Kostner D, Luchterhand B, Junker A, Volland S, Daniel R, Büchs J, Liebl W, Ehrenreich A (2015) The consequence of an additional NADH dehydrogenase paralog on the growth of *Gluconobacter oxydans* DSM3504. Appl Microbiol Biotechnol 99 (1):375-386. doi:10.1007/s00253-014-6069-9

Krajewski V (2008) Modifikation des Glucosestoffwechsels in *Gluconobacter oxydans*. Dissertation, University of Düsseldorf, Germany

Krajewski V, Simić P, Mouncey NJ, Bringer S, Sahm H, Bott M (2010) Metabolic engineering of *Gluconobacter oxydans* for improved growth rate and growth yield on glucose by elimination of gluconate formation. Appl Environ Microbiol 76 (13):4369-4376. doi:10.1128/aem.03022-09

Kruger NJ, von Schaewen A (2003) The oxidative pentose phosphate pathway: structure and organisation. Curr Opin Plant Biol 6 (3):236-246

Kulhanek M (1989) Microbial dehydrogenations of monosaccharides. Adv Appl Microbiol 34:141-181

Lancaster CR, Kröger A, Auer M, Michel H (1999) Structure of fumarate reductase from *Wolinella succinogenes* at 2.2 A resolution. Nature 402 (6760):377-385. doi:10.1038/46483

Lau FT, Fersht AR (1987) Conversion of allosteric inhibition to activation in phosphofructokinase by protein engineering. Nature 326 (6115):811-812. doi:10.1038/326811a0

Levering PR, Weenk G, Olijve W, Dijkhuizen L, Harder W (1988) Regulation of gluconate and ketogluconate production in *Gluconobacter oxydans* ATCC 621H. Arch Microbiol 149 (6):534-539

Lightfield J, Fram NR, Ely B (2011) Across bacterial phyla, distantly-related genomes with similar genomic GC content have similar patterns of amino acid usage. PLoS One 6 (3):e17677. doi:10.1371/journal.pone.0017677

Macauley S, McNeil B, Harvey LM (2001) The genus *Gluconobacter* and its applications in biotechnology. Crit Rev Biotechnol 21 (1):1-25. doi:10.1080/20013891081665

Majumdar R, Guest JR, Bridger WA (1991) Functional consequences of substitution of the active site (phospho)histidine residue of *Escherichia coli* succinyl-CoA synthetase. Biochim Biophys Acta 1076 (1):86-90

Mamlouk D, Gullo M (2013) Acetic Acid bacteria: physiology and carbon sources oxidation. Indian J Microbiol 53 (4):377-384. doi:10.1007/s12088-013-0414-z

Matsushita K, Fujii Y, Ano Y, Toyama H, Shinjoh M, Tomiyama N, Miyazaki T, Sugisawa T, Hoshino T, Adachi O (2003) 5-keto-D-gluconate production is catalyzed by a quinoprotein glycerol dehydrogenase, major polyol dehydrogenase, in *Gluconobacter* species. Appl Environ Microbiol 69 (4):1959-1966

Matsushita K, Nagatani Y, Shinagawa E, Adachi O, Ameyama M (1989) Effect of extracellular pH on the respiratory chain and energetics of *Gluconobacter suboxydans*. Agr Biol Chem 53 (11):2895-2902

Matsushita K, Shinagawa E, Adachi O, Ameyama M (1987) Purification, characterization and reconstitution of cytochrome *o*-type oxidase from *Gluconobacter suboxydans*. Biochim Biophys Acta 894 (2):304-312

Matsushita K, Toyama H, Adachi O (1994) Respiratory chains and bioenergetics of acetic acid bacteria. Adv Microb Physiol 36:247-301

Matsutani M, Suzuki H, Yakushi T, Matsushita K (2014) Draft genome sequence of *Gluconobacter thailandicus* NBRC 3257. Stand Genomic Sci 9 (3):614-623. doi:10.4056/sigs.4778605

McNeil MB, Clulow JS, Wilf NM, Salmond GP, Fineran PC (2012) SdhE is a conserved protein required for flavinylation of succinate dehydrogenase in bacteria. J Biol Chem 287 (22):18418-18428. doi:10.1074/jbc.M111.293803

McNeil MB, Fineran PC (2013 a) Prokaryotic assembly factors for the attachment of flavin to complex II. Biochim Biophys Acta 1827 (5):637-647. doi:10.1016/j.bbabio.2012.09.003

McNeil MB, Fineran PC (2013 b) The conserved RGxxE motif of the bacterial FAD assembly factor SdhE is required for succinate dehydrogenase flavinylation and activity. Biochemistry 52 (43):7628-7640. doi:10.1021/bi401006a

Merfort M, Herrmann U, Bringer-Meyer S, Sahm H (2006 a) High-yield 5-keto-D-gluconic acid formation is mediated by soluble and membrane-bound gluconate-5-dehydrogenases of *Gluconobacter oxydans*. Appl Microbiol Biotechnol 73 (2):443-451. doi:10.1007/s00253-006-0467-6

Miller MJ, Gennis RB (1985) The cytochrome *d* complex is a coupling site in the aerobic respiratory chain of *Escherichia coli*. J Biol Chem 260 (26):14003-14008

Miura H, Mogi T, Ano Y, Migita CT, Matsutani M, Yakushi T, Kita K, Matsushita K (2013) Cyanide-insensitive quinol oxidase (CIO) from *Gluconobacter oxydans* is a unique terminal oxidase subfamily of cytochrome *bd*. J Biochem 153 (6):535-545. doi:10.1093/jb/mvt019

Mogi T, Ano Y, Nakatsuka T, Toyama H, Muroi A, Miyoshi H, Migita CT, Ui H, Shiomi K, Omura S, Kita K, Matsushita K (2009) Biochemical and spectroscopic properties of cyanide-insensitive quinol oxidase from *Gluconobacter oxydans*. J Biochem 146 (2):263-271. doi:10.1093/jb/mvp067

Nishikura-Imamura S, Matsutani M, Insomphun C, Vangnai AS, Toyama H, Yakushi T, Abe T, Adachi O, Matsushita K (2014) Overexpression of a type II 3-dehydroquinate dehydratase enhances the biotransformation of quinate to 3-dehydroshikimate in *Gluconobacter oxydans*. Appl Microbiol Biotechnol 98 (7):2955-2963. doi:10.1007/s00253-013-5439-z

Nishimura JS (1986) Succinyl-CoA synthetase structure-function relationships and other considerations. Adv Enzymol Relat Areas Mol Biol 58:141-172

Olijve W, Kok JJ (1979a) Analysis of growth of *Gluconobacter oxydans* in glucose containing media. Arch Microbiol 121 (3):283-290

Olijve W, Kok JJ (1979b) An analysis of the growth of *Gluconobacter oxydans* in chemostat cultures. Arch Microbiol 121:291-297

Pappenberger G, Hohmann HP (2014) Industrial production of L-ascorbic Acid (vitamin C) and D-isoascorbic acid. Adv Biochem Eng Biotechnol 143:143-188. doi:10.1007/10_2013_243

Park SJ, Chao G, Gunsalus RP (1997) Aerobic regulation of the *sucABCD* genes of *Escherichia coli*, which encode alpha-ketoglutarate dehydrogenase and succinyl coenzyme A synthetase: roles of ArcA, Fnr, and the upstream *sdhCDAB* promoter. J Bacteriol 179 (13):4138-4142

Peters B, Junker A, Brauer K, Mühlthaler B, Kostner D, Mientus M, Liebl W, Ehrenreich A (2013a) Deletion of pyruvate decarboxylase by a new method for efficient markerless gene deletions in *Gluconobacter oxydans*. Appl Microbiol Biotechnol 97 (6):2521-2530. doi:10.1007/s00253-012-4354-z

Peters B, Mientus M, Kostner D, Junker A, Liebl W, Ehrenreich A (2013b) Characterization of membrane-bound dehydrogenases from *Gluconobacter oxydans* 621H via whole-cell activity assays using multideletion strains. Appl Microbiol Biotechnol 97 (14):6397-6412. doi:10.1007/s00253-013-4824-y

Pronk JT, Levering PR, Oiijve W, van Dijken JP (1989) Role of NADP dependent and quinoprotein glucose dehydrogenases in gluconic acid production by *Gluconobacter oxydans*. Enzyme Microb Tech 11 (3):160-164

Prust C, Hoffmeister M, Liesegang H, Wiezer A, Fricke WF, Ehrenreich A, Gottschalk G, Deppenmeier U (2005) Complete genome sequence of the acetic acid bacterium *Gluconobacter oxydans*. Nat Biotechnol 23 (2):195-200. doi:10.1038/nbt1062

Przybyla-Zawislak B, Dennis RA, Zakharkin SO, McCammon MT (1998) Genes of succinyl-CoA ligase from *Saccharomyces cerevisiae*. Eur J Biochem 258 (2):736-743

Puustinen A, Finel M, Virkki M, Wikström M (1989) Cytochrome *o* (*bo*) is a proton pump in *Paracoccus denitrificans* and *Escherichia coli*. FEBS Lett 249 (2):163-167

Raspor P, Goranovič D (2008) Biotechnological applications of acetic acid bacteria. Crit Rev Biotechnol 28 (2):101-124. doi:10.1080/07388550802046749

Rauch B, Pahlke J, Schweiger P, Deppenmeier U (2010) Characterization of enzymes involved in glucose and gluconate utilization in the central metabolism of *Gluconobacter oxydans*. Appl Microbiol Biotechnol 88 (3):711-718. doi:10.1007/s00253-010-2779-9

Reichstein T, Grüssner, A. (1934) Eine ergiebige Synthese der L-Ascorbinsäure (C-Vitamin). Helv Chim Acta 17:311-328

Richhardt J, Bringer S, Bott M (2012) Mutational analysis of the pentose phosphate and Entner-Doudoroff pathways in *Gluconobacter oxydans* reveals improved growth of a Δ*edd* Δ*eda* mutant on mannitol. Appl Environ Microbiol 78 (19):6975-6986. doi:10.1128/AEM.01166-12

Richhardt J, Bringer S, Bott M (2013a) Role of the pentose phosphate pathway and the Entner-Doudoroff pathway in glucose metabolism of *Gluconobacter oxydans* 621H. Appl Microbiol Biotechnol 97 (10):4315-4323. doi:10.1007/s00253-013-4707-2

Richhardt J, Luchterhand B, Bringer S, Büchs J, Bott M (2013b) Evidence for a key role of cytochrome bo_3 oxidase in respiratory energy metabolism of *Gluconobacter oxydans*. J Bacteriol 195 (18):4210-4220. doi:10.1128/JB.00470-13

Roche B, Aussel L, Ezraty B, Mandin P, Py B, Barras F (2013) Iron/sulfur proteins biogenesis in prokaryotes: formation, regulation and diversity. Biochim Biophys Acta 1827 (3):455-469. doi:10.1016/j.bbabio.2012.12.010

Saichana N, Matsushita K, Adachi O, Frebort I, Frebortova J (2015) Acetic acid bacteria: A group of bacteria with versatile biotechnological applications. Biotechnol Adv 33 (6 Pt 2):1260-1271. doi:10.1016/j.biotechadv.2014.12.001

Schedel M (2000) Regioselective oxidation of aminosorbitol with *Gluconobacter oxydans*, a key reaction in the industrial synthesis of 1-deoxynojirimycin. Kelly DR (ed) Biotechnology; Wiley-VCH, Weinheim vol 8b (Biotransformations II):pp 296–308

Shinagawa E, Matsushita K, Adachi O, Ameyama M (1990) Evidence for electron transfer via ubiquinone between quinoproteins D-glucose dehydrogenase and alcohol dehydrogenase of *Gluconobacter suboxydans*. J Biochem (Tokyo) 107 (6):863-867

Siedler S, Bringer S, Blank LM, Bott M (2012) Engineering yield and rate of reductive biotransformation in *Escherichia coli* by partial cyclization of the pentose phosphate pathway and PTS-independent glucose transport. Appl Microbiol Biotechnol 93 (4):1459-1467. doi:10.1007/s00253-011-3626-3

Sievers M, Gaberthuel C, Boesch C, Ludwig W, Teuber M (1995) Phylogenetic position of *Gluconobacter* species as a coherent cluster separated from all *Acetobacter* species on the basis of 16S ribosomal RNA sequences. FEMS Microbiol Lett 126 (2):123-126

Soini J, Ukkonen K, Neubauer P (2008) High cell density media for *Escherichia coli* are generally designed for aerobic cultivations - consequences for large-scale bioprocesses and shake flask cultures. Microb Cell Fact 7:26. doi:10.1186/1475-2859-7-26

Sugiyama M, Suzuki S, Tonouchi N, Yokozeki K (2003) Transaldolase/glucose-6-phosphate isomerase bifunctional enzyme and ribulokinase as factors to increase xylitol production from D-arabitol in *Gluconobacter oxydans*. Biosci Biotechnol Biochem 67 (12):2524-2532

Svitel J, Tkac J, Vostiar I, Navratil M, Stefuca V, Bucko M, Gemeiner P (2006) *Gluconobacter* in biosensors: applications of whole cells and enzymes isolated from *Gluconobacter* and *Acetobacter* to biosensor construction. Biotechnol Lett 28 (24):2003-2010. doi:10.1007/s10529-006-9195-3

Tonouchi N, Sugiyama M, Yokozeki K (2003) Coenzyme specificity of enzymes in the oxidative pentose phosphate pathway of *Gluconobacter oxydans*. Biosci Biotechnol Biochem 67 (12):2648-2651

Van Vranken JG, Na U, Winge DR, Rutter J (2015) Protein-mediated assembly of succinate dehydrogenase and its cofactors. Crit Rev Biochem Mol Biol 50 (2):168-180. doi:10.3109/10409238.2014.990556

Verkhovskaya ML, Garcia-Horsman A, Puustinen A, Rigaud JL, Morgan JE, Verkhovsky MI, Wikström M (1997) Glutamic acid 286 in subunit I of cytochrome bo3 is involved in proton translocation. Proc Natl Acad Sci U S A 94 (19):10128-10131

Weenk G, Olijve W, Harder W (1984) Ketogluconate formation by *Gluconobacter* species. Appl Microbiol Biotechnol 20 (6):400-405

Wolodko WT, Kay CM, Bridger WA (1986) Active enzyme sedimentation, sedimentation velocity, and sedimentation equilibrium studies of succinyl-CoA synthetases of porcine heart and *Escherichia coli*. Biochemistry 25 (19):5420-5425

Yamada Y, Hosono R, Lisdyanti P, Widyastuti Y, Saono S, Uchimura T, Komagata K (1999) Identification of acetic acid bacteria isolated from Indonesian sources, especially of isolates classified in the genus *Gluconobacter*. J Gen Appl Microbiol 45 (1):23-28

Yamada Y, Yukphan P (2008) Genera and species in acetic acid bacteria. Int J Food Microbiol 125 (1):15-24. doi:10.1016/j.ijfoodmicro.2007.11.077

Zahid N, Schweiger P, Galinski E, Deppenmeier U (2015) Identification of mannitol as compatible solute in *Gluconobacter oxydans*. Appl Microbiol Biotechnol 99 (13):5511-5521. doi:10.1007/s00253-015-6626-x

Zhang P, Ma Y, Wang F, Wei D (2014) Phosphorylation of HPr by HPr kinase in *Gluconobacter oxydans 621H*. Protein Pept Lett 21 (6):597-601

6. Appendix

6.1 Supplementary data: Growth of different deletion mutants of *G. oxydans*

Table 1: Constructed strains

Strain	Genotype	Reference
Gluconobacter oxydans		
G. oxydans 621H Δ*upp*	*G. oxydans* 621H derivative with a deletion of GOX0327 coding for uracil phosphoribosyl-transferase (Δ*upp*); Cef^R	A. Ehrenreich (TU Munich), (Peters et al. 2013a)
G. oxydans 621H Δ*upp* Δ*gdhS*	Derivative of *G. oxydans* 621H Δ*upp* with in-frame deletion of GOX2015 (*gdhS*); Cef^R	Kiefler, 2012
G. oxydans 621H Δ*upp* Δ*gdhS* Δ*gdhM*	Derivative of *G. oxydans* 621H Δ*upp* with in-frame deletion of GOX2015 (*gdhS*) and GOX0265 (*gdhM*); Cef^R	Kiefler, 2012
G. oxydans 621H Δ*upp* Δ*gdhS* Δ*gdhM* Δ*pdc*	Derivative of *G. oxydans* 621H Δ*upp* with in-frame deletion of GOX2015 (*gdhS*), GOX0265 (*gdhM*) and GOX1081 (*pdc*); Cef^R	Kiefler, 2012

The deletion mutants *G. oxydans* 621H Δ*upp* Δ*gdhS* (Fig. 1), *G. oxydans* 621H Δ*upp* Δ*gdhS* Δ*gdhM* (Fig. 2) and *G. oxydans* 621H Δ*upp* Δ*gdhS* Δ*gdhM* Δ*pdc* (Fig. 3) were cultivated in a parallel bioreactor system (DASGIP, Juelich, Germany) on glucose (2 % w/v) at a constant pH of 6 and 15 % dissolved oxygen.

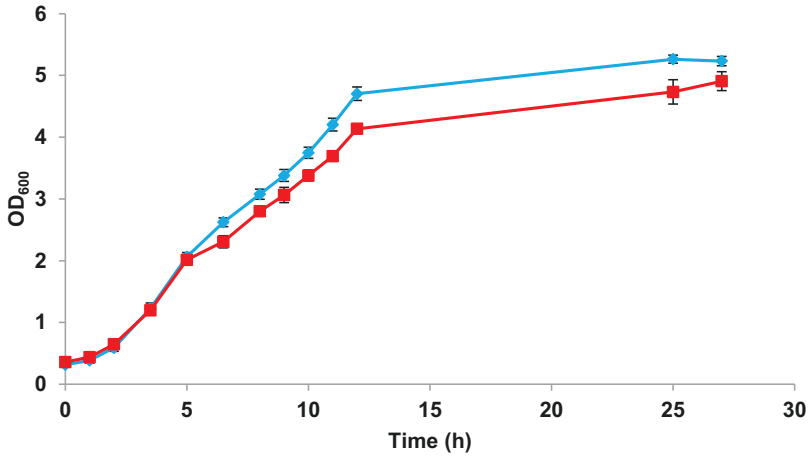

Figure 1: Growth behavior of *G. oxydans* 621H Δ*upp* Δ*gdhS* (■) in comparison to the reference strain *G. oxydans* 621H Δ*upp* (◆). The cultures were grown in glucose (2 % w/v) medium at 15 % dissolved oxygen at pH 6 in a parallel bioreactor system (DASGIP, Juelich, Germany). Mean values and standard deviation from three biological replicates are shown.

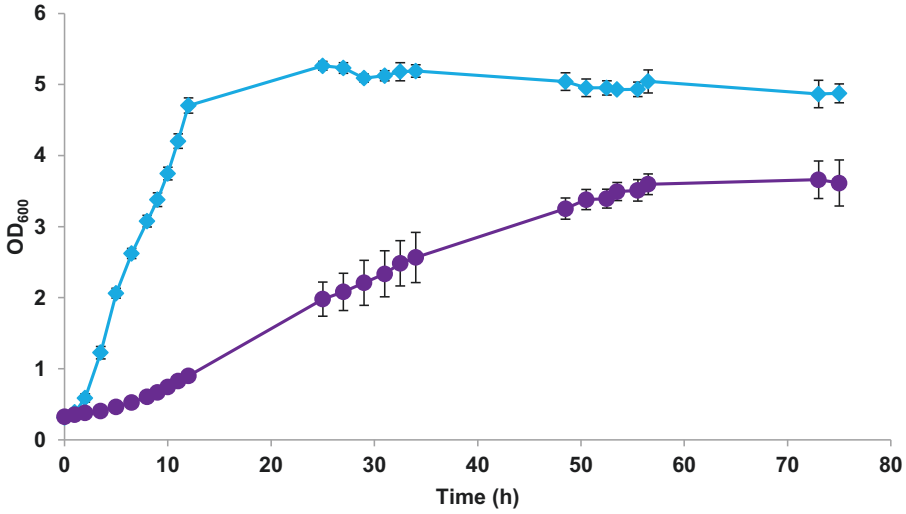

Figure 2: Growth behavior of *G. oxydans* 621H Δ*upp* Δ*gdhS* Δ*gdhM* (■) in comparision to the reference strain *G. oxydans* 621H Δ*upp* (◆).The cultures were grown in glucose (2 % w/v) medium at 15 % dissolved oxygen at pH 6 in a parallel bioreactor system (DASGIP, Juelich, Germany). Mean values and standard deviation from three biological replicates are shown.

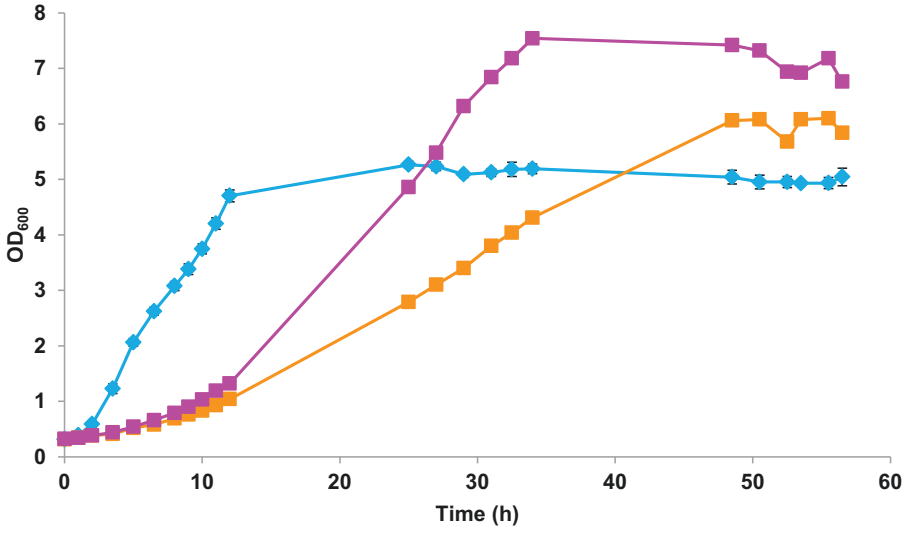

Figure 3: Growth behavior of *G. oxydans* 621H Δ*upp* Δ*gdhS* Δ*gdhM* Δ*pdc* (Clone 1-1 ■, clone 1-3 ■) and the reference strain *G. oxydans* 621H Δ*upp* (◆). The cultures were grown in glucose (2 % w/v) medium at 15 % dissolved oxygen at pH 6 in a parallel bioreactor system (DASGIP, Juelich, Germany). Two different clones of the deletion mutant are shown.

Danksagung

Ein besonderer Dank gilt Prof. Dr. Michael Bott für die Überlassung des herausfordernden Themas, der sich trotz eines straffen Terminkalenders immer die nötige Zeit genommen hat. Vielen Dank für die sowohl hilfreichen Gespräche und Ratschläge als auch für die Durchsicht dieser Arbeit.

Des Weiteren möchte ich mich bei Herrn PD Dr. Ulrich Schulte für die Übernahme des Zweitgutachtens bedanken.

Meiner Gruppenleiterin Dr. Stephanie Bringer danke ich dafür, dass Sie stets ein offenes Ohr für mich hatte und mir immer mit Rat und Tat zur Seite stand. Deine letzte Doktorandin wünscht Dir eine wohlverdiente schöne Zeit nach der Arbeit!

Helga, ohne Dich wären die Wachstumskurven in dieser Arbeit wohl nicht zustande gekommen. Danke, dass du immer auf mich aufgepasst hast.

Mein Dank gilt auch den Mitarbeitern des IBG-1 für die positive Arbeitsatmosphäre und die Gespräche, durch die ich Vieles lernen durfte.

Mama und Papa, Ihr seid immer für mich da und dafür danke ich Euch von ganzem Herzen! Eure Unterstützung, Eure Geduld mit mir, und Euer steter Glaube an mich, haben mich gestärkt und mir in meinem Leben immer weitergeholfen.

Ich möchte auch meinen Großeltern danke sagen. Ihr ward und seid bis heute eine Bereicherung in meinem Leben.

Markus, ich bin dankbar Dich an meiner Seite zu haben! Ich danke Dir für das Bisherige und freue mich auf das Zukünftige.

Mirj, meine Beste, danke! Dass Du bist wie Du bist und wir uns auch ohne ein Wort verstehen.

Meine Mädels! Wenn wir zusammen sind, ist alles andere egal und dafür danke ich Euch!

Erklärung

Ich versichere an Eides Statt, dass die Dissertation von mir selbständig und ohne unzulässige fremde Hilfe unter Beachtung der „Grundsätze zur Sicherung guter wissenschaftlicher Praxis an der Heinrich-Heine Universität Düsseldorf“ erstellt worden ist. Ich habe bisher keine erfolglosen Promotionsversuche unternommen. Diese Dissertation wurde bisher an keiner anderen Fakultät vorgelegt.

Jülich, den 30.03.2016

Ines Kiefler

Band / Volume 68
Modifikationen der Atmungskette in *Corynebacterium glutamicum* und Rolle des Flavohämoproteins Hmp
L. Platzen (2013), IV, 119 pp
ISBN: 978-3-89336-931-7

Band / Volume 69
L-Cystein-Bildung mit *Corynebacterium glutamicum* und optische Sensoren zur zellulären Metabolitanalyse
K. Hoffmann (2014),vi, 83 pp
ISBN: 978-3-89336-939-3

Band / Volume 70
Metabolic engineering of Corynebacterium glutamicum for production of the adipate precursor 2-oxoadipate
M. Spelberg (2014), 118 pp
ISBN: 978-3-89336-954-6

Band / Volume 71
Design and application of metabolite sensors for the FACS-based isolation of feedback-resistant enzyme variants
G. Schendzielorz (2014), 129 pp
ISBN: 978-3-89336-955-3

Band / Volume 72
The development and application of a single cell biosensor for the detection of L-methionine and branched-chain amino acids
N. Mustafi (2014), 137 pp
ISBN: 978-3-89336-956-0

Band / Volume 73
Metabolic engineering of *Corynebacterium glutamicum* for production of L-leucine and 2-ketoisocaproate
M. Vogt (2014), VI, 92 pp
ISBN: 978-3-89336-968-3

Band / Volume 74
Pupylierung in *Corynebacterium glutamicum*
A. Küberl (2014), VI, 163 pp
ISBN: 978-3-89336-969-0

Band / Volume 75
Tat-translocase composition in *Corynebacterium glutamicum* and the effect of TorD coexpression
D. Oertel (2014), v, 117 pp
ISBN: 978-3-89336-996-6

Band / Volume 76
The 6C RNA of *Corynebacterium glutamicum*
J. Pahlke (2014), II, 144 pp
ISBN: 978-3-95806-003-6

Band / Volume 77
Anaerobes Wachstum von *Corynebacterium glutamicum* durch gemischte Säurefermentation
A. Michel (2014), 145 pp
ISBN: 978-3-95806-010-4

Band / Volume 78
Engineering of *Corynebacterium glutamicum* towards utilization of methanol as carbon and energy source
S. Witthoff (2015), V, 113 pp
ISBN: 978-3-95806-029-6

Band / Volume 79
Interaction of the two-component systems HrrSA and ChrSA in *Corynebacterium glutamicum*
E. Hentschel (2015), V, 118 pp
ISBN: 978-3-95806-053-1

Band / Volume 80
Strukturelle und funktionelle Untersuchungen zur Kupfer-Homöostase in *Corynebacterium glutamicum*
X. Schuplezow (2015), 114 pp
ISBN: 978-3-95806-085-2

Band / Volume 81
Development and application of single cell biosensors for the improvement of amino acid production in *Escherichia coli* and *Corynebacterium glutamicum*
R. Mahr (2016), IV, 179
ISBN: 978-3-95806-145-3

Band / Volume 82
Strain development of *Gluconobacter oxydans*: Complementation of non-functional metabolic pathways and increase of carbon flux
I. Kiefler (2016), III, 103 pp
ISBN: 978-3-95806-158-3

Weitere ***Schriften des Verlags im Forschungszentrum Jülich*** unter
http://wwwzb1.fz-juelich.de/verlagextern1/index.asp

Gesundheit / Health
Band / Volume 82
ISBN 978-3-95806-158-3

JÜLICH
FORSCHUNGSZENTRUM